Depletion of ABCC10 in human colorectal Caco-2 cancer cells using the CRISPR-Cas9 system

Sajeevani S. K. Narasinghe

A thesis submitted to the Auckland University of Technology, in fulfilment of the requirements of the degree of Master of Philosophy

Faculty of Health and Environment Sciences, School of Science

March 2024

Abstract

Colorectal cancer (CRC) is one of the most prominent cancers detected worldwide. Cancer treatment with standard chemotherapy has led to improved CRC patients' overall survival rate. However, in more than 40% of patients, the standard chemotherapy achieves only a brief or no tumour response or unexpected toxicity, leading to therapeutic failure. Accumulating evidence identified a family of cell membrane transporter proteins (ABC transporters) that transport various chemotherapeutics across cell membranes and, in this way, may control the cellular accumulation, antitumour activity, and toxicity of front-line therapeutics. Multi-drug resistant proteins (MRPs) belong to the ABCC subfamily, and overexpression of ABCC transporters in tumour cells results in multi-drug resistance, which is when tumour cells are able to resist the antitumour cytotoxicity of a range of structurally diverse anticancer drugs (e.g.: Oxaliplatin, 5-Fluorouracil). MRP7 (encoded by *ABCC10* gene) has recently been reported to confer resistance to the antitumor drug docetaxel and oxaliplatin. However, previous ABCC10 work was undertaken by using siRNA gene knockdown and pharmacological inhibitors, but those experiments were confounded by the off-target effects. Therefore, we hypothesized that CRISPR-cas9 gene editing technology could be used to achieve precise and permanent disruption of the functional expression of ABCC10 transporter protein and reverse the drug resistance in human colorectal cancer Caco-2 cells. To test our hypothesis, Caco-2 cells were transfected with ABCC10 guideRNA-Cas9 protein ribonucleoprotein complexes through liposome-mediated delivery. The efficiency of the *ABCC10* gene disruption was analysed using the T7 Endoneuclease1 cleavage efficiency assay. The single clones of ABCC10 knockouts were obtained from limiting dilution. The variation of the ABCC10 (MRP7) protein expression in the wild Caco-2 cells and the transfected clones was assessed following western blot analysis. The sensitivity towards a model ABCC10 substrate docetaxel and its concentration-dependent cytotoxicity was determined by using MTT [3-(4,5-dimethylthiazol-2-yl)-2,5-diphenyltetrazolium bromide] assay. The cleavage efficiency of disrupting the *ABCC10* gene was 13.98% in Caco-2 cells. Following western blotting, both wild Caco-2 cells and the gRNA/Cas9 transfected clones produced the signal corresponding to ABCC10. However, one clone 6G2 developed significantly increased sensitivity towards

docetaxel ($P < 0.05$), with docetaxel IC50 values of 1.84 μM and 0.27 μM in wildtype Caco-2 cells and single clone 6G2, respectively. Therefore, the sensitivity of the isolated single clone towards the anticancer drug docetaxel has been increased approximately tenfold. The finding of this study demonstrates that CRISPR-Cas9 transfection of Caco-2 cells is feasible in reverse ABCC10-mediated resistance towards docetaxel. Therefore, our research provides proof-of-principle evidence that disruption of the *ABCC10* gene reduces the function of the ABCC10 and could convert a less effective drug (e.g. docetaxel) into an exceptional one for CRC treatment.

Table of Contents

1. Introduction 15
   1.1. Colorectal Cancer 15
      1.1.1. Trends of Colorectal Cancer Worldwide 15
      1.1.2. Prevalence of Colorectal Cancer in New Zealand 17
      1.1.3. Risk Factors 18
      1.1.4. Symptoms and Stages of Colorectal Cancer 22
      1.1.5. Diagnosis of Colorectal Cancer 24
      1.1.6. Treatments for Colorectal Cancer 26
   1.2. Multi-Drug Resistance 29
      1.2.1. Multi-Drug Resistant Proteins (MRP) 29
      1.2.2. MRP 7/ABCC10 31
   1.3. Docetaxel 33
      1.3.1. History of Docetaxel Development 33
      1.3.2. Structure of Docetaxel 35
      1.3.3. Mechanism of Action 36
      1.3.4. Clinical Uses 36
      1.3.5. Pharmacokinetics of Docetaxel 40
      1.3.6. Toxicities related to Docetaxel 42
      1.3.7. Limitations and Future Perspectives 43
   1.4. CRISPR-Cas9 44
      1.4.1. Mechanism of the CRISPR-Cas9 system 44
      1.4.2. CRISPR-Cas9 in cancer therapeutics 45
      1.4.3. Factors Affecting Therapeutic Efficacy 48
   1.5. Research hypotheses and aims 52
2. Materials and Methods 53
   2.1. Chemicals and reagents 53
   2.2. Reviving Cell Culture from Frozen Cells 53
   2.3. CRISPR-Cas 9 Transfection 53
      2.3.1. Preparation of sgRNA working solution 54
      2.3.2. Seeding Cells 54
      2.3.3. Transfection 54
   2.4. Cleavage Efficiency Assay 56
      2.4.1. Harvest Cells 56
      2.4.2. Cell lysis and DNA extraction 57
      2.4.3. Preparing primer working solution 57
      2.4.4. PCR amplification 57
      2.4.5. PCR Products Gel Analysis 58
      2.4.6. PCR product verification 58
      2.4.7. Cleavage Assay 58

2.4.8. Cleavage Products Gel Analysis 59
2.5. Selection of Single Clones 60
2.6. Western Blotting 61
2.6.1. Preparation of cell lysate 61
2.6.2. Western blot gel electrophoresis 62
2.6.3. Staining with antibodies and visualizing 62
2.6.4. Western blot method optimisation 63
2.6.5. Western Blot analysis of isolated clones 64
2.7. MTT assay 64
2.7.1. Definition of linear range 65
2.7.2. Method Development to detect IC50 of wildtype Caco-2 cells 66
2.7.3. Docetaxel sensitivity of the knockout clones 68
3. Results 69
3.1. Gene Alteration with CRISPR-Cas9 69
3.1.1. Selection of sgRNA and primers 69
3.1.2. PCR Analysis 70
3.1.3. Genomic Cleavage Assay 71
3.2. Selection of Single Clones 73
3.3. Western Blotting 77
3.3.1. Protocol development for ABCC10 western blot analysis 77
3.3.2. Single clones ABCC10 expression comparison with Western blot 79
3.4. MTT Assay 80
3.4.1. Linear range detection 81
3.4.2. Protocol Development of MTT Assay for IC50 Detection 81
3.4.3. Comparison of cell viability of the single clones 86
4. Discussion 88
4.1. Introduction 88
4.2. Major Findings of the Study 89
4.3. Active transportation of Docetaxel via ABCC10 90
4.4. Improvement of chemotherapy with gene editing 91
4.5. Gene knockout efficiency and off-target effect 92
4.6. Future Directions 93
4.7. Conclusion 95
References 96
Annex 104

List of Figures

Figure 1.1. Number of new cancer cases and cancer-related deaths reported in 2022 16
Figure 1.2. Structure of Docetaxel 35
Figure 2.1. Composition of Transfection Solutions 55
Figure 2.2. Layout of transfection 6-well plate 55
Figure 2.3. The layout of the 96-Well plate for limiting dilution 60
Figure 2.4. The Layout of the 96-well plate for linearity range detection 65
Figure 2.5. The layout of the 96-well plate of docetaxel treatment for 24 hours on 10,000 wild Caco-2 cells 66
Figure 2.6. The layout of the 96-well plate of docetaxel treatment for 72 hours on 10,000 wild Caco-2 cells 67
Figure 2.7. The layout of a 96-well plate, Comparison of docetaxel sensitivity in wild Caco-2 cells and knockout clones 68
Figure 3.1. Products of PCR Analysis 70
Figure 3.2. *ABCC10* gene sequence amplified by PCR 70
Figure 3.3. Products of Genomic Cleavage Assay 71
Figure 3.4. ABCC10 signal in DTT cell lysates 77
Figure 3.5. Effect of different lysis buffers on ABCC10 signal. 78
Figure 3.6. Western Blot of Single Clones - Set 1 79
Figure 3.7. Total Protein Image - Clones set 1 79
Figure 3.8. Western Blot of Single Clones - Set 2 80
Figure 3.9. Linearity Range Detection 81
Figure 3.10. Percentage cell viability of 10,000 Caco-2 cells treated with docetaxel for 24 h 82
Figure 3.11. Percentage cell viability of 10,000 Caco-2 cells treated with docetaxel for 72 h 83
Figure 3.12. Percentage cell viability of 5,000 Caco-2 cells treated with docetaxel for 72 h 83
Figure 3.13. Comparison of cell survival with respect to concentration of drug-treated 84
Figure 3.14. IC50 detection of docetaxel for wild Caco-2 cells (96-Well plate following MTT assay) 85
Figure 3.15. Cell viability variations among Caco-2 cell clones treated with docetaxel (2 μM) for 72 h. 86
Figure 3.16. Cell viability of WT and clone 6G2 in different docetaxel concentrations 87
Figure 3.17. Concentration-dependant effect of docetaxel on clone 6G2 (5000 cells per well). 87

List of Tables

Table 1.1. Cancer incidences by prioritized ethnicity in New Zealand in 2021 17
Table 1.2. CRC Statistics New Zealand 2012 to 2021 17
Table 1.3. Summary of ABCC subfamily members 30
Table 1.4. Chronology of Taxol Development 34
Table 2.1. Chemicals and reagents used for the study with their supplier 53
Table 2.2. Temperature program for cell lysis 57
Table 2.3. Composition of the PCR mixture 58
Table 2.4. Temperature program of PCR reaction 58
Table 2.5. Temperature program of re-annealing cycle 59
Table 2.6. Composition of Dithiothreitol containing Laemmli sample buffer. 61
Table 2.7. Composition of cell lysate mixture 64
Table 3.1. In silico sgRNA design 69
Table 3.2. In silico Primer Design 69
Table 3.3. Morphological changes of the single clones 73
Table 3.4. Linearity Range Detection 81
Table 3.5. Percentage cell viability of 10,000 Caco-2 cells treated with docetaxel for 24 h 82
Table 3.6. Percentage cell viability of 10,000 Caco-2 cells treated with docetaxel for 72 h 82
Table 3.7. Percentage cell viability of 5,000 Caco-2 cells treated with docetaxel for 72 h 83
Table 3.8. Percentage cell viability of 5,000 cells 6G2 clone treated with docetaxel for 72 h ... 87

Attestation of Authorship

I hereby declare that this thesis is my work and that, to the best of my knowledge, it contains no material previously published or written by another person. Except for work that has been explicitly defined and acknowledged.

Signed:

Name: Sajeevani S. K. Narasinghe

Date: 14th March 2024

Acknowledgments

I completed my thesis successfully because of the endless support of my supervisors, family, and friends. Therefore, I would like to express my heartfelt gratitude to all of them.

First of all, I would like to thank my primary supervisor, Associate Professor Yan Li, for allowing me to work on a project I had always dreamt of. The skills you have taught me and the experience I gained while working with you are invaluable and will be beneficial for my career. Prof. Yan has much experience in biomedical research and always has a solution for whatever issues occur during my research. He was very patient and encouraged me to complete my thesis on time. I sincerely thank him for guiding me throughout this project.

I also would like to thank my secondary supervisor, Joe Chang, for allowing me to work with him and utilize the facilities at the AUT Roche Laboratory. Thank you very much for all the support given to me from the start of this project.

I want to thank everyone who worked in the AUT cell culture lab for being very friendly and supportive and making my stay there a pleasurable experience. A special thanks to our lovely technician, Matt Oudshoorn, who was always there to support us whenever we were in need and especially for being my lab buddy despite his busy schedule.

My greatest appreciation to my parents for supporting me financially and providing me moral support, being by my side, and encouraging me in whatever I do. I could not have made my dream come true without your support, for which I will be forever indebted to both of you.

Finally, I would like to thank my husband, who was behind me throughout this whole process, supporting and encouraging me whenever I was disappointed. I am genuinely grateful for your sacrifices to help me achieve my target. Thank you very much.

Abbreviations

µl - microliter

^{0}C - Degree Celsius

3DCRT - 3-dimensional conformal radiotherapy

AAV - adeno-associated viruses

ABC - ATP-binding cassette

AC - adenocarcinomas

AICD - activation-induced cell death

ANOVA – analysis of variance

APC - adenomatous polyposis coli

ASR - age-standardized rates

AUC - area under the curve

bp - base pair

CAR - chimeric antigen receptor

CBCT - cone beam computer tomography

CEA - carcinoembryonic antigen assay

CFTR - cystic fibrosis transmembrane conductance regulator

CI - confidence interval

CRC - colorectal cancer

CRISPR - clustered regularly interspaced short palindromic repeats

CRM - circumferential resection margin

CT scan - computed tomography scan

CTLA – 4 - cytotoxic T lymphocyte-associated antigen - 4

CYP3A - cytochrome P450-3A

DMEM - Dulbecco’s modified eagle medium

DMSO - dimethyl sulfoxide

DNA - deoxyribose nucleic acid

DSB - double stranded break

DTT - dithiothreitol

E217βG - 17β-estradiol-(17-β-D-glucuronide)

EDTA - ethylenediaminetetraacetic acid

EGF - epidermal growth factor

EMT - epithelial-mesenchymal transition

EORTC - European organization for research and treatment of cancer

FAP - familial adenomatous polyposis

FBS - fetal bovine serum

FDA - food and drug administration

FOBT - fecal occult blood test

g - gram

GCD - genomic cleavage detection

GI - gastrointestinal

GLOBOCAN - the global cancer observatory

GOS - Glasgow osteogenic sarcoma

gRNA - guide RNA

GTP - guanosine triphosphate

HDR - homology-directed repair

HEK - human embryonic kidney

HNPCC - hereditary nonpolyposis colon cancer

HRP - horseradish peroxidase

IBD - inflammatory bowel disease

IGRT - image-guided radiotherapy

IMRT - intensity-modulated radiation therapy

IRR - incidence rate ratios

LDM - low-dose metronomic

LDS - lithium dodecyl sulfate

lncRNA - long noncoding RNA

M - Molar concentration

MAC - mucinous adenocarcinomas

miRNA - microRNA

mol - mole

MRI scan - magnetic resonance imaging scan

MRP - multi-drug resistant proteins

MSD - membrane-spanning domains

MTT - [3-(4,5-dimethylthiazol-2-yl)-2,5-diphenyltetrazolium bromide]

NBD - nucleotide binding domains

NHEJ - non-homologous end joining

OTE - off-target effects

P - probability

PAM - protospacer adjacent motif

PBS - phosphate-buffered saline

PCR - polymerase chain reaction

PD-1 - programmed cell death protein

PDX-1 - pancreatic duodenal homeobox-1

PET scan - positron emission tomography scan

pmol - picomole

RIPA buffer - radioimmunoprecipitation assay buffer

RNA - ribonucleic acid

RT/PCR - reverse transcription polymerase chain reaction

SBRT - stereotactic body radiation therapy

SC - signet-ring cell carcinomas

SCCHN - squamous cell carcinoma of the head and neck

SDS - sodium dodecyl sulfate

sgRNA - single guide RNA

SNP - single nucleotide polymorphisms

SpCas9 - Cas9 derived from *Streptococcus pyogenes*

SUR 1 - sulfonylurea receptor 1

T7E1 - T7 endoneuclease1

TALEN- transcription activator-like effector nuclease

TBE - Tris-borate-EDTA buffer

TBST - Tris-buffered saline with 0.1% Tween® 20 detergent

TE buffer - Tris-EDTA buffer

VEGF - vascular endothelial growth factor

ZFN - zinc finger nucleases

1. Introduction

1.1. Colorectal Cancer

1.1.1. Trends of Colorectal Cancer Worldwide

The Colon and rectum are crucial components of the digestive tract. The colon lies between the small intestine and the rectum and is divided into four main sections: ascending, transverse, descending, and sigmoidal colon. The colon's primary functions mainly include the absorption of nutrients, minerals, and water and the storage of the waste material that forms the faeces. Due to their physiological nature, the colon and the rectum are highly exposed to different chemical, physical, and biological agents, which makes them highly vulnerable to pathologies that will lead to conditions such as cancer (Arvelo et al., 2015). Due to the similarities between colon and rectum cancers, they are classified into one main category and named colorectal cancers.

Colorectal Cancer (CRC) is one of the significant forms of cancer diagnosed annually. CRC is a severe health hazard that is more prominent in older people who are above 50 years of age. It is the third most prominent cancer, which falls behind breast and lung cancer. In 2022, the total number of new cancer cases reported was 19,976,499; out of that, 1,926,425 (9.6%) were colorectal cancer cases (Figure 1.1).

CRC is the third most prominent cancer form detected in males, while the most common form is lung cancer, and the second form is prostate cancer. In the year 2022, according to the reports published by GLOBOCAN, out of the 10,311,610 males diagnosed with cancer, 1,069,446 (10.4%) were of colorectal cancer. In women, breast cancer is the most prominent form (2,296,840 = 23.8%), while colorectal cancer is the third most common (856,979 = 8.9%) among this group. CRC has the second-highest mortality rate and corresponds to 9.3% of cancer-related deaths in the year 2022. The incidence trend and mortality rate of CRC is expected to increase annually despite all the improvements in the treatment and diagnosis process. It is predicted that in the year 2040, there will be 3.2 million new CRC cases detected, while 1.6 million deaths are expected to be reported (Morgan et al., 2023)

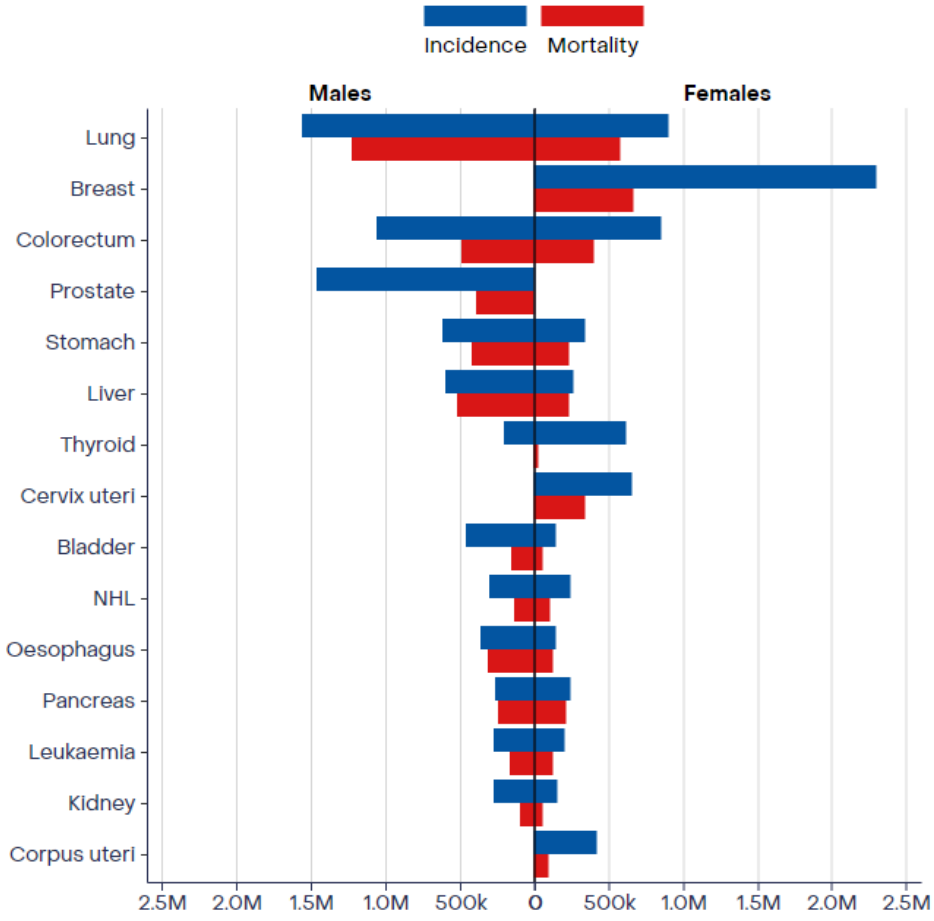

Rates worldwide in 2022 among male and female

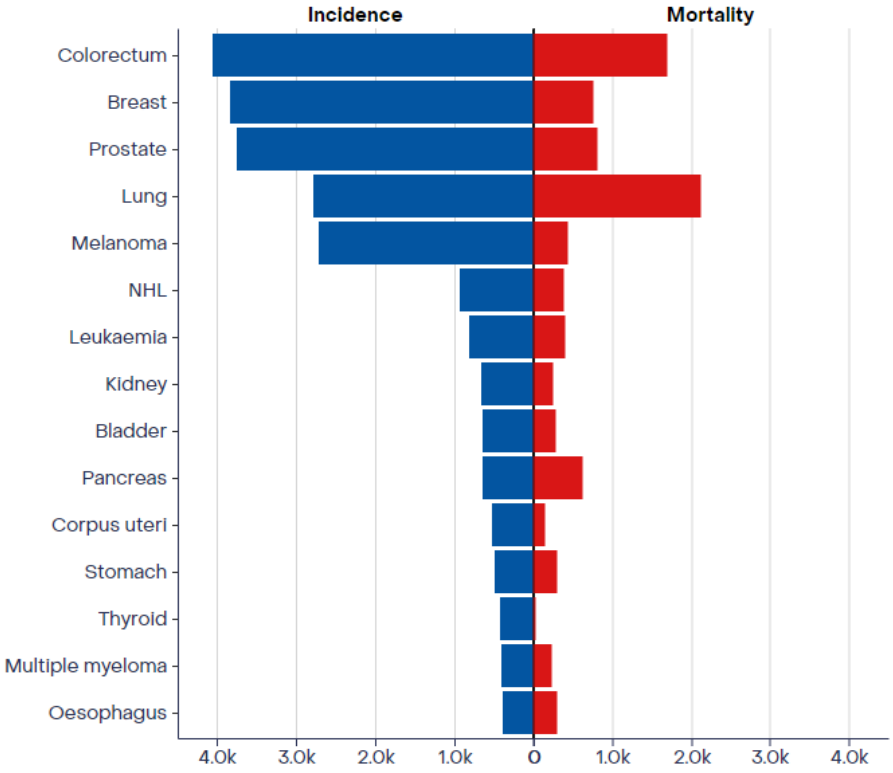

Rates in New Zealand among both sex

Note: Adopted from (The Global Cancer Observatory, 2022)

Figure 1.1. Number of new cancer cases and cancer-related deaths reported in 2022

1.1.2. Prevalence of Colorectal Cancer in New Zealand

According to global cancer records, Oceania had the highest age standardized rates (ASR) in 2022 (The Global Cancer Observatory, 2022) when considering new cases of all cancer forms. Oceania reported an ASR of 409.0, and New Zealand reported an ASR of 427.3.

When considering the data from the New Zealand Cancer Registry and New Zealand Mortality Collection, the Māori reported higher rates of new cancer cases as well as deaths compared to the other prominent ethnic groups in New Zealand (Table 1.1). CRC and other GI cancers are the third most common cause of cancer deaths among Māori and non-Māori males and females reported in the year 2021 and account for 39.9% of all new cancer registrations in NZ. (Health New Zealand, 2023)

Table 1.1. Cancer incidences by prioritized ethnicity in New Zealand in 2021

	Ethnicity	Registrations			Deaths		
		All Sex	Male	Female	All Sex	Male	Female
Number	Māori	3435	1536	1899	1274	605	669
	Pacific	1262	554	708	473	222	251
	Asian	1556	697	859	456	223	233
	European/Other	21616	12137	9479	8285	4516	3769
	Total	27869	14924	12945	10488	5566	4922
Age Standardized Rate per 100,000 (ASR)	Māori	432.2	412.5	452	167	173.1	163.8
	Pacific	383.8	359.1	412.2	149.8	150.2	149.3
	Asian	187	185.3	189.2	57.5	62.3	54.1
	European/Other	346.3	388	309.5	106.4	122.7	93.5
	Total	341.2	369.6	317.5	110.8	125	99.7
Note: Adopted from (Health New Zealand, 2023)							

Table 1.2. CRC Statistics New Zealand 2012 to 2021

Year	Registrations			Deaths		
	All Sex	Male	Female	All Sex	Male	Female
2012	2956	1559	1397	1262	652	610
2013	3022	1602	1420	1223	644	579
2014	3211	1700	1511	1249	637	612
2015	3101	1621	1480	1243	678	565
2016	3167	1637	1530	1268	639	629
2017	3031	1611	1420	1214	669	545
2018	3206	1718	1488	1221	639	582
2019	3327	1735	1592	1213	661	552
2020	3420	1845	1575	1266	671	595
2021	3368	1806	1562	1306	644	662
Note: Adopted from (Health New Zealand, 2023)						

There were 4,070 new Colorectal Cancer patients diagnosed in New Zealand in the year 2022, corresponding to 10.7 % of the total cancer patients diagnosed in that year (38,157). CRC is the

most prominent cancer form detected, while Breast and prostate cancer take second and third place, respectively (The Global Cancer Observatory, 2022). Similar to other developed countries, the number of new cases of CRC and CRC-related deaths in the past ten years were reported to have similar values (Table 1.2), indicating that further measures are needed to increase early-stage diagnosis and effective treatment for metastasis cancer.

1.1.3. Risk Factors

Several factors significantly contribute to increasing the risk of being diagnosed as colorectal cancer patients. It is crucial to identify these factors as it helps the clinical practitioner's early diagnosis of patients and prevent metastasis. The main risk factors contributing to increased CRC incidence and mortality are inherited risk factors, dietary and lifestyle patterns, age, sex, and ethnicity. These factors contribute to increasing the prognosis of colorectal cancer as follows.

1.1.3.1. Hereditary Factors

A family history of colorectal cancer is one of the main factors that increase the risk of developing CRC in relatives. This risk increases if the relative is a first-degree relative, such as parents and siblings, the age at which the relative first developed symptoms, the number of family members recognized with CRC, and the co-occurrence of other forms of abnormalities (Sawicki et al., 2021). Previous studies indicate that the risk is 2.1 times higher than one with no family history, and this risk is 3.7 times higher when the relative is diagnosed with CRC before the age of 45 (St. John et al., 1993). Furthermore, it is stated that 5% to 10% of CRC are developed from hereditary syndromes. The most common are Familial Adenomatous Polyposis (FAP) and hereditary nonpolyposis colon cancer (HNPCC) (Amersi et al., 2005).

1.1.3.2. Inflammatory Bowel Disease (IBD)

The risk of developing colorectal cancer is very high among patients who have been suffering from IBD for many years (Bernstein et al., 2001). The two primary forms of IBD are Ulcerative Colitis and Crohn's Disease. According to previous studies, patients with ulcerative Colitis have a 3.7% higher risk of developing colorectal cancer in the future (Eaden et al., 2001). In contrast,

people with Crohn's Disease have an increased risk of 2.5% of developing CRC in the latter stage of life (Canavan et al., 2006).

1.1.3.3. Colon Polyps

Colon polyps can be either neoplastic or non-neoplastic; hamartomas, hyperplastic, inflammatory, and mucosal polyps come under benign polyps, and adenomatous polyps become mostly malignant (Amersi et al., 2005). Adenoma polyps have three histological variants: tubular, tubulovillous, and villous. 75% to 85% of adenoma polyps fall under the tubular category and have less than a 5% chance of developing into a malignant state. Tubulovillous represents 10% to 15% of adenomas and can become malignant at 20% to 25%. In contrast, the least number of adenomas are of villous form, which is about 5% to 10%, but is the most potent, and about 35% to 40% of these polyps are malignant.

According to previous studies, the cumulative risk of diagnosing colorectal cancer in 5, 10, and 20 years was 2.5%, 8%, and 24%, respectively (Stryker et al., 1987). Furthermore, studies have also demonstrated that early diagnosis and removal of polyps has significantly reduced future incidence of colorectal cancer (Muller & Sonnenberg, 1995).

1.1.3.4. Cholecystectomy

Cholecystectomy is the process of removal of the Gallbladder through surgery. Earlier studies have proposed possible outcomes in changes in the secretion and composition of bile acids in the absence of the bladder. There will be a continuous flow of bile acid, converted to secondary bile acids and producing reactive oxygen and nitrogen species. They will damage colonic epithelial cells, induce DNA damage, and disrupt mitochondria and cell membranes, leading to cancer (Ajouz et al., 2014; Nguyen et al., 2018).

1.1.3.5. Gut Microbiota

A Healthy person relies on a microbiome to absorb nutrients and metabolite and eliminate xenobiotics and drugs. However, the pathogenic microbiome will produce toxic metabolites and induce dysfunction in the gut epithelial barrier, activating proinflammatory cytokinin's, interleukin-6, and tumour necrosis factor-α. Some bacterial species, such as Bacteroides fragilis

and Enterococcus faecalis, produce endotoxins and reactive oxygen species that can cause DNA damage (Saus et al., 2019). It is recommended that a person's diet should be enriched with high fibre, probiotics, polyphenols, and polyunsaturated fatty acids to regulate healthy levels of gut microbiota (Sánchez-Alcoholado et al., 2020).

1.1.3.6. Diabetes Mellitus

Previous studies have indicated that patients who have diabetes have a high risk of being diagnosed with colorectal cancer (Pang et al., 2018; Peeters et al., 2015). Hyperinsulinemia may contribute to colorectal cancer directly by inducing colonic cell proliferation and indirectly by inducing proinflammatory cytokines, interleukin-6, tumour necrosis factor-α and increasing the levels of insulin-like growth factor-1 (Ma et al., 2018).

1.1.3.7. Overweight and Obesity

Obesity is associated with inflammation and tends to increase adipose tissue-derived inflammatory factors such as tumour necrosis factors, insulin-like growth factors, leptin, and adipokines. These compounds promote cell growth and oxidative stress and suppress immune systems. Furthermore, estrogen has a protective function against CRC. Therefore, obese women are less prone to cancer compared to men (Murphy et al., 2019). Earlier studies have demonstrated that there is a significant increase in CRC risk among obese subjects (Abar et al., 2018; Peeters et al., 2015).

1.1.3.8. Physical Inactivity

According to a previous study performed on people 40 years of age, physically active people were less prone to lower digestive system cancer (Keum et al., 2016). In contrast, physically inactive groups are more likely to be diagnosed with cancer. Studies have proven this among groups who spend more time watching television. A study reported that colon cancer risk is 1.54 times higher for television viewers and 1.24 times for occupational sitting time (Schmid & Leitzmann, 2014). Another study reported that 2 hours per day of television viewing was associated with a 1.07 relative risk (95% CI 1.05–1.10, P<.001). In contrast, two hrs. of occupational sitting is associated with a 1.04 risk of developing colorectal cancer (Ma et al., 2017).

1.1.3.9. Dietary Patterns

A diet high in red and processed foods may contain heterocyclic amines, polycyclic aromatic hydrocarbons, and N-nitroso compounds produced during cooking. These and heme present in red meat are known to contribute to carcinogenesis (Keum & Giovannucci, 2019). According to previous studies, western dietary pattern was linked with a 1.25 risk of CRC (95% CI 1.11, 1.40), whereas prudent dietary patterns had a negative correlation (Garcia-Larsen et al., 2019).

Dietary fibre helps easy excretion of faeces limiting the time spent in the colon and, therefore, reducing the exposure time for carcinogens. Furthermore, it aids the actions of microbiota. Studies revealed that 10 g of dietary fibre intake is associated with a reduced risk of CRC. The risk is further reduced to three daily servings (Aune et al., 2011). Furthermore, it is reported that patients who increase their fibre levels by 5 g daily after diagnosis of CRC have an 18% low mortality rate (Song et al., 2018).

High consumption of dairy products, particularly milk, is necessary as it is a source of vitamins and minerals, mainly vitamin D and Calcium. Vitamin D is essential for Calcium homeostasis. Calcium binds to secondary bile acids and ionized fatty acids, limiting its ability to modify the colorectal lumen and reducing its carcinogenic effect. Studies have reported that a calcium intake of 300 mg daily can reduce CRC risk by 8% (Keum et al., 2014).

1.1.3.10. Smoking and Alcohol Consumption

Tobacco smoke contains many carcinogenic compounds such as Nicotine, N-nitrosamines, polycyclic aromatic hydrocarbons, aromatic amines, aldehydes, and metals, which are known to damage DNA and lead to mutations that will generate polyps and lead to adenocarcinoma (Sawicki et al., 2021). A previous study reported that smoking any tobacco has an increased risk of CRC (OR = 1.90, 95% CI: 1.02-3.54) (Cross et al., 2014). Another study reported that the incidence of CRC risk is 1.18 (95% confidence interval [CI], 1.11-1.25) and the mortality rate is 1.25 (95% CI, 1.14-1.37) compared to never-smokers (Botteri et al., 2008).

The intermediate product of ethanol metabolism, acetaldehyde, is a known carcinogen. In addition, genetic polymorphisms may also lead to an increase in the activity of alcohol

dehydrogenase and accumulate acetaldehyde, increasing carcinogenesis (Rossi et al., 2018). A previous study conducted among Japanese men demonstrated that alcohol intakes of 23-45.9 g/day, 46-68.9 g/day, 69-91.9 g/day, and 92 g/day or more significantly increase the risk of CRC incidence concerning alcohol intake. It was reported as 1.42 (95% confidence interval (CI): 1.21, 1.66), 1.95 (95% CI: 1.53, 2.49), 2.15 (95% CI: 1.74, 2.64), and 2.96 (95% CI: 2.27, 3.86), respectively (Mizoue et al., 2008).

1.1.3.11. Age, Sex, and Race

Colorectal cancer symptoms are diagnosed more often among people above 50 years of age. Furthermore, men are more prone to CRC susceptibility as well as deaths compared to women of all age groups. Smoking, alcohol consumption, and hormonal levels such as estrogen are supposed to be the cause of this difference. The median age of diagnosis is 72 for women and 68 for men (Sawicki et al., 2021). According to records, the CRC risk among men is 2.75%, while it is 1.83% among men. Similarly, the mortality rate is 1.14% in men and 0.72% in women (Mattiuzzi et al., 2019). It is reported that 60.4% of CRC cases are between 50 and 74 years of age, and only 10% are below 50. Furthermore, 50% of CRC deaths were between 50 and 74 years old (Morgan et al., 2023).

Colorectal cancer incidence prevalence varies among different races; this may be due to differences in their genetics, lifestyle, and dietary patterns. A previous study has reported that non-Hispanic black had a 50% incidence of early-stage CRC (incidence rate ratios (IRR), 1.5; 95% confidence interval (CI) 1.4–1.6) and 40% incidence of late-stage CRC (IRR, 1.4; 95% CI, 1.3–1.5). Early-stage CRC incidence among Non-Hispanic black women is 60%, and late-stage incidence (IRR, 1.6; 95% CI, 1.4–1.7) is 40% among the same group (IRR, 1.4; 95% CI, 1.3–1.5) (Ellis et al., 2018).

1.1.4. Symptoms and Stages of Colorectal Cancer

The most common symptoms of colorectal cancer are abdominal pain, changes in bowel habits, passing of blood with stools, anaemia, unexplained weight loss, bloating, feeling tired and

vomiting (Sawicki et al., 2021). However, these symptoms may not be visible in the early stage of cancer. Diagnosing at the early stages is crucial as it increases the survival rate. According to data published by the American Cancer Society, the 5-year relative survival rate of localized colon cancer patients is 91% (Stage I, IIA, IIB); in the regional stage, it is 73% (stage IIC and III) and 13% in distant stage (stage IV). Similarly, patients diagnosed with rectal cancer are 90%, 74%, and 18% in localized, regional, and distant stages, respectively (American Cancer Society, 2020). Cancer development can be divided into five stages, from 0 to IV.

1.1.4.1. Stage 0

The abnormal cells are found in the mucosa layer, called Carcinoma in situ. These cells may become cancerous and spread to nearby normal tissue.

1.1.4.2. Stage I

Cancer has formed in the innermost layer of the colon, the mucosa, and spread to the next layer of tissues, the submucosa or even the muscle layer.

1.1.4.3. Stage II

Stage IIA – Cancer spreads through the muscle layer to the outermost layer of the serosa.

Stage IIB – Cancer has spread through the serosa to the tissue lines and the organs in the abdomen.

Stage IIC – Cancer has spread through the serosa to nearby organs.

1.1.4.4. Stage III

Stage III is also subdivided into stages IIIA, IIIB, and IIIC, depending on the number of layers the cancer has spread and the number of lymph nodes it has been involved in.

Stage IIIA - Cancer has spread to the muscle layer and one to three lymph nodes / nearby tissue. Alternatively, the cancer has spread to the submucosa and four to six lymph nodes.

Stage IIIB - Cancer has spread from the mucosa to the visceral peritoneum and one to three lymph nodes or spread until the serosa, and four to six lymph nodes or spread up to the muscle layer and seven or more lymph nodes.

Stage IIIC - The cancer has spread from the mucosa to the visceral peritoneum and four to six lymph nodes or spread to the serosa and seven or more lymph nodes, either spread to the serosa and one or more lymph nodes and spread to nearby tissue or organs.

1.1.4.5. Stage IV

The cancer has spread to other parts of the body through the blood and lymph system and is also known as metastatic cancer.

1.1.5. Diagnosis of Colorectal Cancer

Different diagnostic methods are available for preliminary screening and advanced techniques for further diagnosing the extent of spreading. In addition, other methods are available to detect colon cancer, depending on the location of origin. Furthermore, detection is required during the treatment process to determine the efficiency of the treatment and plan future treatments.

1.1.5.1. Rectal Examination

The rectum is examined for any presence of lumps or abnormality with the help of a lubricated, gloved finger. This initial evaluation of a symptomatic patient cannot be considered a screening test (National Cancer Institute, 2022).

1.1.5.2. Fecal Occult Blood Test (FOBT)

This is used to detect the blood present in stools. However, the presence of blood can be due to cancer, polyps, or other clinical conditions. There are two methods of FOBT. The first method is the Guaiac FOBT, where feces are placed on a guaiac paper. In the presence of Heme, the paper turns into a blue colour. However, this is not specific only to human haemoglobin. The reaction takes place in the presence of food containing peroxidase. Therefore, the patient should avoid uncooked vegetables and red meat three days before the test and avoid non-steroidal anti-inflammatory drugs seven days before. The second is Immunochemical FOBT, which is more sensitive than the Guaiac FOBT as it contains an antibody specific to the human heme group (Granados-Romero et al., 2017).

1.1.5.3. DNA Analysis is faeces.

PCR analysis is performed on the DNA samples present in the stool to identify any mutations in genes (ex, Pancreatic Duodenal homeobox-1/PDX-1, Adenomatous Polyposis Coli/APC, K-ras, and p53 gene mutations) specific for cancer (Hsieh et al., 2005).

1.1.5.4. Carcinoembryonic antigen (CEA) assay

Carcinoembryonic antigen assay is performed on blood samples to detect if the level is higher than the accepted amount, which may indicate colon cancer or other conditions.

1.1.5.5. Sigmoidoscopy

This method uses a thin, tube-like instrument with a light and a lens to view the colon's lowest part. It covers only the rectum and the lower sigmoidal colon for polyps or any abnormality.

1.1.5.6. Colonoscopy

It is a method similar to sigmoidoscopy but can cover the entire colon area; therefore, it is more sensitive.

1.1.5.7. Computed Tomography scan (CT scan)

Multiple X-ray images are taken at different angles using a rotating X-ray tube. The images are processed on a computer using tomographic reconstruction algorithms. Previous studies have used the tomographic images produced from CT scans to differentiate the types of colorectal cancer ex: adenocarcinomas (AC), mucinous adenocarcinomas (MAC), and signet-ring cell carcinomas (SC) (Li et al., 2017).

1.1.5.8. Magnetic Resonance Imaging scan (MRI scan)

This method uses strong magnetic fields to generate images of organs in the body. MRI scan produces images with better contrast of soft tissues and, therefore, can be used to image the abdomen and rectum. The circumferential resection margin (CRM) is the closest distance from the most profound tumour invasion to the surgical margin of the mesentery. It is a crucial factor in the treatment and prognosis of rectal cancer. MRI scans can access the CRM; therefore, it is the primary method for detecting the stage in rectal cancer patients (Torkzad et al., 2010).

1.1.5.9. Positron Emission Tomography scan (PET scan)

Injects a radioactive substance (ex, Fluorodeoxyglucose) into the body, which emits positron and interacts with electrons and annihilates to produce gamma rays, which are detected with gamma cameras and create a three-dimensional image. It allows for capturing metastatic cancer (Gallamini et al., 2014).

1.1.6. Treatments for Colorectal Cancer

Several standard treatments are available depending on the extent of the cancer progression. Furthermore, combinations of treatments are used for cancer in the latter stage. Follow-up treatments are essential to prevent reoccurrence.

1.1.6.1. Surgery

This is the most common treatment for all cancers. However, the type of surgery may differ depending on the cancer stage.

1.1.6.1.1. Local Excision

If the cancer is in an early stage, the clinicians will use the colonoscopy method with a tool to cut the tumour out without cutting through the abdominal wall (Nivatvongs, 2000). If this technique is used to cut a cancer found in a polyp, this method is called polypectomy.

1.1.6.1.2. Anastomosis

This method is used when the can is spread to a much larger area. The area around the cancer is cut, and the end of the remaining colon is joined. Colorectal anastomotic leak is one primary concern in this method (Ho & Ashour, 2010).

1.1.6.1.3. Colostomy

In situations where the end join is not possible following the colectomy, the ends of the colon are left open (stoma), and a colostomy bag is used to collect the secretions. This colostomy can be permanent or temporary until the colon is healed (Maria & Lieske, 2020).

1.1.6.2. Cryosurgery

This method uses extremely low temperatures to destroy cancer cells and is mainly used in the metastasis stage (Ravikumar et al., 1997).

1.1.6.3. Radiofrequency ablation

In this method, a current is generated through radio waves and directed to the tumour using a needle via the skin or through surgery. The current increases the temperature to 50-100 ^{0}C degrees, leading to tumour coagulation and necrosis (Cirocchi et al., 2012).

1.1.6.4. Radiation Therapy

This treatment uses ionization radiation to destroy cancer cells. This high-energy radiation damages the genetic material, Deoxyribonucleic acid (DNA) of cells and prevents them from dividing and proliferating. This therapy combines other treatments, such as surgery, chemotherapy, and immunotherapy. If applied before surgery, its purpose is to shrink the tumour; if applied after surgery, it destroys the leftover tumour residues. Two methods are used to deliver this radiation. The most common method is external beam radiation, where high-energy radiation targets the tumour location from outside the body. The second method is internal radiation, also known as brachytherapy, where the radioactive sources are directed to the tumour site using a sealed catheter (Baskar et al., 2012).

The drawback of this method is that it affects both cancer and normal cells. However, normal cells have a higher ability to repair themselves and retain their functions. Advanced techniques have been developed to produce higher doses, penetrate deeper skin, and minimize side effects. Some of these techniques are Intensity-modulated radiation therapy (IMRT), Image-guided radiotherapy (IGRT), 3D Conformal radiotherapy (3DCRT), Stereotactic body radiation therapy (SBRT), and Cone beam computer tomography (CBCT) (Abshire & Lang).

1.1.6.5. Targeted Therapy

In targeted therapy, monoclonal antibodies target cellular compounds produced specifically from cancer cells. Therefore, this treatment will target only the cancer cells and reduce the impact on normal cells. During cancer, the immune system is highly affected. Thus, antibodies are designed

to target immune checkpoints. “Lpilimumab” is used to target cytotoxic T lymphocyte-associated antigen-4 (CTLA-4), and “Pembrolizumab” targets programmed cell death protein (PD-1), which activates T cells and kills the tumour cells (Zahavi & Weiner, 2020).

Some monoclonal antibodies target molecules over-expressed in cancer cells. (i) Alemtuzumab targets CD52, overexpressed in malignant lymphocytes, granulocytes, macrophages, and natural killer cells, and is approved as a treatment for lymphocytic leukaemia. (ii) Bevacizumab binds to vascular endothelial growth factor (VEGF). It blocks its binding to the VEGF receptor, inhibiting the formation and growth of blood vessels and restricting the growth of tumours. (iii) Panitumumab and Cetuximab bind to the Epidermal growth factor (EGF) receptor and prevent the division and growth of cancer cells (Scott et al., 2012). In addition, monoclonal antibodies labelled with isotopes are used for selective radiation delivery to cancer cells to treat cancers unresponsive to other treatments and to determine the extent of cancer spread (Pento, 2017).

1.1.6.6. Chemotherapy

New Zealand and international clinical practice guidelines, based on robust evidence from randomised controlled trials, now recommend oxaliplatin-based chemotherapy as the preferred regimen for the treatment of metastatic colorectal (National Comprehensive Cancer, 2009) and other GI cancer (Lordick et al., 2022) types. This treatment uses cytotoxic chemicals to reduce or eradicate the tumour, reduce symptoms, and increase survival. Chemotherapy is mainly done intravenously but can also be administered orally. In some instances, if the cancer is developed only in a particular region, the chemotherapy is administered only to the affected area, e.g., the abdominal cavity or cerebrospinal fluid. Each cytotoxic drug has its mechanism of action; therefore, a combination of drugs is commonly administered to increase efficiency.

Alkylators and alkylator-related agents bind to macromolecules such as DNA and interrupt gene expression and cell division. Platinum drugs, too, act in the same way, e.g., Oxaliplatin. Antimetabolites have mechanisms similar to normal molecules and, therefore, replace the normal molecules in DNA and RNA synthesis and disturb the function, e.g., Fluorouracil and Methotrexate. Topoisomerase inhibitors disrupt the function of topoisomerase. Topoisomerases are essential for DNA replication and repair. This inhibition leads to permanent breaks in DNA,

e.g., Doxorubicin. Microtubule-interacting agents interrupt the cellular cytoskeleton. Cell structure is necessary for molecule transportation, cell division, and adhesion. Disruption of cell structure leads to loss of function and growth arrest, e.g., docetaxel.

However, chemotherapy drugs develop resistance. Many factors are affecting, and the function of multi-drug resistant proteins is crucial. Therefore, measures are needed to overcome this challenge (Nygren, 2001).

1.2. Multi-Drug Resistance

Although oxaliplatin-based chemotherapy has been widely adopted as the standard and preferred regimen for treating many types of GI cancer, its dose-limiting toxicities and tumour resistance are major limitations for many patients in clinical practice. In a New Zealand clinical study, more than 40% of patients receiving chemotherapy including oxaliplatin stopped that chemotherapy early due to either severe toxicity or lack of efficacy (Jackson et al., 2015). Chemotherapeutic regimens induce a short-lived response in many GI cancer patients whose tumours progress and developed multi-drug resistance (MDR). Accumulating evidence suggests that ATP-binding cassette (ABC) proteins mediated tumour resistance represents one of the most common causes of MDR (Robey et al., 2018).

1.2.1. Multi-Drug Resistant Proteins (MRP)

Multi-drug resistance is one of the curial phenomena responsible for chemotherapeutic resistance in cancer treatments and is an area that needs further understanding and development to combat cancer. ATP-binding cassette (ABC) proteins are a large family that is responsible for active transmembrane transport of a wide range of substances, including inorganic anions, peptides, sugars, metal ions, amino acids, hydrophobic compounds, metabolites, and play a prominent role in maintaining homeostasis. Forty-eight protein-coding genes and one pseudogene correspond to ABC protein synthesis in humans. This family is divided into seven subfamilies named from ABCA to ABCG based on their amino acid sequence similarities (Dvorak et al., 2017).

The ABCC subfamily is also called the Multi Drug Resistant proteins (MRP), as nine (9) of its members are primarily involved in drug resistance. Overexpression of these proteins in cancer cells leads to the efflux of endogenous substances and resistance to xenobiotics. The ABCC7/ Cystic Fibrosis Transmembrane Conductance Regulator (CFTR), ABCC 8/ Sulfonyl Urea Receptor 1 (SUR1), and ABCC9/ Sulfonyl Urea Receptor 2 (SUR2) do not confer multi-drug resistance (Sodani et al., 2012). The symbol, alternate name gene accession number, chromosomal location, protein accession number, number of amino acids, and their similarity percentage with respect to MRP1 are compared in Table 1.3.

Depending on their topology, these nine main multidrug-resistant proteins can be classified into two groups. Group one, named the "short" MRP, has the typical ABC structure with two membrane-spanning domains (MSD1 and MSD2), and in between are the two nucleotide-binding domains (NBD1 and NBD 2). MRP 4, 5, 8, and 9 fall under this group. MRP 1,2,3,6 and 7 come under the "long" group, which has additional membrane-spanning domains (MSD0) at the amino-terminal. MSD 1 and MSD2 are composed of 6 transmembrane α-helices through which the substrates cross the membrane, and the two NBDs form a sandwich-dimer in a head-to-tail formation. Each MRP is located either apical or basolateral in the membranes and has a different tissue distribution. Therefore, they can transport structurally diverse molecules and show limited substrate overlapping (Chen & Tiwari, 2011).

Table 1.3. Summary of ABCC subfamily members

Symbol	Alternate name	Gene accession number	Chromosomal localization	Protein accession number	Amino acids	Amino acid Identity (%)
ABCC1	MRP1	NM_004996	16p13.1	NP_004987	1531	100
ABCC2	MRP2	NM_000392	10q24	NP_000383	1545	50
ABCC3	MRP3	NM_003786	17q22	NP_003777	1527	58
ABCC4	MRP4	NM_005845	13q32	NP_005836	1325	41
ABCC5	MRP5	NM_005688	3q27	NP_005679	1437	38
ABCC6	MRP6	NM_001171	16p13.1	NP_001162	1503	46
ABCC7	CFTR	NM_000492	7q31.2	NP_000483	1480	30
ABCC8	SUR1	NM_000352	11p15.1	NP_000343	1581	36
ABCC9	SUR2A	NM_005691	12p12.1	NP_005682	1549	35
ABCC9	SUR2B	NM_020297	12p12.1	NP_064693	1549	36
ABCC10	MRP7	NM_033450	6p12.1	NP_258261	1492	35
ABCC11	MRP8	NM_033151	16q12.1	NP_149163	1382	33
ABCC12	MRP9	NM_033226	16q12.1	NP_150229	1356	36
Note: Adopted from (Fromm & Kim, 2010)						

1.2.2. MRP 7/ABCC10

There is increasing evidence that ABCC10 contributes to drug resistance and tumour development. *ABCC10* gene, initially discovered in 2001 by Hopper et al., is located in chromosome 6p12. ABCC10 cDNA codes for 1492 amino acids and synthesizes a protein named ABCC10 with a molecular weight of around 158 kDa. In the same study, signals were observed when RT/PCR analysis was conducted in samples obtained from the skin, testis, spleen, stomach, colon, kidney, heart, and brain. However, no apparent signals were detected in RNA blot analysis on the same tissue samples, indicating that the expression of ABCC10 is low in these tissues (Hopper et al., 2001). In another study, a splice variant of human ABCC10 is described, which has a 15 amino acid deletion between the second membrane-spanning domains and the second nucleotide-binding domain, which is recognized as MRP7A (Kao et al., 2003).

1.2.2.1. Single Nucleotide Polymorphisms in *ABCC10* gene

Two single nucleotide polymorphisms (SNP) are observed in the *ABCC10* gene. The first is rs9349256, located in intron 4, and the second is rs2125739 in exon 12. The mutation in the exon leads to an amino acid change of Ile920Thr, which leads to a change in ABCC10 expression. The minor allele frequency of rs2125739 varies in different populations. It is 26.7% among Northern and Western Europeans, 34.2% among Sub-Saharan Africans, and 3.4% among Han Chinese (Pushpakom et al., 2011).

1.2.2.2. Physiological substrates and inhibitors of ABCC10

In a previous study (Chen et al., 2003), a ATP-dependent transport of 17β-estradiol-(17-β-D-glucuronide) (E217βG) were observed in human embryonic kidney cells (HEK 293) overexpressing ABCC10 but not in parental HEK293 cells. Further analysis of kinetics data unravels E217βG is an ABCC10 substrate with Km and Vmax values of 57.8 ± 15 μM and 53.1 ± 20 pmol/mg/min. Leukotriene C4 (LTC4) also exhibited to a lesser extent. However, substrates of other MRP family members were not transported by ABCC10, demonstrating its substrate selectivity. Furthermore, E217βG transportation was inhibited entirely by amphiphiles, such as leukotriene C4, glycolithocholate 3-sulfate, and MK571, and lipophilic agents such as

cyclosporine A. These findings proved that ABCC10 is a lipophilic anion transporter (Chen et al., 2003).

1.2.2.3. ABCC10 mediated drug resistance

As a recently discovered member of the MRP family, limited data is available on the drug-resistant profile of ABCC10. Studies conducted on MPR7 transfected HEK 293 cells have demonstrated a higher resistance level towards the taxanes group drug "Docetaxel." Interestingly, ABCC10 is the only member of the long MRP family that has been reported to confer resistance towards "Docetaxel." MRP1, MRP2, MRP3, and MRP6 have not been reported to confer drug resistance towards taxane family drugs. The ABCC10 transfected HEK293 cells had the highest resistance towards docetaxel, followed by paclitaxel, vincristine, and vinblastine (Hopper-Borge et al., 2004).

Further studies have demonstrated that ABCC10 confers resistance to nucleoside-based agents, cytarabine and gemcitabine. Furthermore, it transport other cancer drugs, such as daunorubicin and epothilone B (Hopper-Borge et al., 2009). A study conducted in the same lab demonstrated that embryo fibroblasts derived from ABCC10-knockout ($ABCC10^{-/-}$) mice developed hypersensitivity towards paclitaxel, docetaxel, vincristine, and cytarabine, which is associated with cellular accumulation of ABCC10 drug substrates compared with WT controls (Hopper-Borge et al., 2011). In addition, mice treated with paclitaxel developed neutropenia-associated toxicity in bone marrow, as well as toxicity in the thymus and spleen. Therefore, it suggests that ABCC10 transporter (ABCC10) plays a crucial role in anticancer drug resistance in vivo (Hopper-Borge et al., 2011).

1.2.2.4. Synthetic inhibitors of MRP7 / ABCC10

As discussed above, ABCC10 confers resistance to many anticancer drugs, preventing its function and aiding cancer cell proliferation and mortality. Therefore, mechanism based ABCC10 inhibitors are desired to reverse drug resistance. The function of ABCC10 inhibitors is to bind to the transporter and block the channel. This will lead to drug substrate accumulation in the cancer cells and increase DNA damage, leading to inhibition of metabolism, cell cycle arrest, and finally, cancer cell death, which stops proliferation and improves survival rate.

Researchers are attempting to develop compounds that are potential inhibitors of ABCC10. Cepharanthine, an herbal extract isolated from Stephania cepharantha Hayata, has successfully reversed the drug resistance towards paclitaxel of HEK293 cells transfected with ABCC10 (Zhou et al., 2009). Similarly, it has been reported that the tyrosine kinase inhibitors imatinib and nilotinib could also reverse the drug resistance of ABCC10 towards paclitaxel. However, the western blotting analysis showed that the ABCC10 expression was not significantly affected (Shen et al., 2009).

Furthermore, in the presence of epidermal growth factor receptor inhibitors, lapatinib and erlotinib, the sensitivity towards docetaxel, paclitaxel, vinblastine, and vinorelbine was increased in ABCC10-transfected HEK293 cells but not in parental HEK293 cells. Lapatinib was a more potent ABCC10 inhibitor compared to Erlotinib. Therefore, it proves that combinational therapy can overcome drug resistance and increase the efficiency of chemotherapy (Kuang et al., 2010).

In addition, phosphodiesterase type 5 inhibitors, sildenafil and vardenafil too enhanced the sensitivity of paclitaxel, docetaxel, and vinblastine in HEK 293 cells transfected with ABCC10 but not in parental HEK293 cells (Chen et al., 2012). Similarly, a third-generation ABCB1 inhibitor, tariquidar, was able to increase the sensitivity of paclitaxel, docetaxel, vincristine, vinblastine, and vinorelbine (Sun et al., 2013). Furthermore, in the presence of FMS-like tyrosine kinase 3 inhibitor, tandutinib, the sensitivity of paclitaxel and vincristine has increased in ABCC10-transfected HEK293 cells but not in parental HEK293 cells (Deng et al., 2013). Therefore, combining chemotherapy with an ABCC10 inhibitor is a promising strategy to overcome drug resistance and improve therapeutic efficacy.

1.3. Docetaxel

1.3.1. History of Docetaxel Development

The first taxane was extracted from the bark of the Pacific yew or western yew tree (*Taxus brevifolia*). It was supplied to Dr. JonathanL Hartwells' lab in 1964 by the National Cancer Institute from the collection of Botanists Arthur S. Barclays 650 plant samples collected from

bark, twigs, leaves, and fruit of *Taxus brevifolia* from Washington State in August 1962 (Wall & Wani, 1995).

The plant was extracted in Dr. Hartwells' lab, and its crude was obtained in 1964 following a laborious process. Next, the name "taxol" was given, and its structure was deduced in 1971 in the same lab (Wani et al., 1971). Furthermore, it was evident that the extracts had antitumor activity against leukaemia, melanoma and several *in vivo* rodent assays (Wall & Wani, 1995).

In 1979, the mechanism of action of taxol was identified by Dr. Susan B. Horwitz and her group (Schiff et al., 1979). From 1982 to 1994, there was a rapid development in chemical synthesis and clinical trials of taxol (Table 1.4).

In 1991, the Cancer Institute conducted a competition, and the Cooperative Research and Development Award was issued to Bristol-Myers Squibb, which filed a Food and Drug Administration (FDA) approval for marketing a New Drug and received the application to trademark Taxol in December 1992 (Wall & Wani, 1995).

Table 1.4. Chronology of Taxol Development

Event	Year
Structure Determination	1971
Antitumor Activity	1975 - 1976
Preclinical Development	1977
Mechanism of Action	1979
Animal Toxicology	1982
Phase I Clinical Trials	1983 – 1984
Phase II Clinical Trials	1985 – 1986
Synthesis of Taxol side chain	1986
Semi Synthesis of Taxol	1988
Improved Synthesis of Taxol Side Chain	1990 - 1993
Food and Drug Administration Approval	1992
Total Synthesis of Taxol	1994
Note: Adopted From (Wall & Wani, 1995)	

However, as Taxol (Paclitaxel) was derived from an exhaustible sauce, there was a need to develop a similar drug from a synthetic method. Therefore, in 1981, a French Chemist, Pierre Potier, developed Taxotere (Docetaxel) semi-synthetically by esterifying 10-Deacetylbaccatin III obtained from the needles of *Taxus Baccata*, a European yew tree. Clinical trial phase I studies of docetaxel were initiated in 1990, and phase II studies were conducted in 1992. Docetaxel was further developed by an American Chemist, Robert. A. Holton. FDA approval was obtained to

treat breast cancer in 1996, non-small-cell-lung cancer in 1999, metastatic hormone-refractory prostate cancer in 2004, and head and neck cancer in 2006. Currently, new formulations are undergoing to improve the efficiency of the drug and targeted drug delivery (Ojima et al., 2016).

1.3.2. Structure of Docetaxel

The chemical formula of docetaxel is C43H53NO14; it has an anhydrous molecular weight of 807.9 g/mol, and the weight of the trihydrate form ($C_{43}H_{53}NO_{14}.3H_2O$) is 861.9 g/mol (Clarke & Rivory, 1999).

Docetaxel has the main taxane ring to which a four-membered oxetane side ring is attached at carbon 4 and 5; in addition, at carbon 13, there is a bulky ester side chain attached, which plays a central role in its anti-tumour function (Figure 1.2). Both docetaxel and paclitaxel have the above-mentioned main taxane structure, explaining their similarity in function. However, it differs in only two positions, leading to a slight change in their functionality. In Paclitaxel, an acetyl group is attached to Carbon 10, which is replaced by a hydroxyl group in docetaxel, making it more hydrophilic (Fauzee et al., 2011). In addition, the 3' position on the lateral carbon 13 is attached to a benzamide group in Paclitaxel, whereas it contains a tert-butyl carbamate in docetaxel.

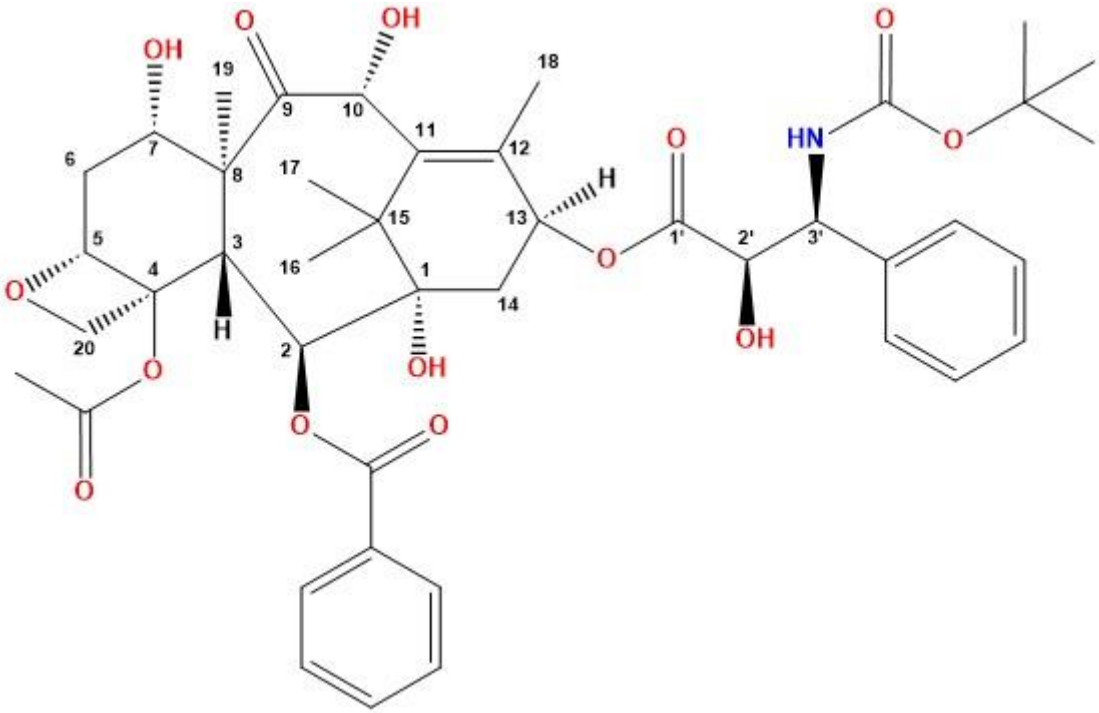

Figure 1.2. Structure of Docetaxel
Note: Adopted from PubChem

1.3.3. Mechanism of Action

Taxanes have a mechanism of action different from all other anti-cancer drugs, which is called hyper-stabilization of microtubules. Taxanes bind to microtubules and stabilize them, while vinca alkaloids and colchicine inhibit microtubule polymerization (Montero et al., 2005). The bulky ester side chain at C-13 is essential for binding the β-subunit of the tubulin heterodimer. The microtubules produced by docetaxel are larger than the tubules made by paclitaxel. Furthermore, docetaxel binds more strongly to the tubulin and retains it longer (Vaishampayan et al., 1999). The taxanes stabilize the microtubules in a guanosine triphosphate (GTP) independent manner, disrupting the physiological disassembly of microtubules and arresting the cell cycle at the metaphase/anaphase boundary. This affects the mitotic spindles and inhibits cell division and chromatic separation, leading to cell death. These drugs are mitotic inhibitors and cause frozen mitosis, often called “mitotic Poisons” (Fauzee et al., 2011).

1.3.4. Clinical Uses

In human and mouse studies, docetaxel has proven anticancer activity against a broad range of cancers, both in vitro and in vivo. Docetaxel displayed cytotoxicity in murine embryonic cells (SVras) and leukaemia (P388) as well as human epidermoid carcinoma (KB), small cell lung carcinoma (N417), colon adenocarcinoma (HCT116), bladder carcinoma (T24) and breast carcinoma (Calc18) cell lines. Furthermore, docetaxel displayed 1.3 to 12 times more potency than paclitaxel (Riou et al., 1992).

In in vivo studies, docetaxel antitumor activity was tested against several transplantable tumours in mice. Following IV administration of docetaxel B16 melanoma (B16), pancreatic ductal adenocarcinoma 03 (P03) and colon adenocarcinoma 38 (C38) were reduced significantly. In the same study, Lewis lung carcinoma (3LL), Glasgow osteogenic sarcoma (GOS), lymphoid leukaemia (L1210), and lymphocytic leukaemia (P388) responded to a lesser extent (Bissery et al., 1991).

Docetaxel has produced promising results at higher doses as well as lower doses. Previous studies have demonstrated that low-dose metronomic therapy (LDM) is cytotoxic to proliferating

endothelial cells and inhibiting tumour vasculogenesis (Muta et al., 2009). Therefore, LDM therapy may still show activity even after tumours have become taxane-resistant.

During phase I, II, and III clinical trials, docetaxel demonstrated a positive effect on patients diagnosed with several cancer types when administrated alone or in combination with other anticancer drugs. Lung cancer is one of the most prevalent and non-operable diseases. Many studies provide evidence for a positive response for docetaxel among patient groups suffering from non-small cell lung cancer as well as small cell lung cancer. A phase II study administered docetaxel for 29 patients with unresectable stage III and IV Non-small cell lung cancer at a dose of 100 mg/m2 intravenously (IV) over 1 hour every 21 days. The primary objective response was observed among 38%, and the median duration of response was 5.3 months (P. A. Francis et al., 1994). Another study displayed a similar response rate where 33% achieved partial response during 14 weeks (Fossella et al., 1994). The same dose was administered to 34 patients with small cell lung cancer, and 25% reported a partial response rate; the duration of response was 3.5 to 12.6 months (Smyth et al., 1994).

Docetaxel is a prominent drug used to treat breast cancer. It is very active, and some patients demonstrate complete response during clinical trials. Docetaxel is administered to cancer patients who are previously untreated, as well as those who have previously undergone treatments such as surgery, radiotherapy, and other chemotherapy. There are several studies demonstrating the efficacy of docetaxel. A study by the EORTC (European Organization for Research and Treatment of Cancer) Early Clinical Trials Group administered docetaxel 100 mg/m2 every three weeks as a 1-hour infusion. In this study, 24 patients were treated as second-line therapy; 13 achieved partial remission, and 1 achieved complete remission (overall response rate 58%). Eight patients were treated as first-line therapy; 2 achieved partial response, and 1 achieved complete response. The median response duration was 38 weeks (ten Bokkel Huinink et al., 1994). Another study demonstrated that in phase II trials, the overall response rate was 73% in patients receiving docetaxel as first-line therapy. In contrast, the rate was 38% in patients receiving it as second-line therapy (Eisenhauer & Trudeau, 1995). Furthermore, docetaxel seems to be superior to paclitaxel in breast cancer treatment. In a phase III study with 449 patients, 225 patients were randomly

assigned to receive 100 mg/m^2 docetaxel, and 225 patients were randomly assigned to receive 175 mg/m^2 paclitaxel. Both the overall survival rate and median time to progression were higher among the group who received docetaxel (Jones et al., 2005).

Another most common cancer that is treated with docetaxel is ovarian cancer. In four phase II trials, which study 340 ovarian cancer patients treated with docetaxel 100 mg/m^2 as 1-hour infusions every three weeks, previously treated with cisplatin or carboplatin therapy, the overall response rate was 30%. Among the patients who were once resistant to treatments, the response rate was 28%. Response duration was 4 to 17 months (Kaye et al., 1997). Another study selected 97 patients who had disease relapse or disease progression within 12 months from platinum-based first-line or second-line therapy and injected the same dose of docetaxel as mentioned above. The overall response rate was 23.5 % whose tumour progressed in the most recent platinum treatment. The median progression-free period was 3.9 months, and overall survival was 8.4 months (Piccart et al., 1995). A similar response was observed among another study group that had administered docetaxel to patients who were already resistant to platinum-based drugs. 35% observed partial response, and the median response duration was five months (P. Francis et al., 1994). Therefore, treatment with docetaxel is a solution to overcome platinum resistance among ovarian cancer patients.

Prostate cancer is one of the leading causes of death among men. Mitoxantrone is one of the main treatments provided along with prednisone. This combination has been able to reduce pain and increase quality of life. However, the survival rate still needs to be improved. When combined with prednisone, docetaxel has a higher survival rate than Mitoxantrone. One thousand six men treated with 5 mg of prednisone twice daily were randomly divided into three groups and administered either 12 mg/m^2 of Mitoxantrone every three weeks, 75 mg/m^2 docetaxel every three weeks or 30 mg/m^2 docetaxel weekly until six weeks. The median survival was 16.5 months, 18.9 months, and 17.4 months, respectively. The predefined pain reduction was 22%, 35%, and 31%, respectively. Furthermore, the improvement in quality of life was 13%, 22%, and 23%, respectively, suggesting the docetaxel treatment every three weeks in combination with prednisone gave the best overall expected outcome (Tannock et al., 2004). Another study

compared two groups of men with androgen-independent prostate cancer; the first group was administered 60 mg of Dexamethasone, 60 mg/m2 docetaxel, and 280 mg of Estramustine, and the second group was administered 12 mg/m^2 of Mitoxantrone and 5 mg of prednisone. The first group had a median survival of 18 months, whereas the second group had 15 months. Furthermore, the median progression time was six months and three months, respectively. The response rates were 17% and 10%, respectively, which too proved that docetaxel is a better treatment for patients with androgen-independent prostate cancer (Petrylak et al., 2004).

Squamous cell carcinoma of the head and neck (SCCHN) is another malignancy which docetaxel treats. In a study, 31 patients were treated with 100 mg/m^2 as a 1-hour infusion every three weeks. 13% demonstrated a complete response, and 29% had a partial response. The duration of response was from 2 to 14 months (Dreyfuss et al., 1996). In another study, the same dose was given to 43 patients. Of them, ten had a partial response, and two yielded complete responses confirming the use of docetaxel against SCCHN (Catimel et al., 1994). Docetaxel is responsive against metastatic melanoma, too. Docetaxel was administered 100 mg/m^2 as a 1-hour infusion every three weeks to 37 patients with no prior chemotherapy. One complete and one partial response was observed (Einzig et al., 1996). When the same dose was administered to 29 patients with metastases of soft tissue sarcomas, 5 had a partial response (17%, C.I. 6%-36%) (van Hoesel et al., 1994). Docetaxel displayed less activity against renal carcinoma. Only one of the twenty patients in the phase II trial demonstrated a mixed response (Mertens et al., 1994). Similar results were obtained in another study group, confirming its less activity towards renal carcinoma (Bruntsch et al., 1994). Docetaxel displays a desirable response against pancreatic adenocarcinoma. In the phase II study, 40 patients were treated with 100 mg/m^2 as a 1-hour infusion every three weeks. 6% had a partial response, and 38% displayed stable disease conditions. The median duration of response was 5.1 months, and the median pain control time was 4.5 months (Rougier et al., 2000).

Docetaxel is an active agent against advanced gastric cancer. In a phase II study, 33 patients were treated with 1-hour infusions of 100 mg/m2 docetaxel every three weeks; the dose was reduced as necessary. Eight of the evaluable patients achieved partial remission during a median of 7.5 months. In addition, 11 patients developed stabilization of the disease (Sulkes et al., 1994). In a

phase II study, 75 mg/m2 docetaxel combined with 75 mg/m2 cisplatin and 750 mg/m2 fluorouracil (DCF) every three weeks shows a more desirable effect in advanced gastric cancer patients. Four hundred forty-five patients were randomly assigned to be treated with DCF or 75 mg/m^2 cisplatin and 750 mg/m^2 fluorouracil (CF) every four weeks. The group that received DCF treatment exhibited a longer time to progression than the CF group. The two-year survival rate was 18% in DCF and only 9% among the CF group (Van Cutsem et al., 2006). Meta-analysis studies further confirm these results (Li et al., 2019).

However, when administered in the normal phase II dose, 1-hour infusions of 100 mg/m^2 docetaxel every three weeks display limited activity towards colorectal cancer. Of thirty-three evaluable patients treated, only one achieved a complete response, and two achieved a partial response (Sternberg et al., 1994). A similar pattern was obtained in other studies, too (Clark et al., 1998; Pazdur et al., 1994). However, it displayed promising results in animal studies and in vitro studies. Therefore, further measures should be taken to enhance the effect, such as varying the dose, testing the combination of drug treatments, and moving on to advanced methods such as genetic modifications.

1.3.5. Pharmacokinetics of Docetaxel

Docetaxel displays linear pharmacokinetics when administered between 20 mg/m2 and 115 mg/m^2. Therefore, the area under the curve increases with increasing dose. The plasma clearance was biexponential at lower concentrations (Concentrations below 70 mg/m2), and at higher concentrations, it displayed a triexponential curve with three half-lives α, β, and γ, and for concentration 115 mg/m2; it was reported as 5 minutes, 60 minutes, and 10 to 18 hours respectively. The mean terminal half-life was recorded as 13.5±7.5 h, the plasma clearance was 21.2±5.3 liters/h/ m2, and the distribution volume was 72±40 $litres/m^2$ (Extra et al., 1993).

The pharmacokinetic models' studies using paediatrics demonstrated a bicomponent model with a distribution half-life of 0.09 hours and an elimination half-life of 1.4 hours. The plasma clearance was higher than adults and was reported as 33 liters/h/ m^2 (Clarke & Rivory, 1999).

1.3.5.1. Metabolism of Docetaxel

Due to its low solubility during intravenous administration, docetaxel is formulated with pharmaceutical vehicles, and in recent years, it has mostly been polysorbate 80. About 98% of docetaxel within the body is protein-bound, mainly serum albumin, lipoprotein, and α1-acid glycoproteins. The concentration of α1-acid glycoproteins varies among patients, and this could contribute to the varied amount of free docetaxel observed in cancer patients. A meagre percentage is associated with erythrocytes, and the majority is present in the plasma component of blood. Also, it is reported that the drugs co-administered will not modify the plasma binding of docetaxel (Urien et al., 1996).

Docetaxel distribution is evident in many tissues and was observed at the highest level in the liver, bile duct, and intestine. However, a limited amount is presented among the central nervous system and testis. The brain is protected from taxane thanks to efflux by P-glycoproteins at blood-brain barriers. The exposure to docetaxel is higher in tumour tissues than in other tissues, but peak tumour levels are low. However, as the elimination from tumour tissues is low, the area under the curve is about five-fold higher than in plasma (de Weger et al., 2014). As it has low solubility, oral administration of docetaxel is limited. Furthermore, orally administrated docetaxel is extensively excreted from the intestine by P-glycoproteins, metabolized by CYP3A enzymes. Preclinical studies have demonstrated that oral co-administration of docetaxel with a CYP3A inhibitor, ritonavir, has increased the plasma docetaxel level by 50-fold. However, intravenous and oral administration displayed similar tissue distribution and plasma protein binding.

Docetaxel is mainly metabolized by the hepatic cytochrome P450-3A subfamily of isoenzymes (CYP3A) to inactive metabolites. Around 70-80% of dosed docetaxel is excreted through hepatic clearance into bile by P-glycoproteins and MRP2 transporters as metabolites or parent drugs and passes through faeces. Renal clearance is only about 5-10%, whereas excretion through breath is not detected. It cleared entirely after seven days, and most recovered within the first two days.

Metabolism mainly occurs in the C-13 side chain, tert-butyl carbamate, where M2 is formed by oxidation of one side chain methyl group. Next, the unstable aldehyde and acid, intermediates of

the alcohol, are spontaneously cycled to form diastereoisomers M1 and M3 and a ketone metabolite M4 (Royer et al., 1996).

The metabolites of docetaxel showed minimal cytotoxic activity (Sparreboom et al., 1996). Docetaxel is the preferred drug for older adults with renal disease and impaired creatinine clearance as it has limited usage of renal clearance. However, the dose must be altered when treating patients with hepatic dysfunction as the docetaxel is mainly metabolized via the liver. The clearance rate is reduced from 12- 27% among patients with elevated liver enzymes. Therefore, this population's recommended dose is reduced to 75 mg/m^2 over a 1-hour infusion (Clarke & Rivory, 1999).

1.3.6. Toxicities related to Docetaxel

Neutropenia was the most common dose-related toxicity observed in all studies. Several other side effects also occur depending on the duration of the infusion and dosage. In the phase one study with a five-day schedule, 1 mg/m^2 docetaxel was infused continuously for five consecutive days. This process was repeated every three weeks, and the dose was increased each time. Initially, the dose was increased by 100% until biological activity was detected. At this stage, the dose is increased by 50% until grade 2 toxicity is observed; subsequently, the dose is increased by 25% until the maximum tolerated dose. Granulocytopenia and concurrent mucositis were observed starting at 12 mg/m^2. However, different patients began to develop toxicities at different doses. The area under the curve for plasma concentration and duration of exposure was directly correlated with neutropenia. Therefore, dose modification is recommended according to the AUC reported on the first day of the treatment (Pazdur et al., 1992).

Other toxic signs are visible when the infusion lasts longer than 1 hour. One study compared infusion doses of 100 mg/m^2 for 2 hours and 115 mg/m^2 for 6 hours, repeated every three weeks. Alopecia was observed in this study, which was absent in the previous study, with lower doses administered in less time. The transient rash was observed in both groups but was more common in 2-hour infusions, whereas Mucositis was more common among 6-hour infusions. Hypersensitivity reactions were visible only among some patients (Burris et al., 1993). Another

study treated 110 mg/m^2 for 1 hour on days one and eight. It repeated the process every three weeks, displayed neutropenia, alopecia, and hypersensitivity reactions, and, in addition, showed asthenia, skin toxicity, and edema. Furthermore, paresthesia aggravated in patients with preexisting history, and new sensory symptoms developed in others (Tomiak et al., 1994). Another study that tested 5 - 115 mg/m^2 doses during 1-2 hour infusions observed alopecia and delayed cumulative skin reaction doses above 70 mg/m^2 (Extra et al., 1993). However, neither cardiac nor neurotoxicity were observed in the above studies. Acute hypersensitivity reactions could be controlled by pretreatment of 32 mg of methylprednisolone, 10 mg of cetirizine, and 1 mg of ketotifen. Furthermore, skin toxicity is reduced with ointments of chlorhexidine and glycerin (Schrijvers et al., 1993).

1.3.7. Limitations and Future Perspectives

Patients must visit the hospitals regularly as the pharmaceutical excipients cause hypersensitive reactions. Therefore, new formulas should be developed for intravenous administration with the same anticancer activity and can simultaneously reduce hypersensitivity reactions. Initial steps have been taken to develop an albumin-bound paclitaxel, bringing about a satisfactory effect (Blum et al., 2007). Therefore, these developments must be applied to docetaxel as well.

The bioavailability is less following oral administration. However, if developed to increase bioavailability, it could be more accessible to administer and produce less hypersensitive reactions. One group used nano micelles to improve the uptake of paclitaxel (Lian et al., 2013). Therefore, similar approaches should be tested for docetaxel in the future.

Preclinical studies have demonstrated that docetaxel can increase plasma concentration when administered with ritonavir. Therefore, further studies are essential to demonstrate its effect on patients. Other combinations of drug forms should be tested, which will not reduce the antitumor activity but increase the plasma concentration by delaying metabolism.

Most importantly, it is reported that the ABCC10 transporter is responsible for the drug resistance developed among patients treated with taxanes. Therefore, possible drug combinations must be

tested to act as ABCC10 inhibitors. Also, novel approaches, such as gene editing using the CRISPR technique, should be tested to alter the ABCC10 gene.

1.4. CRISPR-Cas9

1.4.1. Mechanism of the CRISPR-Cas9 system

CRISPR-Cas9 is derived from the bacterial immune system. It disrupts foreign plasmids or viruses that invade the organism (Saber et al., 2020). CRISPR-Cas9 is currently recognized as a promising tool for gene editing due to its ability to induce site-specific breaks in the DNA double-strand (Ghosh et al., 2019).

The CRISPR-Cas9 system is comprised of two crucial constituents: a single-guide RNA (sgRNA) and Cas9 nuclease. Cas9, typically derived from Streptococcus pyogenes (SpCas9), can cleave double-stranded DNA. The Cas9 protein is characterized by two nuclease domains: HNH and RuvC-like. The HNH domain cuts the complementary DNA strand, while the RuvC-like domain cuts the non-complementary strand (Saber et al., 2020). The sgRNA, a typical 20 bp nucleotide sequence, is designed to pair with the target DNA sequence through Watson-Crick base pairing (Xia et al., 2019). The sequence of the sgRNA determines the precision of CRISPR-Cas9 genome editing, as the first 10-12 nucleotides at the 3' end of the gRNA are involved in recognizing and binding to the target sequence (Liu et al., 2019). Upon binding of the sgRNA to the designated site provides guidance for the sgRNA-Cas9 complex, which is positioned at the protospacer adjacent motif (PAM). This triggers a conformational alteration in the Cas9 protein, forming two nuclease domains that cleave both strands of the target DNA, thereby generating double-strand breaks (DSBs) approximately three nucleotides before the PAM site. SpCas9, a widely utilized Cas9 variant, can recognize the typical PAM sequence NGG. This recognition site commonly occurs in the genome and exhibits less restrictive requirements for target site selection. A mutation occurring in a single amino acid in one of the two nuclease domains of the Cas9 protein will lead to a single-stranded DNA break instead of the formation of DSBs. If both nuclease domains of Cas9 are mutated, its ability to cleave DNA will be compromised (Xia et al., 2019).

After double-strand breaks (DSBs) occur in mammalian cells, two main repair pathways are promptly activated: non-homologous end joining (NHEJ) and homology-directed repair (HDR) (Ghosh et al., 2019). NHEJ, being the primary pathway, mends DSBs by chemically rejoining the two ends together (Baliou et al., 2018). Although this pathway is efficient, it often results in small insertions or deletions at the site of the break (Xia et al., 2019). These insertions/deletions can lead to frameshift mutations or premature stop codons, ultimately causing disruption to the target gene (Karimian et al., 2019).

On the contrary, while less efficient, the HDR pathway is more precise. In this mechanism of gene repair, a DNA template searches for a homologous position at the flanking site of the DSB to reconstitute dysfunctional genes and restore gene function (Xia et al., 2019). The phase of the cell cycle influences the choice of the repair pathway. NHEJ is commonly employed when the cell is in the G1, S, or G2 phases, whereas HDR can only be utilized in cells during the S and G2 periods (Baliou et al., 2018).

These two pathways are utilized differently in genomic editing based on their repair mechanisms. The NHEJ pathway is typically employed for gene disruption, which may involve causing small deletions or insertions, duplications, and inversions. Conversely, since the HDR mechanism can introduce new genetic information into the genome, it is usually applied for large deletions, insertions, and replacements (Baliou et al., 2018).

1.4.2. CRISPR-Cas9 in cancer therapeutics

Cancer represents a complex series of events involving the accumulation of genetic alterations, including mutations, genome rearrangements, and epigenetic changes occurring in oncogenes and tumour suppressor genes. Investigating both normal and cancerous cell genomes is crucial for understanding the initiation processes and assessing the therapeutic responses of cancer cells to facilitate the development of treatments (Rodríguez-Rodríguez et al., 2019). Consequently, CRISPR-Cas9 technology, serving as a gene-editing tool, holds vast potential applications in this domain. It can be utilized either to elucidate the underlying molecular mechanisms of tumour growth or directly participate in various therapeutic approaches (Baliou et al., 2018).

1.4.2.1. Association of CRISPR-Cas9 and cancer related genes

Due to the potential mutations and variations in genomic instability, cancer cells often exhibit diverse genomic features as they progress through cancer development. Therefore, through CRISPR/Cas 9, identifying mutant proteins that drive tumour proliferation can reveal cancer-specific targets for drug development (Guo et al., 2017).

By applying CRISPR-Cas9 to different cell lines, shared essential genes across various cancer types have been identified. By deducing these shared essential genes, CRISPR-Cas9 technology provides an opportunity to pinpoint context-specific fitness genes in specific tumour cells. For example, recent studies comparing four cancer types have identified several context-specific fitness genes in glioblastoma, colorectal carcinoma, cervical carcinoma, and melanoma, demonstrating the potential of genome sequencing and functional genomic screens for patient categorization (Hart et al., 2015).

Furthermore, CRISPR-Cas9 has facilitated the correlation of functional genomic data with known pathological features, aiding in the development of specific genetic mutation models for rare tumours (Hong et al., 2016).

1.4.2.2. CRISPR libraries to combat drug resistance

Drug resistance in tumour cells is associated with multiple cellular mechanisms, including epithelial-mesenchymal transition (EMT), alterations in autophagy and glycolysis, suppression of apoptosis, epigenetic modifications, and changes in drug metabolism. New genomic changes are triggered by treatment and tumour heterogeneity. Therefore, the treatment plan should be altered to suit the new molecular features of the tumour (Saber et al., 2020)

To combat drug resistance, understanding the mechanisms behind it is crucial. Thus, CRISPR libraries are employed for screening purposes to evaluate synthesized drugs or to test random mutations, aiming to identify potential therapeutic targets (Kurata et al., 2018). Genome-wide CRISPR activation (CRISPRa) and CRISPR knockout (CRISPRn) screens are utilized to assess the effects of gain or loss of function in various genes on tumour drug response. By modifying genomic DNA at the single nucleotide level or knocking out specific genes, the CRISPR-Cas9

system offers a platform to investigate the mechanisms of drug resistance across different cancer types (Konermann et al., 2015).

1.4.2.3. Role in examining noncoding regulators of cancer

Apart from protein-coding genes, numerous non-coding genome regions play crucial roles in regulating protein-encoding gene expression. CRISPR-Cas9 offers a powerful tool for exploring the potential therapeutic utility of these non-coding regions in cancer therapy.

Utilizing CRISPR interference (CRISPRi), researchers have identified nine distal enhancers located within a one-megabase sequence near the MYC and GATA1 oncogenes. These noncoding regulators can be manipulated and potentially harnessed for novel cancer treatment strategies (Fulco et al., 2016).

Moreover, besides targeting enhancer binding sites, CRISPR screening using saturation mutagenesis or deletion can identify various other oncogenic modulators, including long noncoding RNAs (lncRNAs) (Zhu et al., 2016), microRNAs (miRNAs) (Golden et al., 2017), and other critical noncoding regions such as introns and untranslated exons (Kataoka et al., 2016). This broader approach enables the detection of a wide range of potential targets involved in cancer progression and drug resistance.

1.4.2.4. Application in cancer immunotherapy

One of the most impactful applications of CRISPR-Cas9 technology in cancer therapy lies in its integration into cancer immunotherapy, which stands as one of the most promising treatment strategies for cancer. The immune system, particularly T lymphocytes, plays a pivotal role in recognizing tumour-specific antigens, thereby potentially eradicating cancerous cells.

CRISPR-Cas9 technology has emerged as a powerful tool for eliminating genes encoding immune checkpoint molecules, such as programmed cell death protein 1 (PD-1) and cytotoxic T-lymphocyte-associated protein 4 (CTLA-4), which are expressed in T cells. In cancer patients, chimeric antigen receptor (CAR)-T cells can lead to exhaustion. Additionally, tumour cells can upregulate the expression of PDL-1, resulting in reduced immune response. Universal T-donor

cells have been successfully generated by CRISPR-Cas9-mediated simultaneous knockout of four loci of PD-1 and CTLA-4. (Ren et al., 2017).

Similarly, CRISPR-Cas9 technology has been utilized to overcome the Fas receptor member of the tumour necrosis factor α family of death receptors. Fas/FasL-dependent activation-induced cell death (AICD) has been reported to contribute to attenuating CAR-T cell activity. Therefore, Fas-induced cell death was reported to be prevented by knocking out the Fas receptor using CRISPR-Cas9 technology (Ren et al., 2017).

In conclusion, this method holds significant implications for personalized cancer therapy, as genetically modified T cells carrying tumour-targeting receptors have achieved positive therapeutic outcomes in patients with various haematological malignancies such as leukaemia and lymphomas (Mollanoori et al., 2018).

1.4.3. Factors Affecting Therapeutic Efficacy

While CRISPR-Cas9 technology has demonstrated promising advancements in previous clinical trials, several factors continue to influence its effectiveness and safety for widespread clinical application. These factors primarily revolve around the fitness of the edited cells, editing efficiency, delivery methods, and the potential for off-target effects. Ensuring that the edited cells are robust and functionally viable is essential for therapeutic success. Additionally, optimizing editing efficiency to achieve precise and accurate modifications without off-target editing is critical. Moreover, the development of efficient delivery methods that can effectively transport CRISPR-Cas9 components to target cells in vivo remains a significant challenge. Addressing these challenges will be crucial for harnessing the full potential of CRISPR-Cas9 technology in clinical settings while ensuring its safety and efficacy for therapeutic purposes.

1.4.3.1. Fitness of edited cells

One of the challenges in the clinical use of CRISPR-Cas9 technology is the fitness changes in edited cells. Fitness changes refer to alterations in the adaptability, proliferation capacity, and viability of genetically edited cells compared to their unedited counterparts. If edited cells exhibit improved proliferation and adaptability, they may gain a selective advantage over unedited cells,

reducing the initial cell number needed to reverse the antitumor effect (Cox et al., 2015). Conversely, if edited cells experience fitness defects, such as reduced proliferation and differentiation capabilities compared to unedited cells, they may be concealed by diseased counterparts. This scenario increases the threshold for modification and diminishes treatment efficiency. Therefore, the gene that leads to producing such unfit cells is not considered a suitable candidate for gene editing therapy (Xia et al., 2019). Thus, understanding and managing fitness changes are crucial considerations for the successful implementation of CRISPR-Cas9 in clinical settings.

In certain types of cancer, edited cells may not exhibit changes in fitness, proliferation, or differentiation, potentially necessitating editing a larger initial cell population for therapeutic effect. If diseased counterparts surpass modified cells, there remains hope for curing the disease through in vitro CRISPR-mediated genome editing, in which edited cells are expanded sufficiently in vitro before reintroducing into the patient. Furthermore, cancer cells mainly possess more significant growth advantages than normal cells, including rapid proliferation. However, there is a risk of spontaneous mutation in p53 in edited cells, and Cas9 may induce a p53-mediated DNA damage response. Therefore, monitoring p53 function is critical to ensure that patients' cells retain functional p53 before and after engineering (Chen et al., 2019). This emphasizes the importance of thoroughly assessing and managing potential risks associated with CRISPR-Cas9 gene editing therapies in cancer treatment.

1.4.3.2. Editing efficiency

The repair pathway of double-strand breaks (DSBs) significantly influences editing efficiency. NHEJ induces frameshift mutations or premature stop codons, making it suitable for gene knockout studies. In contrast, HDR targets transgenes or replaces specific genomic mutations with exogenous sequences. The choice between NHEJ and HDR-mediated repair mechanisms results in noticeable differences in editing efficiency, observed across different cell types and within different cell states. Generally, NHEJ pathways exhibit higher activity and efficiency in most cell types compared to HDR pathways. In germ cells, replication occurs, increasing the chance of integrating homologous chromosomes into the genome. However, in somatic cells, replication

primarily occurs from the identical sister chromatids, resulting in a low integration rate of donor DNA. Furthermore, HDR is limited to the S/G2 stages of the cell cycle, where sister chromatids are available for repair. Utilizing sequences from sister chromatids or homologous chromosomes enhances the accuracy of DNA repair in the HDR pathway (Devkota, 2018).

In summary, NHEJ is generally more flexible and efficient for generating indels to knock out carcinogenic genes, while HDR offers precise genetic modification but is relatively slower. The activity of the DSB repair pathway dictates the speed of gene editing, thus affecting the efficacy of most gene-editing processes. Enhancing the efficiency of the HDR repair pathway presents a significant challenge. The DNA repair machinery can be manipulated to favour either NHEJ or HDR based on experimental requirements. Strategies to increase HDR repair pathway efficiency include activating HDR chemically or genetically or suppressing NHEJ activity. Cells can be arrested at the S/G2 cell cycle stage to provide more time for HDR. (Cox et al., 2015).

1.4.3.3. Editing and Delivery Methods

For the comprehensive implementation of CRISPR-Cas9-mediated gene therapy in clinical applications, selecting appropriate editing and delivery methods poses a significant challenge. Currently, two main editing methods are available: in vitro and in vivo. The in vitro method includes removing targeted cells from the patients, editing outside the body, and re-engrafting. However, for this process, the cells should be capable of surviving outside the human body. In contrast, in vivo methods include altering the genes inside the body. It can be either by targeted local injection or by editing a wide range of tissue types (Cox et al., 2015).

The success of gene editing comprises effective cell targeting, rapid clearance, and minimal cytotoxicity within the CRISPR system. However, achieving all these criteria simultaneously with current delivery methods is challenging. Reducing off-target effects and immune responses is crucial for realizing sufficient clinical benefit. Additionally, programmable nucleases must be transiently delivered appropriately to avoid possible off-target cleavage and immune response activity. Moreover, the choice of delivery method impacts whether the nuclease expression in the target cell is transient or permanent.

Delivery methods generally fall into three categories: physical delivery, viral vectors, and non-viral vectors. Standard physical delivery methods include microinjection and electroporation. Viral delivery vectors encompass specifically engineered adeno-associated viruses (AAV), full-sized adenoviruses, and lentiviruses, with viral vectors being the predominant choice for in vivo CRISPR-Cas9 delivery. Although less common, non-viral vector delivery offers several advantages over viral vectors and is an area of growing research. Non-viral vector systems include nanoparticles (Chen et al., 2019).

1.4.3.4. Off-target effects

Off-target effects (OTEs) in CRISPR-mediated gene editing can arise from various events, including unintended DNA cleavage or binding at genomic sites and subsequent editing or regulatory events. Studies have shown that OTEs often lead to the generation of insertions or deletions (indels) at undesired genomic loci. The specificity of CRISPR-related nucleases is influenced by factors such as the genomic locus, host cell type, culture conditions, and the dose and duration of nuclease presence. Continuous genetic modification increases the risk of off-target cleavage and reduces editing specificity, potentially causing unnecessary mutations and toxicity. CRISPR-Cas9 has been found to pose a higher risk of off-target effects in human cells compared to other genome editing methods like zinc finger nucleases (ZFNs) and transcription activator-like effector nuclease (TALENs). Off-target effects can lead to genomic toxicity, carcinogenesis, genomic instability, disruption of functional genes, epigenetic changes, cell death, and cell transformation (Xia et al., 2019).

The successful monitoring of on-target changes in genome-edited cells can be achieved through targeted analysis of genomic loci using various assays. Detection and mapping of off-target effects (OTEs) allow for the assessment of the specificity of a particular guide RNA (gRNA). However, the impact of detected OTEs on the interpretation of experimental results remains uncertain. Despite techniques available for assessing the specificity of particular guide RNAs, off-target effects can still impact the interpretation of experimental results. Therefore, it is crucial to minimize and control off-target effects. Previous studies have developed strategies using a range of design tools, engineered reagents, and experimental procedures to mitigate off-target effects.

These strategies aim to increase the specificity of nuclease-mediated cleavage at the target site or restrict the duration of nuclease expression to minimize off-target mutations (Chen et al., 2019).

Multiple strategies are implemented in experimental design and downstream phenotypic assessment to reduce OTEs and derive meaningful conclusions. Proper selection of the gRNA is crucial, with target sequences chosen for lower homology and careful control of CRISPR-Cas9 dosage. Modifications to the structure and composition of the gRNA, such as using truncated sgRNAs, can reduce off-target effects. Additionally, high-fidelity Cas9 nuclease variants have been developed, showing a significant reduction in off-target cleavage events while maintaining on-target editing capability (Campenhout et al., 2019).

The choice of delivery method can also influence off-target effects, as different methods result in varying levels and durations of Cas9 and gRNA expression. While cell lines with stable and constitutive Cas9 expression are beneficial for gene knockout, continuous high-level expression of Cas9 may increase off-target effects due to increased mismatch tolerance. Despite efforts to reduce OTEs, they cannot be entirely avoided. Therefore, steps should be taken in experimental design to control these effects and increase confidence in the results (Cox et al., 2015).

In summary, CRISPR-Cas9 holds excellent promise as a gene-editing tool in anticancer therapies. Despite challenges, systematic optimization of its efficacy, safety, and specificity can lead to the development of effective biological treatments, enhancing patient outcomes in the future.

1.5. Research hypotheses and aims

We hypothesize that *ABCC10* gene (encoding MRP7) can be silenced by using CRISPR-Cas9 system in human colorectal Caco-2 cells. This thesis aims to investigate the deletion of ABCC10 by using liposome-mediated delivery of ABCC10 guide-RNA/Cas9 protein ribonucleoprotein complexes and to evaluate the effect of ABCC10 silencing on the proliferation of colorectal Caco-2 cells and their sensitivity to docetaxel.

2. Materials and Methods

2.1. Chemicals and reagents

The chemicals and reagents used in this study are listed below in Table 2.1.

Table 2.1. Chemicals and reagents used for the study with their supplier

Chemicals	Supplier
Lipofectamine™ CRISPRMAX™ Cas9 transfection kit	Thermo Fisher (Pub.No.MAN0014545)
TrueCut™ Cas9 Protein v2	Thermo Fisher (Pub.No.MAN0017066)
DMEM	Thermo Fisher
Opti-MEM medium	Thermo Fisher
Fetal Bovine Serum (FBS)	Moregate biotech
Phosphate Buffered Saline (PBS)	Thermo Fisher
TrypLE™ express enzyme	Thermo Fisher
GeneArt® genomic cleavage detection kit (GCD)	Thermo Fisher

2.2. Reviving Cell Culture from Frozen Cells

The Caco-2 cell lines already available at AUT University were defrosted by immersing the frozen cells containing vials in a 37 ^{0}C water bath for a few minutes with continuous agitation. Complete media was prepared by adding 10% Fetal Bovine Serum (FBS) to Dulbecco's Modified Eagle Medium (DMEM). Next, 5 ml of complete medium was added to a T25 flask, and the defrosted Caco-2 cells were added to it. The cells were placed in a CO_2 incubator at 37 ^{0}C for 24 hours. The next day, the medium was removed, 5 ml of new complete medium was added, and the cells were allowed to grow in the CO_2 incubator at 37 ^{0}C until confluent.

2.3. CRISPR-Cas 9 Transfection

A CRISPR-Cas9 Transfection was carried out to produce an ABCC10/MRP7 knockout Caco-2 cell line. The contents of the Lipofectamine™ CRISPRMAX™ Cas9 transfection kit, TrueCut™ Cas9 Protein v2 and the Invitrogen™ TrueGuide™ Synthetic gRNA were used in this reaction. The steps followed are explained below.

2.3.1. Preparation of sgRNA working solution

The 1.5 nmol dry sgRNA from Thermo Fisher was dissolved in 15 µl of 1X TE buffer to prepare 100 pmol/µl stock sgRNA solution. The working solution (15 pmol/µl sgRNA) was prepared by dissolving 15 µl of the stock solution in 85 µl of nuclease-free water.

2.3.2. Seeding Cells

Once the Caco-2 cells were about 70-80% confluent in the T25 flask, the complete medium was removed, and the cells were washed with 5 ml of pre-warmed PBS. Next, 2ml of TrypLE^{TM} was added to the flask and incubated for 5 minutes at 37 ^{0}C. Once the cells were detached, 4 ml of complete medium was added to the flask, and the contents were transferred to a 15 ml centrifuge tube. The cells were centrifuged at 1200 rpm for 5 minutes. The supernatant was discarded, and the cell pellet was resuspended in 1 ml of complete medium.

For the cell counting, 10 µl of the resuspended cells were added onto a parafilm and mixed with 10 µl of Trypan Blue. Trypan blue is added to stain the cells to ease the cell counting. The mixture was loaded to one side of the haemocytometer until it filled the area under the cover slip. The haemocytometer was kept under a microscope and observed under a 10X objective. The total number of cells in the four corner squares was counted, and the cell number was calculated using the following equation.

Number of cells per ml = Average number of cells X dilution factor X 10^4

The cell concentration was adjusted to 100,000 cells/ml, and 1 ml of this solution was added to five wells of the 6-well plate to have a final Caco-2 cell concentration of 100,000 cells per well (Figure 2.2). The cells were grown in a CO_2 incubator at 37 ^{0}C. The following day, transfection was carried out as described below.

2.3.3. Transfection

Two separate solutions (solution 1 and solution 2) were prepared with a mixture of different reagents, as shown in Figure 2.1 below. Solution 1 had four different compositions; therefore, it was prepared in four separate tubes labelled from A to D.

Solution 1			
Tube A (gRNA only)	**Tube B (Cas9 only)**	**Tube C (15 pmol/µl gRNA + Cas9)**	**Tube D (45 pmol/µl gRNA + Cas9)**
1 A	**1 B**	**1 C**	**1 D**
50 µl Opti-MEM + 3 µl gRNA + 5 µl Cas9 Plus lipofectamine	50 µl Opti-MEM + 2.5 µl (2500ng) Cas9 Protein + 5 µl Cas9 Plus lipofectamine	50 µl Opti-MEM + 2.5 µl (2500ng) Cas9 Protein + 1 µl gRNA + 5 µl Cas9 Plus lipofectamine	50 µl Opti-MEM + 2.5 µl (2500ng) Cas9 Protein + 3 µl gRNA + 5 µl Cas9 Plus lipofectamine

Solution 2	
2	12 µl Lipofectamine CRISPRMAX + 200 µl Opti-MEM

Figure 2.1. Composition of Transfection Solutions

Solution 1 (tubes A to D) was incubated at room temperature for 10 minutes. Solution 2 was incubated at room temperature for 1 minute and quickly transferred 50 µl of solution 2 to tubes A, B, C and D. The solutions were mixed and incubated at room temperature for 15 minutes. Finally, add 100 µl of each tube (Tube A to D) into four separate wells of the 6-well plate, as shown below in Figure 2.2.

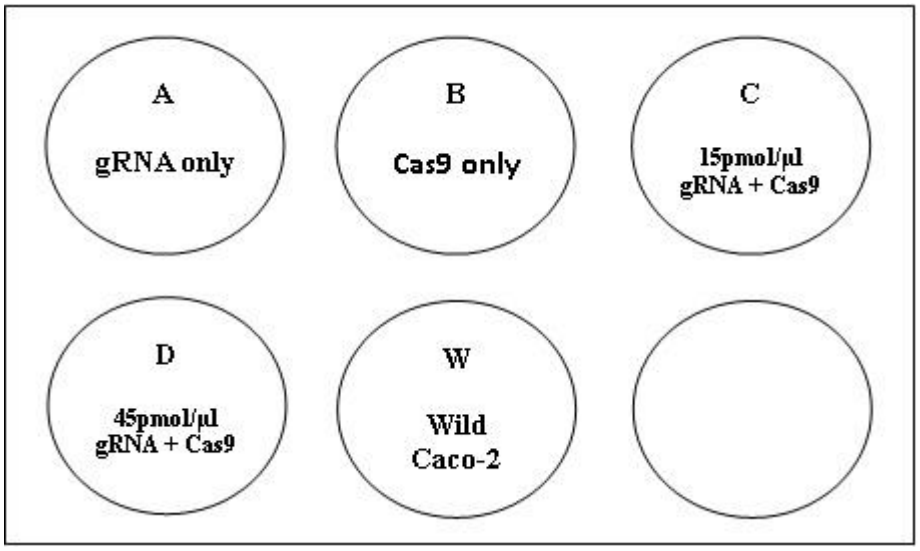

Figure 2.2. Layout of transfection 6-well plate

The plate was incubated at 37 ^{0}C for two days. After two days, the culture medium was removed, and the cells were washed with 500 µl of PBS. Next, the cells of each well were prepared to detect the cleavage efficiency.

2.4. Cleavage Efficiency Assay

This study used a GeneArt® genomic cleavage detection kit purchased from Thermo Fishers. The gene editing efficiency was detected according to the manufacturer's instructions supplied with the kit.

In the process of creating ABCC10/MRP7 knockouts, a gRNA specific for the *ABCC10* gene is used. Following the CRISPR-Cas9 transfection process, double-stranded breaks will be created, and during the process of non-homologous end joining, indels will be incorporated into the DNA strand.

In this method, the gene target that contains the indels will be amplified by PCR using pre-designed primers for the interested region. The PCR product will be subjected to several cycles of denaturing and reannealing. Mismatches will be generated when the strands with indels are re-annealed with complementary stand with no indels. The product will be cleaved with the T7 Endonuclease 1 (T7E1) Detection Enzyme provided in the kit. Only the DNA regions with mismatches will be cleaved by the enzyme. Therefore, the correctly transfected cells will have three bands, while the un-transfected cells will only have the band corresponding to the PCR product. The digested product will be visualized using agarose gel electrophoresis. The cleavage efficiency will be calculated by band densitometry. Each stage of this process is explained below.

2.4.1. Harvest Cells

The cells ready for cleavage analysis were centrifuged at 200 g for 5 minutes at 4 ^{0}C. The supernatant was removed, and the cell pellet was stored at -80 ^{0}C until prepared for the reaction.

2.4.2. Cell lysis and DNA extraction

A Cell lysis buffer and Protein degrader mix was prepared by mixing 250 µl of cell lysis buffer with 10 µl of the protein degrader in a microcentrifuge tube. An aliquot of 50 µl of this mixture was added to each cell pellet obtained from the tubes containing cell pellets of wells A, B, C, D, and W (of the transfected 6-well plate). The cells were resuspended, and all the content was transferred to five separate PCR tubes. The following program (Table 2.2) was run on a thermocycler, and the product was used for the downstream PCR analysis step.

Table 2.2. Temperature program for cell lysis

Temperature	Time
68^0C	15 minutes
95^0C	10 minutes
4^0C	Hold

2.4.3. Preparing primer working solution

The forward (sequence - GAGGTGAGGGGTATGTCTGG) and reverse (sequence - CACAACACGGTCAGCACTAG) primers were designed using the Invitrogen TrueDesign Genome Editor software (Thermo Fisher Scientific, NZ). Both primers had a higher GC content, between 40-60%. The primers were designed to amplify the region, which included the indels. Furthermore, they were designed to produce bands of two distinguished sizes following cleavage with the T7E1 Detection Enzyme.

Both forward and reverse primers' stock solution was 100 µM, whereas their working solution was 10 µM. The dry forward primer (32.6 nmol) was dissolved in 326 µl of the TE buffer to prepare a 100 µM stock solution. Similarly, the reverse primer (26.7 nmol) was dissolved in 267 µl of the TE buffer. Both the stock solutions were diluted ten times to prepare the working solutions.

2.4.4. PCR amplification

The cell lysate prepared as described in section 2.4.2 was vortexed and added 2 µl of it along with the other components mentioned in (Table 2.3) according to the specified volumes to PCR tubes. The final mixture was placed in a thermocycler, and the temperature was changed according to the PCR program mentioned in (Table 2.4)

Table 2.3. Composition of the PCR mixture

Component	Sample	Control
Cell lysate	2 µL	-
10 µM F/R primer mix	1 µL	-
Control template primers	-	1 µL
ampliTaq Gold 360 Master Mix	25 µL	25 µL
Water	22 µL	24 µL
Total	**50 µL**	**50 µL**

Table 2.4. Temperature program of PCR reaction

Stage	Temp	Time	Cycles
Enzyme activation	95 ℃	10 minutes	1X
Denature	95 ℃	30 second	40 X
Anneal	58.9 ℃ (Tm)	30 second	
Extend	72 ℃	30 second	
Final Extension	72 ℃	7 minutes	1X
Hold	4 ℃	Hold	1X

2.4.5. PCR Products Gel Analysis

A 2% agarose gel was prepared by dissolving 1 g of agarose in 50 ml of 1X TBE buffer in a 100 ml conical flask. The flask was heated for 2 minutes in a microwave oven until the solution became clear with no clumps. Red-safe dye was added to this solution and was poured onto a tray while hot. Once the gel became cool and solid, the comb was removed, and the samples were loaded after placing the gel in a gel tank.

2.4.6. PCR product verification

A ladder was loaded to the first well (1 µl ladder (100 bp Thermo Fisher) + 2 µl dye (10X blue juice supplied with ladder) + 11 µl water) to compare the band size. To the rest of the wells, 10 µl of the PCR products were added after mixing with 2 µl of gel loading dye. Gel electrophoresis was performed at 50 V for 10 minutes, and the voltage was later increased to 100 V and continued for 1.5 hours. Following the electrophoresis, the gel was observed using MS major Science, Gel documentation system. If a single band of the expected band size was obtained for the PCR products, proceed to the denaturing and reannealing step to form mismatches. The PCR products were stored at -20 ^{0}C until the next step was performed.

2.4.7. Cleavage Assay

The PCR product (2 µl) was mixed with 1 µl of the 10X Detection reaction buffer in a PCR tube. Added 6 µl of nuclease-free water to make the final volume 9 µl. The mixture was then placed in

a LightCycler® 480 Real-time PCR System (Roche Molecular Systems, Inc), and the re-annealing program was performed, as shown below in Table 2.5.

Table 2.5. Temperature program of re-annealing cycle

Stage	Temperature	Time	Temperature/Time
1	95 °C	10 minutes	-
2	95–85 °C	-	−2 °C/s
3	85 °C	1 minute	-
4	85–75 °C	-	−0.3 °C/s
5	75 °C	1 minute	-
6	75–65 °C	-	−0.3 °C/s
7	65 °C	1 minute	-
8	65–55 °C	-	−0.3 °C/s
9	55 °C	1 minute	-
10	55–45 °C	-	−0.3 °C/s
11	45 °C	1 minute	-
12	45–35 °C	-	−0.3 °C/s
13	35 °C	1 minute	-
14	35–25 °C	-	−0.3 °C/s
15	25 °C	1 minute	-
16	25–4 °C	-	−0.3 °C/s
17	4 °C	∞	-

Once the temperature program was completed, proceeded to the enzyme digestion. For each sample, 1µl of the detection enzyme and 1µl of water were added for each control. All the mixtures were placed in Mastercycler® Pro (Eppendorf AG) and incubated at 42 ^{0}C for 30 minutes. Following the reaction, immediately proceeded to the gel analysis.

2.4.8. Cleavage Products Gel Analysis

A 2% agarose gel was prepared by dissolving 2 g of agarose in 100 ml of 1X TBE buffer in a 250 ml conical flask. The solution was dissolved, as mentioned in section 2.4.5. above, and 1X SYBR™ Gold stain was added and allowed to be solidified on a gel tray. The cleavage product (10 µl) was mixed with 2 µl of loading dye and loaded into the wells. The rest of the steps were followed, as mentioned in section 2.4.5. Following Gel electrophoresis, the cleavage efficacy was calculated using the equation below.

Cleavage Efficiency = $1 - [(1 - \text{fraction cleaved})^{1/2}]$

Fraction cleaved = sum of cleaved band intensities / (sum of cleaved and parent band intensities)

2.5. Selection of Single Clones

After determining the cleavage efficiency, knockout clones were selected using the limiting dilution method. The Caco-2 cells transfected with 15 pmol/µl gRNA, and Cas9 was used for the downstream process. The cells were seeded as described in section 2.3.2. The seeding cell density was 0.8 cells per well. This amount was seeded to prevent having more than one cell per well. Therefore, 100 µl of 8 cells/ml solution was added to each well of a 96-well plate. Only one well in the corner was seeded with 1000 cells per well. This was to ease focusing the microscope as detecting one cell is difficult. The layout of the 96-well plate for limiting dilution is given below in Figure 2.3.

											1000

Figure 2.3. The layout of the 96-Well plate for limiting dilution
Note: The yellow box indicates 1000 cells per well, and the white colour boxes indicate 0.8 cells per well seeding densities.

The wells were checked under the microspore every 3-4 days, and the wells containing surviving cells were marked. The complete medium was changed weekly, and once the cells were approximately 80% confluent, they were transferred to 12-well plates.

After the cells had reached confluency in the 12-well plate, the surviving cells were transferred to 6-well plates, each having two copies, one for western blotting analysis and the other for MTT analysis.

Once the cells are about 80% confluent, they are transferred to T25 flasks. Following this process, fifteen clones were isolated, those which had undergone both western blotting and MTT assay. These clones were analysed to detect if the expected knockout was produced during the transfecting process.

2.6. Western Blotting

Western Blotting analysis is performed to detect the expression of the protein ABCC10. A signal should be produced at around 158 kD if the protein is expressed in the cells. A western blot was developed to observe the signal corresponding to ABCC10 in the wild Caco-2 cells. Next, the developed method was used to compare the western blot results of the wild Caco-2 cells and the cells of the single clones obtained from CRISPR-Cas9 transfection to detect if the knockout was successful. If a homologous knockout is produced, the signal corresponding to the ABCC10 around 158 kD should be absent in the western blot.

2.6.1. Preparation of cell lysate

Once the wild Caco-2 cells grown in T25 flasks reach about 80% confluency, they will be used for the western blotting. First, the old culture medium is removed, and the cells are washed twice with ice-cold PBS. The PBS was discarded, and 500 µl of Dithiothreitol-containing Laemmli sample buffer was added to the flask at room temperature. The composition of the mixture is given below in Table 2.6.

Table 2.6. Composition of Dithiothreitol containing Laemmli sample buffer.

Solution	Volume
4 X Laemmli Buffer	250 µl
1000 mM Dithiothreitol (DTT)	50 µl
Mili Q water	200 µl
Total	**500 µl**

The volume of the lysis buffer needs to be adjusted according to the confluency; for example, if the cells are about 50% confluent, 300 µl from the final mixture was added because the cells will tend to degrade in the presence of more lysis buffer.

The T25 flask containing the lysis buffer was swirled to uniformly spread the buffer. The lysate was scraped using a cell scraper and collected in a weighing boat. The lysate was passed several times through a 27.5-gauge needle to reduce the viscosity. Next, the lysate was transferred to a microcentrifuge tube and centrifuged at 14,000 g for 15 minutes at 4 ^{0}C. The cell pellet was discarded, and the supernatant was transferred to a new tube kept on ice and stored at -80 ^{0}C until used for further steps in the western blot analysis.

2.6.2. Western blot gel electrophoresis

The gel tank was assembled, and a 10% precast polyacrylamide gel cassette (Mini-PROTEN TGX) was placed in the tank (Bio-RAD mini-PROTEAN® Tetra System). The tank was loaded with 1X running buffer (Tris/Glycine/SDS), and the lysed cells were loaded into the wells with a ladder (Precision Plus Protien™ Dual Xtra Standards). The electrophoresis was conducted by running the gel for 10 minutes at 50 V and next for 1 hour at 100 V in Bio-RAD PowerPac Basic™. After the electrophoresis, the proteins on the gel were transferred to a membrane using Trans-Blot® Turbo™ Mini PVDF Transfer Packs and System. The efficiency of protein transfer will be assessed by MemCode™ Reversible Protein Stain Kit – for PVDF Membranes.

2.6.3. Staining with antibodies and visualizing

The PVDF membrane was blocked with blocking buffer (0.5% milk dissolved in TBST and filtered) for 1 hour at room temperature on a plastic tray with continuous agitation. Next, the membrane was washed with TBST for 5 minutes while shaking. The membrane was incubated with the primary antibody (1 µg/ml) diluted in blocking buffer for 1 hour at room temperature with continuous agitation and left overnight at 4 ^{0}C in a fridge. The next day, the primary antibody-stained membrane was washed thrice with TBST buffer for 3 minutes each. The excess TBST was removed, and the membrane was stained with the secondary antibody (1 µg/ml) conjugated with horseradish peroxidase (HRP) diluted in a blocking buffer for 1 hour at room temperature in a dark environment while shaking. Following the incubation, the membrane was washed twice with TBST for 3 minutes and once with Mili Q water (3 minutes), all the time with continuous shaking to remove unbound antibodies. Meanwhile, a working solution of SuperSignal™ West Atto was freshly prepared by mixing 3ml of each peroxide and substrate solution. This solution was added to the membrane and agitated for 5 minutes at room temperature. The blot was removed from the solution and placed on a tray, carefully ensuring no bubbles were trapped. An image of the blot was captured using the ImageQuant LAS 500. Images were captured using auto exposure, semi auto exposure and adjusting the exposure time from 30 seconds to 3 minutes. The best image was selected from all the images generated.

2.6.4. Western blot method optimisation

The western blot image obtained after following the abovementioned steps did not consist of a clear signal corresponding to ABCC10. Therefore, the western blot was developed using different lysis buffers to select the buffer producing the clearest ABCC10 signal. When the lysis buffer used is strong, it will degrade the protein, and the expected signal will not appear. Therefore, in such a case, a milder buffer is preferred. Detergents such as sodium dodecyl sulfate (SDS) will solubilize proteins but may be harsh for some proteins. Therefore, in this study, different lysis buffers were tested to detect which was best for the antibody used and which produced the expected signal for ABCC10 at 158 kD. The different lysis buffers used in this study are given below.

1. Laemmli Buffer

277.8 mM Tris-HCl, pH 6.8

44.4% (v/v) glycerol

4.4% LDS

0.02% bromophenol blue

2. RIPA Buffer

10 mM Tris-HCl, pH 7.4

150 mM NaCl

0.1% Triton X – 100

0.5% Sodium Deoxycholate

0.1% Sodium Dodecyl Sulfate

3. Tris Buffer

50 mM Tris-HCl, pH 8.0

4. EDTA Buffer

50 mM Tris-HCl, pH 6.8

2% Sodium Dodecyl Sulfate

1 mM Ethylenediaminetetraacetic acid (EDTA)

10% glycerol

5. Triton – X Buffer

50 mM Tris-HCl, pH 8.0

0.1% Triton-X

150 mM NaCl

6. Tris-NaCl Buffer

50 mM Tris-HCl, pH 8.0

150 mM NaCl

Before reacting with the cells, all these buffers were mixed with a phosphatase inhibitor (PhosSTOP) and Protease inhibitor cocktail tablets (supplied by Roche). The final mixture added to the cell lysate is given below.

Table 2.7. Composition of cell lysate mixture

Cell lysate Mixture for 50% confluent T25 flask	
Solution	**Volume**
Cell Lysis Buffer	300 µl
10 X phosphatase inhibitor	30 µl
25 X Protease Inhibitor	24 µl
Total	**354 µl**

The cell lysate will be prepared from the Caco-2 cells grown in the T25 flask using 300 µl of the above lysate mixture. All the other steps followed will be similar to those mentioned in sections 2.6.1 to 2.6.3. According to the images obtained the most suitable lysis buffer will be selected that produced the best signal for ABCC10 around 158 kD.

2.6.5. Western Blot analysis of isolated clones

The single clones isolated following limiting dilution will be lysed using the best lysis buffer selected from above, and the western blot procedure will be followed, as mentioned above, from sections 2.6.1 to 2.6.3. For all blots, a wild Caco-2 cell lysate was added for comparison along with the ladder to verify the size of the signals produced.

If a homologous knockout was produced during the CRISPR-Cas9 transfection, the clones produced will not have the signal corresponding to ABCC10 following western blot analysis. However, if a heterozygous knockout or nor knockout is produced, the signal corresponding to ABCC10 will be visible around 158 kD.

2.7. MTT assay

Western blotting is performed to detect the protein expression changes that occurred due to the transfection. In comparison, the MTT assay is used to detect the functional changes of the clones. MTT assay is used to detect the sensitivity of the cells towards drugs. Therefore, the sensitivity of the wild Caco-2 cells and the knockout clones towards the antitumor drug docetaxel was detected in this study.

2.7.1. Definition of linear range

Before developing a method to detect the sensitivity towards antitumor drugs of the wild Caco-2 cells, the number of cells which behave in the linear range should be detected. The number of cells seeded during the follow-up assays depends on the cell count, which falls within the linear range. Only the number of cells that produce an absorbance in the linear range should be seeded to prevent errors and disrupt the observations.

The cell viability is detected by treating the live cells with MTT [3-(4,5-dimethylthiazol-2-yl)-2,5-diphenyltetrazolium bromide]. The metabolically active cells will react with MTT and reduce it to form Formazan, which is purple. Following the reaction of DMSO (Dimethyl sulfoxide), the formazan produced will be solubilized. Therefore, the purple colour is extracted to the medium, and the colour intensity can be detected by a spectrometer at 540 nm.

In this method, a series of wild CaCo-2 cells will be seeded, as described in section 2.3.2. The seeding density will be varied from 1000 cells/well to 64,000 cells/well. The cells will be seeded in a 96-well plate, as shown below in Figure 2.4. The seeded cells will be allowed to grow for 16-24 hours in a CO_2 incubator at 37 ^{0}C.

		1,000	2,000	4,000	8,000	16,000	32,000	64,000			
		1,000	2,000	4,000	8,000	16,000	32,000	64,000			
		1,000	2,000	4,000	8,000	16,000	32,000	64,000			
		1,000	2,000	4,000	8,000	16,000	32,000	64,000			
		1,000	2,000	4,000	8,000	16,000	32,000	64,000			
		1,000	2,000	4,000	8,000	16,000	32,000	64,000			

Figure 2.4. The Layout of the 96-well plate for linearity range detection
Note: The wells marked in grey contain sterile PBS only, marked in orange are complete medium-only wells, and the yellow-coloured wells contain the wild Caco-2 cells; the seeding density is mentioned, which is between 1,000 to 64,000 cells per well.

The following day, remove all the medium from the 96-well plate kept in the incubator. Prepare a 12 mM MTT solution by dissolving 5 mg of MTT in 1 ml of sterile PBS. Add 700 µl of the 12 mM MTT solution to 7,000 µl of the complete medium. Add 110 µl of this MTT, complete medium mixture, to each well (except the wells containing PBS). Incubate for 3 hours in a CO_2 incubator at 37 ^{0}C. After 3 hours, remove all medium but 25 µl of all wells containing MTT. Add 150 µl of DMSO and shake in an orbit shaker for 30 minutes. Insert the plate into a plate reader,

shake for another 2 minutes, and read the absorbance at 540 nm and 680 nm reference wavelengths to correct the background absorbance.

The absorbance at 540 nm is reduced from the absorbance at 680 nm to correct the background absorbance. Next, the absorbance from the blank is reduced. The corrected absorbance is plotted against the cell number per well. From the graph plotted, the cell numbers that fall within the linear range are detected.

2.7.2. Method Development to detect IC50 of wildtype Caco-2 cells

This study tested the sensitivity of wild Caco-2 cells towards the antitumor drug docetaxel. As described in section 2.3.2, wild Caco-2 cells were seeded in a 96-well plate to have a final concentration of 10,000 cells / 100 µl / well. The cells were incubated for 16-24 hours in a CO_2 incubator at 37^0C. Following the incubation, cells were treated with docetaxel at various concentrations as shown in Figure 2.5. As the IC50 of docetaxel of the wildtype Caco-2 cells is unknown at this stage, a concentration gradient was prepared from 100 µM to 0 µM with a series of 1 in 2 dilution, as shown in Figure 2.5. Each concentration was triplicated.

		100.000µM	50.000µM	25.000µM	12.500µM	6.250µM	3.125µM	1.563µM	0.781µM	0.391µM	
		100.000µM	50.000µM	25.000µM	12.500µM	6.250µM	3.125µM	1.563µM	0.781µM	0.391µM	
		100.000µM	50.000µM	25.000µM	12.500µM	6.250µM	3.125µM	1.563µM	0.781µM	0.391µM	
		0.195µM	0.098µM	0.049µM	0.024µM	0.012µM	0.006µM	0.003µM	0.0015µM	0.000µM	
		0.195µM	0.098µM	0.049µM	0.024µM	0.012µM	0.006µM	0.003µM	0.0015µM	0.000µM	
		0.195µM	0.098µM	0.049µM	0.024µM	0.012µM	0.006µM	0.003µM	0.0015µM	0.000µM	

Figure 2.5. The layout of the 96-well plate of docetaxel treatment for 24 hours on 10,000 wild Caco-2 cells
Note: The wells marked in grey colour contain sterile PBS only, marked in orange are complete medium-only wells, and the yellow-coloured wells contain the wild Caco-2 cells, 10,000 cells per well treated with a concentration range of docetaxel as shown in the figure for 24 hours.

The docetaxel-treated cells were incubated for 24 hours in a CO_2 incubator at 37 ^{0}C, and following the drug treatment, the MTT assay was performed, as mentioned above in section 2.7.1. The percentage of cell viability was calculated using the following equation.

$$\text{Percentage cell viability} = \left(\frac{\text{Absorbance of the docetaxel treated cells}}{\text{Absorbance of the untreated cells}}\right) X\ 100\%$$

The IC50 value is the drug concentration responsible for the 50% reduction of cell viability obtained from the dose-response-inhibition curve. Therefore, the percentage cell viability Vs log concentration was plotted, and the IC50 value of docetaxel was detected using the GraphPad Prism version 6.

The MTT assay was optimized by varying conditions, such as the docetaxel concentration, time incubated after treatment and the number of cells used. In the next step, the concentration range was narrowed as the cells did not show a significant inhibition at very low concentrations, and each concentration was repeated six times. Furthermore, as the doubling time of Caco-2 cells is low, the cells were treated for 72 hours, providing sufficient time for the cells to grow. Or else, cells treated with both high and low drug doses will display low cell viability. Therefore, the experiment was repeated by changing the conditions mentioned above, and all the other steps were the same as those mentioned earlier in section 2.7.2. The concentration range applied, and the layout of the 96-well plate is given below in Figure 2.6.

		100.000µM	50.000µM	25.000µM	12.500µM	6.250µM	3.125µM	1.563µM	0.781µM	0.000µM	
		100.000µM	50.000µM	25.000µM	12.500µM	6.250µM	3.125µM	1.563µM	0.781µM	0.000µM	
		100.000µM	50.000µM	25.000µM	12.500µM	6.250µM	3.125µM	1.563µM	0.781µM	0.000µM	
		100.000µM	50.000µM	25.000µM	12.500µM	6.250µM	3.125µM	1.563µM	0.781µM	0.000µM	
		100.000µM	50.000µM	25.000µM	12.500µM	6.250µM	3.125µM	1.563µM	0.781µM	0.000µM	
		100.000µM	50.000µM	25.000µM	12.500µM	6.250µM	3.125µM	1.563µM	0.781µM	0.000µM	

Figure 2.6. The layout of the 96-well plate of docetaxel treatment for 72 hours on 10,000 wild Caco-2 cells

Note: The wells marked in grey colour contain sterile PBS only, marked in orange are complete medium-only wells, and the yellow-coloured wells contain the wild Caco-2 cells, 10,000 cells per well treated with a concentration range of docetaxel as shown in the figure for 72 hours.

Cells with high seeding density will not be affected significantly at lower drug concentrations. Therefore, the cells will be doubling; their cell growth will be inhibited once they reach confluency due to limited space in the well. The reason for the inhibition was not the dose of the drug but the higher initial seeding cell density. Therefore, the experiment was repeated using 5,000 Caco-2 cells per well. The other conditions are the same as in Figure 2.6. Following the MTT assay, the IC50 of docetaxel for 5,000 wild Caco-2 cells treated for 72 hours was detected using prism software, which was used to compare the sensitivity of the isolated single clones.

2.7.3. Docetaxel sensitivity of the knockout clones

The IC50 value of docetaxel was detected as 2 µM in the wildtype Caco-2 cells. Therefore, 2 µM of docetaxel was used to treat the isolated single clones for 72 hours. Each separate clone isolated was seeded in columns 3 to 10, and the wild type was seeded in column 11 of the 96-well plate; the seeding density was 5,000 cells per well. The wild type and the single clones were treated with 2 µM docetaxel and compared with untreated cells. The layout of the 96-well plate used to compare the cell viability of the knockout clones and wild type is shown in Figure 2.7. Following the treatment, the MTT assay was performed as described in section 2.7.1. The cell viability of the wild Caco-2 cells was compared to that of the isolated transfected clones.

		Clone A	Clone B	Clone C	Clone D	Clone E	Clone F	Clone G	Clone H	WT	
		0.0 µM	0.0 µM	0.0 µM	0.0 µM	0.0 µM	0.0 µM	0.0 µM	0.0 µM	0.0 µM	
		0.0 µM	0.0 µM	0.0 µM	0.0 µM	0.0 µM	0.0 µM	0.0 µM	0.0 µM	0.0 µM	
		0.0 µM	0.0 µM	0.0 µM	0.0 µM	0.0 µM	0.0 µM	0.0 µM	0.0 µM	0.0 µM	
		2.0 µM	2.0 µM	2.0 µM	2.0 µM	2.0 µM	2.0 µM	2.0 µM	2.0 µM	2.0 µM	
		2.0 µM	2.0 µM	2.0 µM	2.0 µM	2.0 µM	2.0 µM	2.0 µM	2.0 µM	2.0 µM	
		2.0 µM	2.0 µM	2.0 µM	2.0 µM	2.0 µM	2.0 µM	2.0 µM	2.0 µM	2.0 µM	

Figure 2.7. The layout of a 96-well plate, Comparison of docetaxel sensitivity in wild Caco-2 cells and knockout clones
Note: The wells marked in grey contain sterile PBS only, marked in orange are complete medium-only wells, the yellow-coloured wells are untreated, and the green-cloured ones are treated with 2 µM of docetaxel for 72 hours. Each column from 3 to 10 is seeded with cells of different clones, and the 11th column is seeded with wildtype Caco-2 cells. (The seeding density of all cell types is 5,000 cells per well).

The percentage cell viability, mean and standard deviation were calculated, and the regression analysis was performed using the GraphPad Prism software. The mean values of the wild type and the isolated clones were compared using one-way ANOVA with Dunnett's multiple comparisons test. Clones with a *P* value less than 0.05 suggests significant changes in sensitivity to docetaxel compared to the wildtype control.

The IC50 value was detected in clones, which produced significant variation as described above in section 2.7.2. The concentration of docetaxel was varied from 50 µM to 0 µM and treated 5,000 cells per well for 72 hours. An MTT assay was conducted after the treatment, and the cell viability Vs log concentration was plotted. Using Prism non-linear regression analysis, the IC50 value of the clones was calculated and compared with the IC50 value of the wild type.

3. Results

This study investigated the efficiency of knocking out the *ABCC10* gene in the Caco-2 cell lines using CRISPR-Cas9 based gene editing. A gRNA designed to target the *ABCC10* gene was transfected with the Cas9 protein. The cleavage efficiency was analysed to determine the extent of transfection. Western Blotting analysis was performed to detect the changes in protein expression. MTT analysis compared the functional differences between the gene-altered single clones and the wild type.

3.1. Gene Alteration with CRISPR-Cas9

3.1.1. Selection of sgRNA and primers

Invitrogen TrueDesign Genome Editor software was used to design the sgRNA sequence. Out of the two sgRNAs generated from in silico analysis, the sequence with the least off-targets (Table 3.1) was selected for the CRISPR-Cas9 system.

Table 3.1. In silico sgRNA design

sgRNA Name	Target Sequence	PAM	Score	Genomic Location	No. of off-targets
ABCC10_C1	ACCCATAGGGCTAGAGGTGT	TGG	98.52	chr6[43432267]	2
ABCC10_C2	TCGCTGGCAATGCCACAACA	CGG	97.87	chr6[43432451]	5

The same software was used to design the primers needed for the PCR amplification flanking the region, including the sgRNA sequence. The system generated Three primer sets (Table 3.2), and the primer pair, which had a melting temperature (Tm) of 58.9 0C, which amplified a 366 bp region, was selected for the PCR amplification. The GC content of the forward primer was 60%, and 55% in the reverse primer.

Table 3.2. In silico Primer Design

Forward Primer (FP)	FP Tm (^{0}C)	Reverse Primer (RP)	RP Tm (^{0}C)	Amplicon Size
AAAGACCCTGGGTTCTGAGG	58.9	GCCAACACCTCTAGCCCTAT	58.9	307
GAGGTGAGGGGTATGTCTGG	58.9	CACAACACGGTCAGCACTAG	58.9	366
TCCTTCCTGCTTTCCGTCTT	58.9	CAGGATGAGCAAGCATAGGC	58.8	315

3.1.2. PCR Analysis

PCR Analysis was performed to amplify the interested 366 bp region, which flanks the sgRNA binding sequence. All the mixtures produced the desired band (Figure 3.1), and the PCR product was used for further analysis. A positive control supplied with the kit (template and primers with a different band size) was used to compare the accuracy of the result.

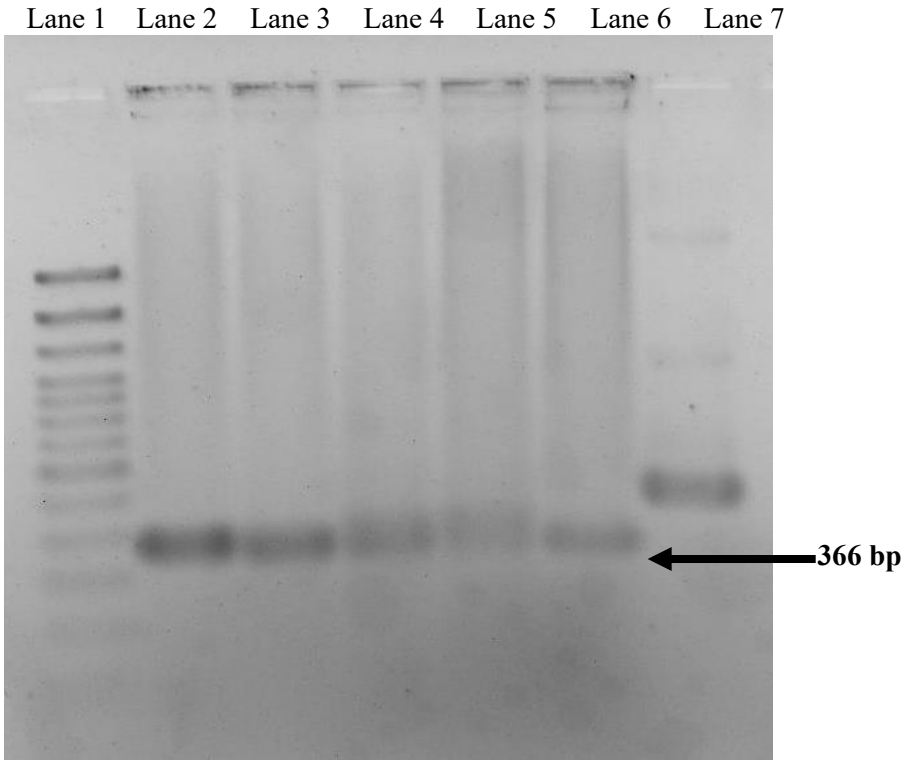

Figure 3.1. Products of PCR Analysis
Note: Lane 1- ladder, lane 2 – 45 pmol/µl sgRNA only, lane 3 - Cas9 only, lane 4 – 15 pmol/µl sgRNA + Cas9, lane 5 – 45 pmol/µl sgRNA + Cas9, treated Caco-2 cells. lane 6 - wild type Caco-2 cells, lane 7 - positive control

The Primers were designed to anneal to the base sequences, as shown in Figure 3.2 below.

```
4441 gagaaaagac cctgggttct gaggtaaagt ggagtaggga taagatgtgc aaggcaggaa
4501 gggagttgat tccttaggta agtgaattat tggaggtgag gggtatgtct ggctcctgag
4561 tcagccacga tgtgcctcct tgtcttcccc cttgtcccca ggagtccaga ttacatccta
4621 ccctgcagtc ctggatggcg cctccgactt gcagcttcct tcctgctttc cgtcttcccg
4681 ctgctagacc ttcttccagt tgctttgcca ccaggggcag gcccaggacc catagggcta
4741 gaggttgttgg cagggtgcgt ggcagctgtg gcctggatca gccacagcct ggccctgtgg
4801 gtgttggcac attcccctca tggccactcc cggggtccct tggccttggc cctggtagcc
4861 ttgctgccag ctccagccct agtgctgacc gtgttgtggc attgccagcg aggcacactt
4921 ctgcccccac ttctcccagg gcccatggcc cgcctatgct tgctcatcct gcagctggct

PRIMERS                                  Cut Site
sgRNA                                    PCR Product 366bp
PAM                                      Digested bands 212bp and 154bp
```

Figure 3.2. *ABCC10* gene sequence amplified by PCR
Note: The PCR amplifies the sequence between the two primers (light blue)

3.1.3. Genomic Cleavage Assay

The PCR product was subjected to further analysis to detect the extent of insertions and deletions (indels) incorporated into the *ABCC10* gene during the CRISPR-Cas9 transfection. Life Technologies GeneArt Genomic Cleavage Detection Kit was used for cleavage efficiency analysis. Only the sgRNA plus Cas9 mixtures (knockout clones) produced the expected band pattern (Figure 3.3), confirming that the CRISPR-Cas9 transfection has been able to generate indels adjacent to the targeted sequence.

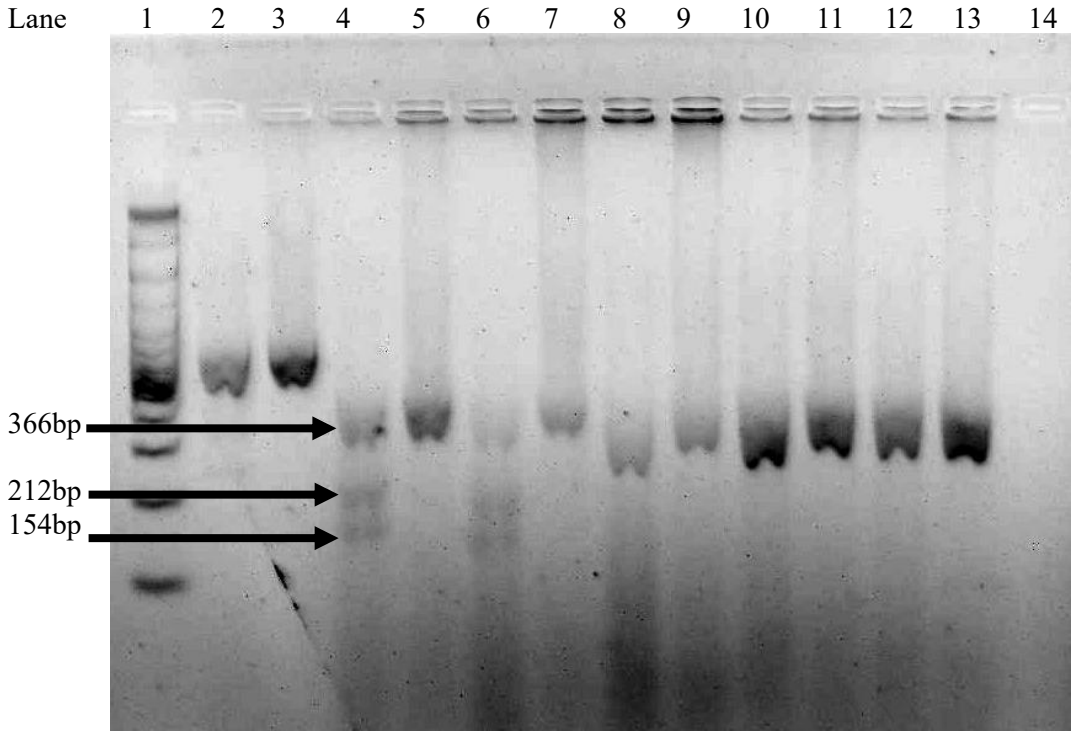

Figure 3.3. Products of Genomic Cleavage Assay
Note: Genomic DNA was extracted from wildtype (WT) Caco-2 cells or Caco-2 cells transfected with Cas9 protein/gRNA ribonucleoprotein complexes targeting human *ABCC10* locus. After re-annealing PCR products, samples were treated with and without T7E1 endonuclease and run on a 2% agarose gel. Lane 1 – ladder, lane 2 – positive control (516 bp in size, provided by Thermo Fisher Scientific, NZ) treated with T7E1 digestion enzyme, lane 3 - positive control (provided by Thermo Fisher Scientific, NZ) without enzyme treatment, lane 4 – T7E1 treated PCR products derived from Caco-2 cells transfected with 15 pmol/µl sgRNA/Cas9 protein , lane 5 - water treated PCR products derived from Caco-2 cells transfected with 15 pmol sgRNA/Cas9 protein; , lane 6 - T7E1 treated PCR products derived from Caco-2 cells transfected with 45 pmol sgRNA/Cas9 protein; , lane 7 - water treated PCR products derived from Caco-2 cells transfected with 45 pmol sgRNA/Cas9 protein , lane 8 – T7E1 treated PCR products derived from WT Coco-2 cells followed by T7E1 enzyme treatment, lane 9 - water treated PCR products derived from WT Coco-2 cells followed by water treatment, lane 10 - T7E1 treated PCR products derived from Caco-2 cells transfected with 45 pmol/µl sgRNA only , lane 11 - water treated PCR products derived from Caco-2 cells transfected with 45 pmol/µl sgRNA only , lane 12 – T7E1 treated PCR products derived from Caco-2 cells transfected with Cas9 only, lane 13 – water treated PCR products derived from Caco-2 cells transfected with Cas9 only, lane 14 – blank

All the reaction mixtures of the PCR were subjected to genomic cleavage assay in the presence of the digestion enzyme and compared with control samples treated with water only. The cleavage bands (212 and 154 bp in size) (Figure 3.3, lanes 4 and 6) is consistent as the predicted (Figure 3.2) and were only detected in T7E1-treated but not in water-treated PCR products, which were derived from Caco-2 cells transfected with Cas9 protein/gRNA ribonucleoprotein complexes targeting human *ABCC10* locus. The water-treated PCR products produced only the parent band (366 bp in size, Figure 3.3, lane 5 and 7), which rules out the possibility of non-specific degradation of PCR products. The T7E1-treated PCR products, which were derived from WT Caco-2 cells (Lane 8), or Caco-2 cells transfected with sgRNA only (lane 10) or Cas9 only (lane 12), generated only the parent band (Figure 3.3), confirming that T7E1-mediated cleavage only occurs in the detection of mismatch mutations. Taken together, this enables us to confirm that the cleavage is exactly due to the indels and that the CRISPR-Cas9 mediated gene editing is on-target.

The sample provided with the kit was used as a positive control (lanes 2 and 3); it produced a band with a different size. This, too, indicates that the reaction has taken place. (If the reaction did not take place accurately, there would not be any bands for the positive control.) However, there are no cleavage bands as it does not have indels.

A reaction mixture with water has been used as the negative control in lane 14; no bands are visible, confirming no contamination.

Only the parent band is visible in the lanes from 8 to 13. Therefore, it confirms that the transfection is successful and can produce indels only in the presence of both sgRNA and Cas9. In the mixtures which have only the sgRNA or Cas9 and in the wild Caco-2 cells, the digestion is not visible as there are no indels incorporated into the amplified target sequence and no Non-Homologous End Joining (NHEJ) has taken place, which leads to the production of blunt ends which is the target of the restriction digestion enzyme.

In lanes 4 and 6, the parent band and two digested bands are observed. The parent band appears at 366bp, and the digested bands are at 212 bp and 154 bp. As the digestion products are better visible in the mixture with 15pmol/µl sgRNA and Cas9 system (lane 4), this product was used for

further analysis (selection of single clones). Therefore, the cleavage efficiency was calculated in this mixture to predict the extent of possible indels incorporated.

The cleavage efficiency was calculated from the results obtained from image J software for each band. According to the calculations, the cleavage efficiency was 13.98 %. Therefore, the CRISPR-Cas9 system has produced indels in the *ABCC10* gene.

Further analysis is needed to detect if this alteration could produce the expected *ABCC10* gene knockout. Therefore, western blotting is performed to check if the protein expression has changed, and the MTT assay is performed to check for any functional changes.

3.2. Selection of Single Clones

The CRISPR-Cas9 transfected Caco-2 cells consist of a mixture of clones. They may have different protein expression and functional levels. Therefore, single clones were separated before further analysis using the limiting dilution method. Next, the single clones were allowed to divide to produce sufficient cells for further analysis. Following limiting dilution, fifteen single clones were isolated. The morphology of the cells after 2,3 and 4 weeks is compared in Table 3.3 below. The figures clearly indicate a variation in these single clones' growth rate and morphology.

Table 3.3. Morphological changes of the single clones

Clone Name	2nd Week	3rd Week	4th Week
1F11	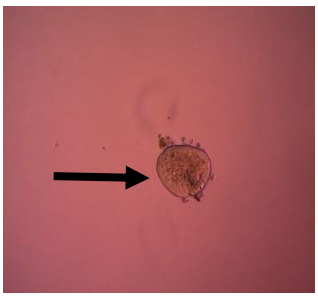	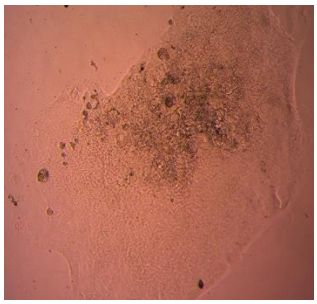	
2D3	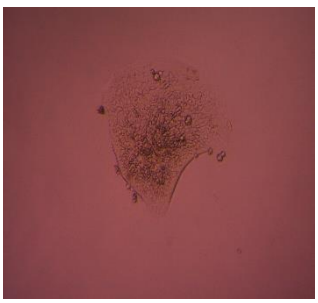		

Clone Name	2nd Week	3rd Week	4th Week
2E5	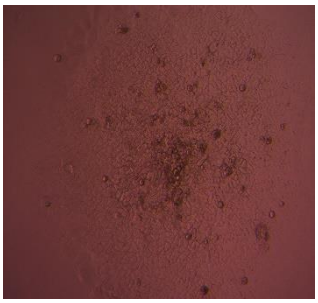	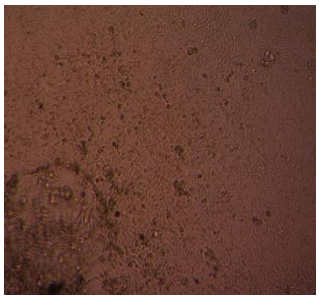	
2G9		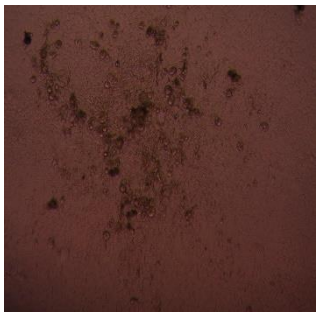	
4D7	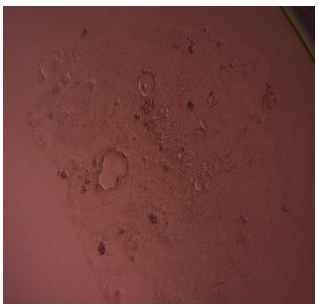	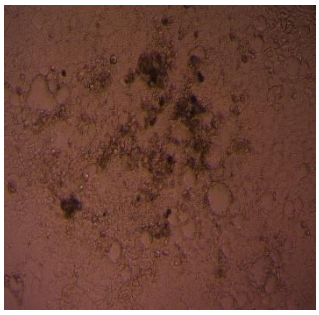	
5C3	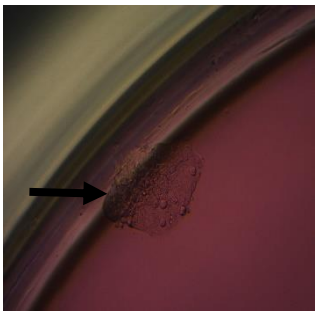	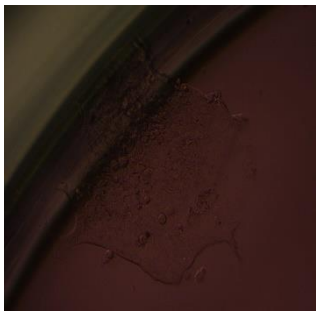	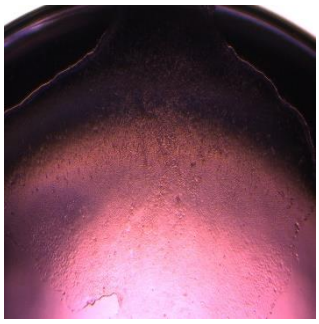
5F2	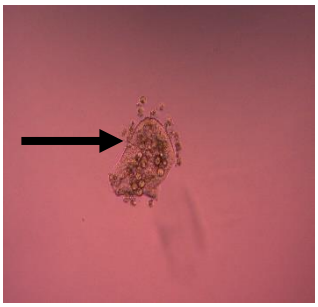	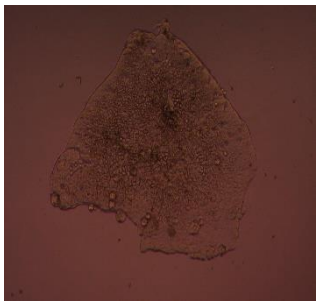	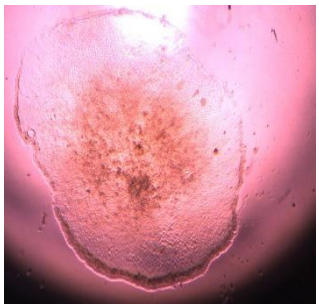

Clone Name	2nd Week	3rd Week	4th Week
5G3	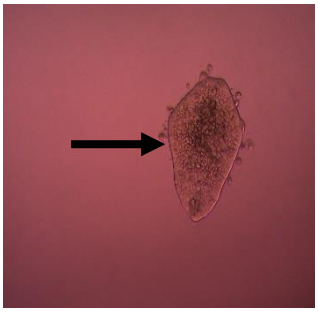		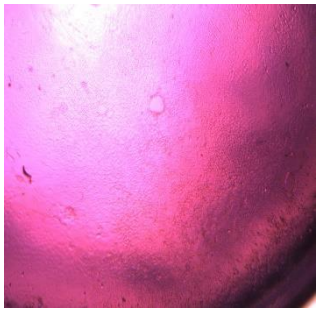
6G2	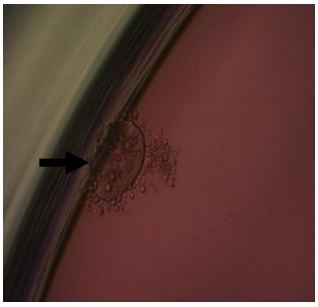		
7B10	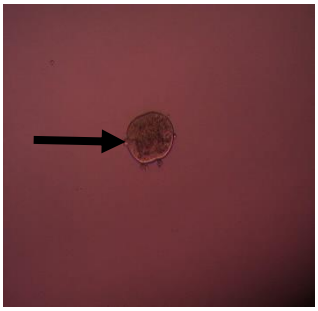		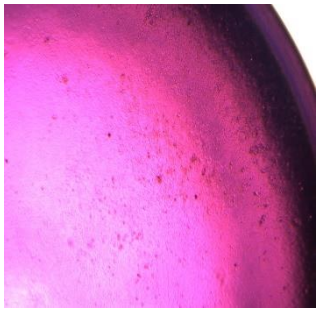
7B11	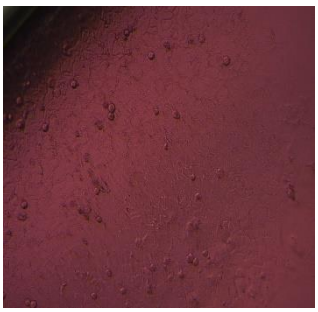	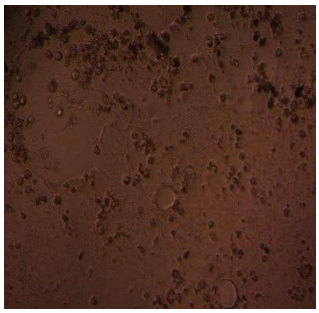	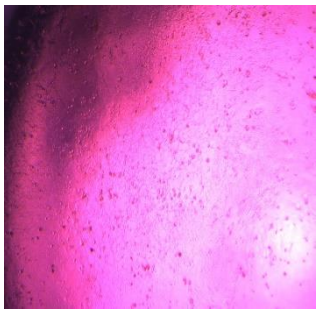
7C9			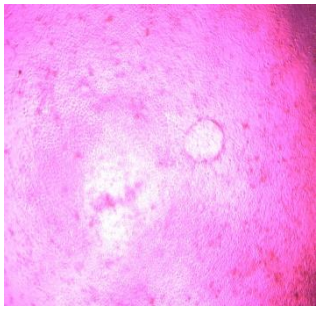

Clone Name	2nd Week	3rd Week	4th Week
7D11	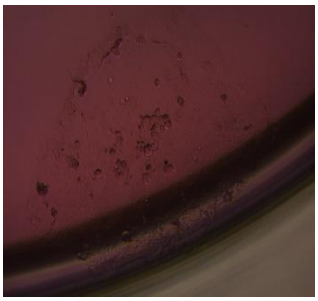	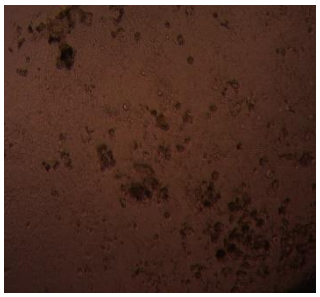	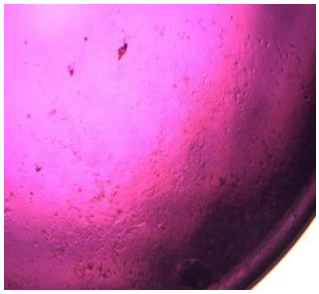
7G6	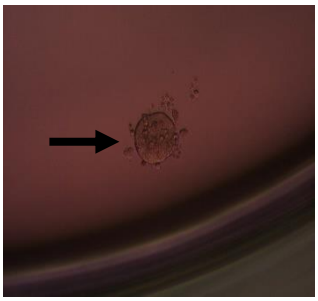		
8B6		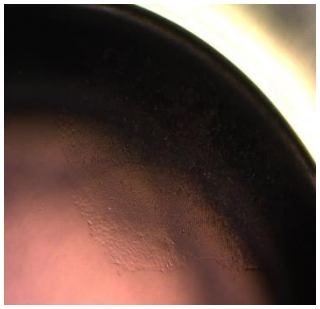	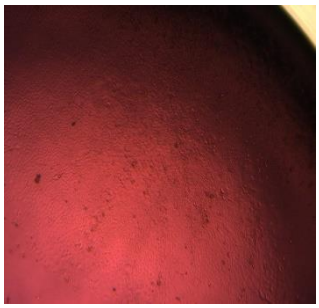

Some of the clones had a speedy growth rate. By the second week, they were spread in a reasonable area in the 96-well plate. By the third week, they were about 50% confluent, and in the fourth week, they were captured at low power (4X) as the cells were spread throughout the well, and the complete area was not visible under high power (10X). In contrast, some colonies were growing very slowly (indicated with arrows). Each of them had a unique morphology. During the first three weeks, they were different from one another. However, once it had reached about 50% confluency, all the colonies were identical.

Once they reached 80% confluency, the colonies were transferred to 12 well plates. When the colonies in the 12 well plates reached 80% confluency, they were divided into two and sub-cultured in 6 well plates. One set was grown for western blotting and the other for MTT assay. When the six-well plates were 80% confluent, transferred to T25 flasks and when sufficient number of cells are available, they were extracted, and the respective tests was performed.

3.3. Western Blotting

Western Blotting analysis compared the protein expression of the wild Caco-2 cells and the isolated single clones. This helps identify whether a complete knockout was generated from the CRISPR-Cas9 transfection.

3.3.1. Protocol development for ABCC10 western blot analysis

As the initial approach, Dithiothreitol (DTT) containing Laemmli sample buffer was used to lyse the wild Caco-2 cells. 350 µl of the DTT lysis buffer was used to extract 80% confluent wild Caco-2 cells grown in a T25 flask. The following results were obtained after western blotting (Figure 3.4).

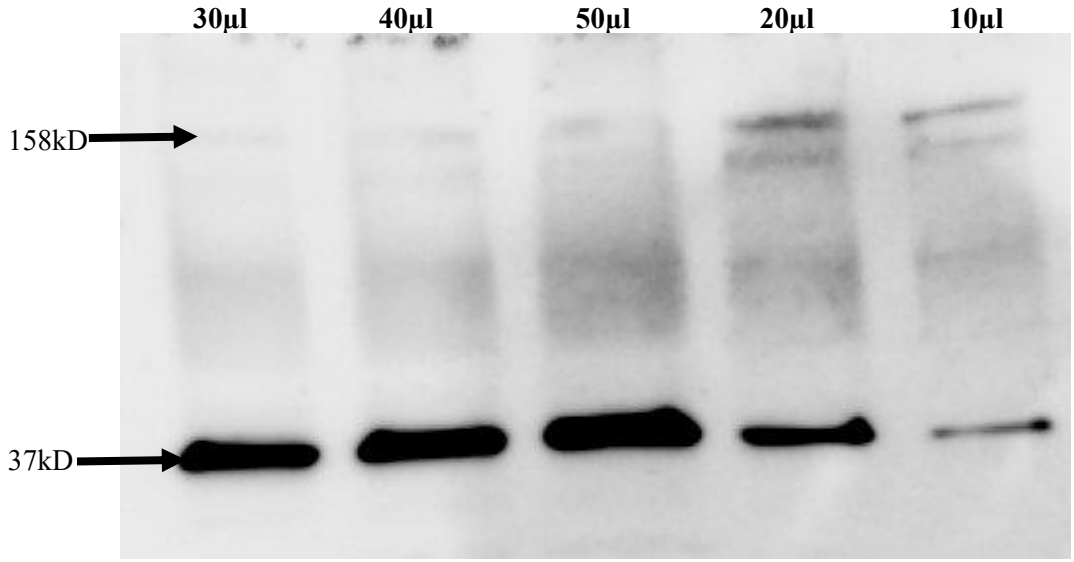

Figure 3.4. ABCC10 signal in DTT cell lysates
Note: Wild Caco-2 DTT lysis buffer cell lysates loaded in different volumes ranging from 10 µl to 50 µl

The band size expected for ABCC10 protein (ABCC10) is ≈ 158 kD. However, the intensity of the desired band was very low in wild Caco-2 lysate extracted from DTT containing Laemmli buffer. Therefore, different buffers were used, and their lysates were subjected to western blotting to select the best lysis buffer, which produces a clear ABCC10 signal.

The wild Caco-2 cells were lysed using different lysis buffers, and before loading into the gel, each lysate was mixed with 1X Laemmli buffer. It contained a dye; therefore, it helped in loading accurately to the wells and helped detect the band's position during electrophoresis.

Lysis solutions prepared with Laemmli buffer, RIPA buffer, 1 mM EDTA + 2% SDS + 10% glycerol + 50 mM Tris-HCl (EDTA buffer), 0.1% Triton-X + 150 mM NaCl + 50 mM Tris-HCl (Triton-X buffer), 150 mM NaCl + 50 mM Tris-HCl (Tris-NaCl buffer) and 50 mM Tris-HCl only (Tris Buffer) was used to lyse wild Caco-2 cells. Western blotting was performed to compare the ABCC10 signal intensity of each cell lysate (Figure 3.5).

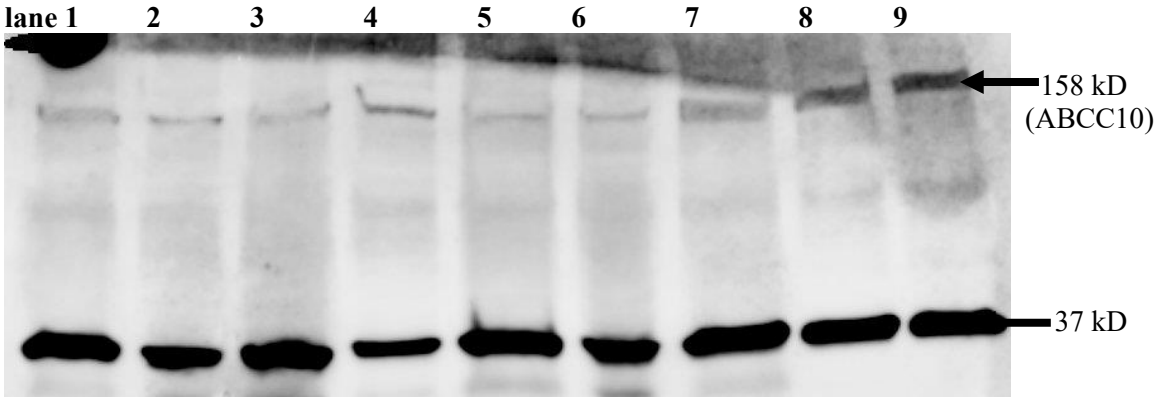

Figure 3.5. Effect of different lysis buffers on ABCC10 signal.
Note:
Lane 1 – 30 µl cell lysate with RIPA buffer + 10 µl Laemmli buffer
Lane 2 – 15 µl cell lysate with RIPA buffer + 5 µl Laemmli buffer
Lane 3 – 30 µl cell lysate with Laemmli buffer
Lane 4 – 15 µl cell lysate with Laemmli buffer
Lane 5 – 30 µl cell lysate with EDTA buffer + 10 µl Laemmli buffer
Lane 6 – 15 µl cell lysate with EDTA buffer + 5 µl Laemmli buffer
Lane 7 – 30 µl cell lysate with Triton-X buffer + 10 µl Laemmli buffer
Lane 8 – 30 µl cell lysate with Tris-NaCl buffer + 10 µl Laemmli buffer
Lane 9 – 30 µl cell lysate with Tris buffer + 10 µl Laemmli buffer

The cell lysate from RIPA, EDTA, and Laemmli buffer was loaded in two volumes (30 µl and 15 µl) to compare if the intensity varied with the amount loaded. There was no significant difference in the ABCC10 signal. However, the band's intensity at 37 kD decreased when the volume loaded was reduced.

The intensity of the interested ABCC10 signal was highest (lane 9) in the cell lysate produced using only 50 mM Tris-HCl (pH=8.00) solution. Therefore, this solution was used to lyse the single clone's cells.

3.3.2. Single clones ABCC10 expression comparison with Western blot

When comparing the ABCC10 expression of the single clones, a lysate from the wild Caco-2 cells was also added to each western blot. 45 µl of each single clone lysate / wild type was mixed with 5 µl of Laemmli buffer before loading. The western blots obtained are given in Figure 3.6 and Figure 3.8 below.

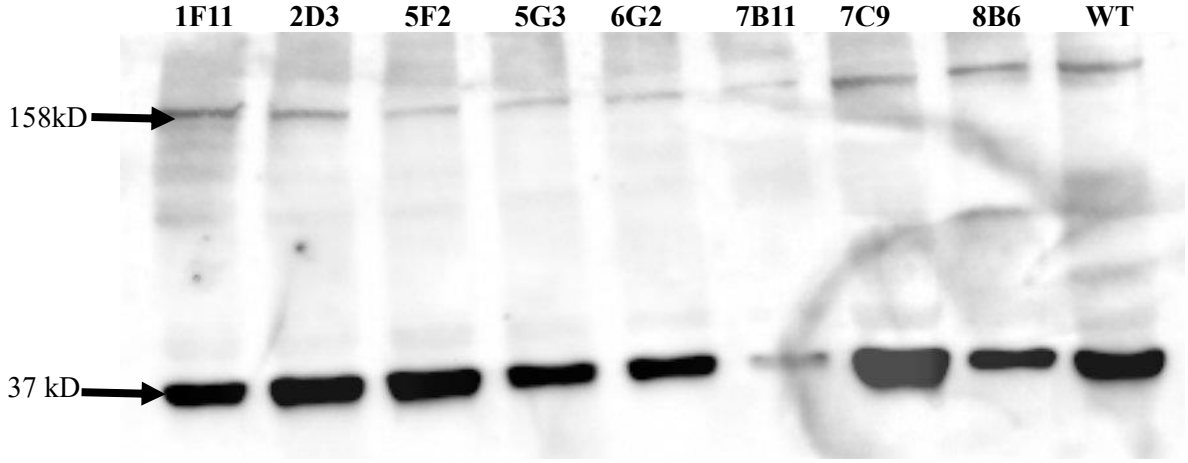

Figure 3.6. Western Blot of Single Clones - Set 1

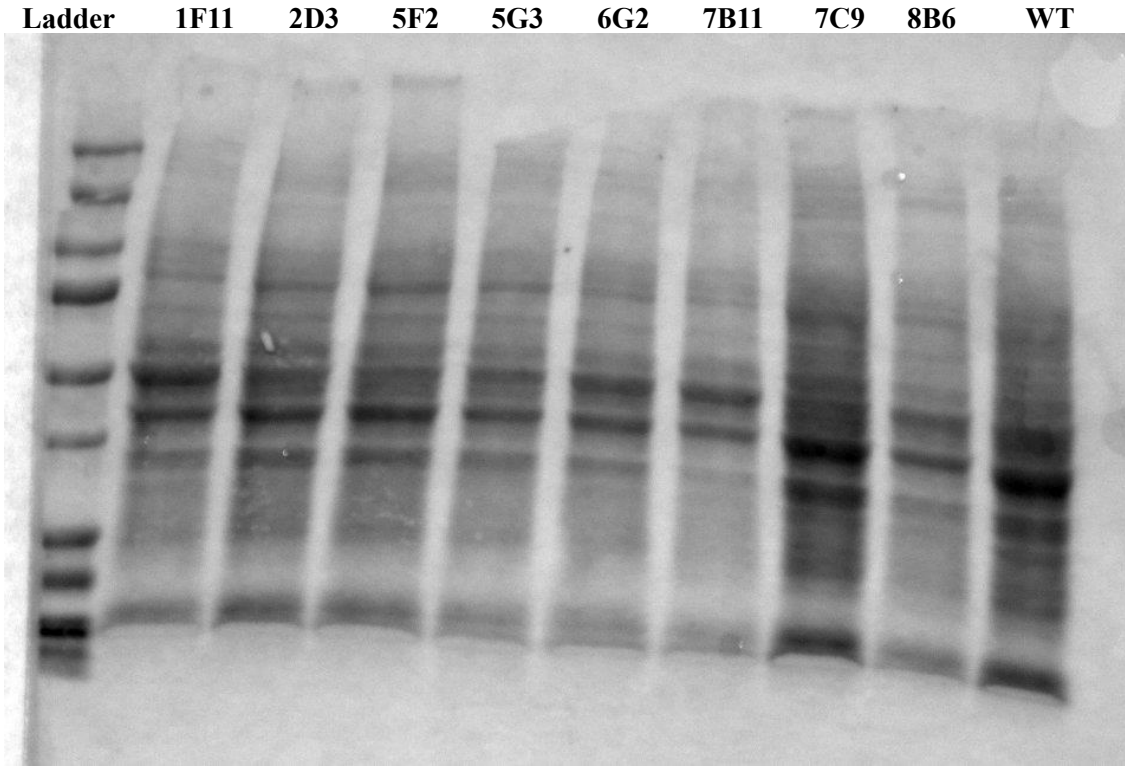

Figure 3.7. Total Protein Image - Clones set 1

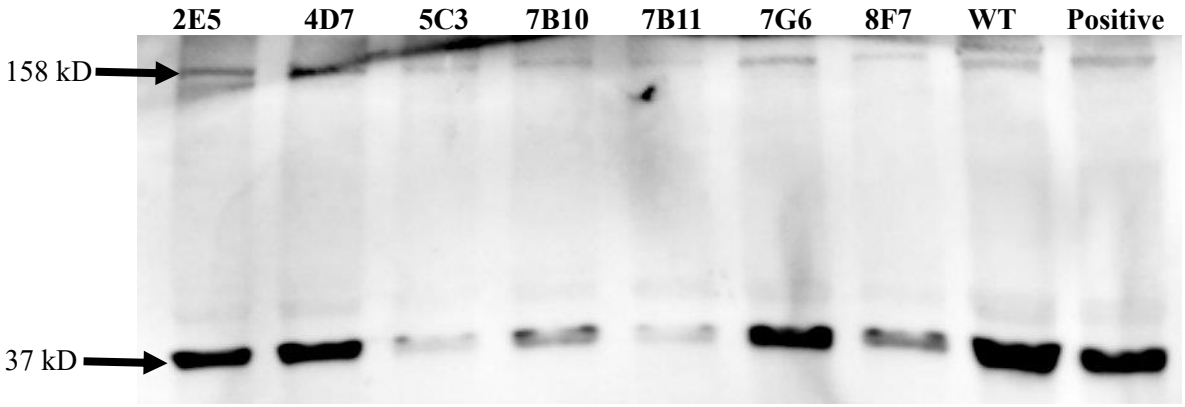

Figure 3.8. Western Blot of Single Clones - Set 2

In the first set of clones, 7B11 produced a light band. Therefore, this sample was repeated with the second set. Again, it produced a band with a lower intensity than the other bands. In the second set, a wild Caco-2 lysate, which produced bands in set 1, was added as a positive control. Therefore, it confirms that all the bands corresponding to 158 kD appear in the same position in all the clones and the wild Caco-2 cells. It confirms that all the single clones isolated produced the signal corresponding to ABCC10. The western blot results show that the ABCC10 protein is expressed in all clones. The total protein analysis is performed as a loading control to normalize the western blot protein band signal. In our experiment as the ABCC10 signal was observed in all clones the total protein analysis is not compulsory. However, we performed a total protein analysis for clone set 1 as clone 7B11 showed very low intensity. The intensities of the bands produced in total protein too was very low for clone 7B11 confirming that the concentration of it is lower compared to other samples (Figure 3.7). Therefore, the reduced intensity of 7B11 in not due to a knockout but due to a dilution or the loaded volume being low compared to others.

3.4. MTT Assay

The MTT assay compares the functional changes that occurred in the single clones due to transfection. The wild Caco-2 cells and the CRISPR-Cas9 transfected cells will be treated with an anticancer drug (Docetaxel), and their cell viability will be compared in this assay.

3.4.1. Linear range detection

This experiment aims to determine the range in which the cell number is proportional to the absorbance. The results obtained are shown in Table 3.4 below.

Table 3.4. Linearity Range Detection

Cell number per well	Absorbance
0	0.000
1000	0.159
2000	0.146
4000	0.282
8000	0.507
16000	0.850
32000	1.246
64000	2.743

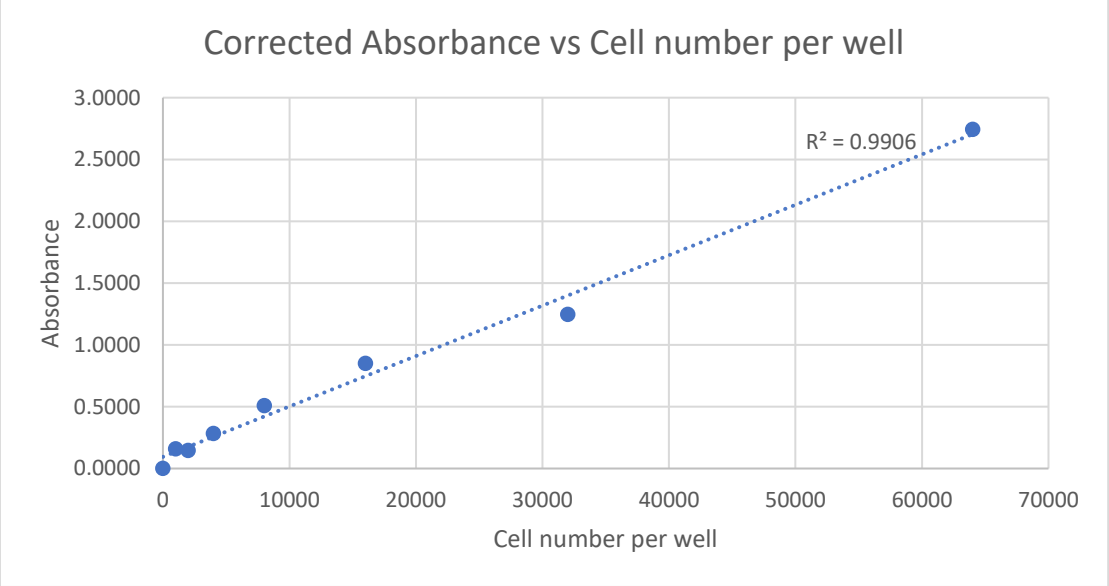

Figure 3.9. Linearity Range Detection

According to the results obtained from a 24-hour analysis, the cell number per well can be varied between 1,000 and 64,000 as they are all within the linear range. Therefore, for the MTT assay developed, the number of cells seeded was either 5,000 or 10,000, as they both fall within the linear range.

3.4.2. Protocol Development of MTT Assay for IC50 Detection

As the first step of MTT assay development, a wide concentration range of the anticancer drug (docetaxel) was used to treat the wild Caco-2 cells. 10,000 Caco-2 cells per well were grown for 16-24 hour. 100 µl of docetaxel was added to each well. (To obtain a final concentration range

from 100 µM to 0 µM). After 24 hours, the MTT assay was performed, and the results are given below in Table 3.5 and Figure 3.10.

Table 3.5. Percentage cell viability of 10,000 Caco-2 cells treated with docetaxel for 24 h

Conc (µM)	100	50	25	12.5	6.25	3.125	1.563	0.781	0.391
% cell viability	26	58	92	124	128	117	121	115	131
Conc (µM)	0.195	0.098	0.049	0.024	0.012	0.006	0.003	0.002	0.000
% cell viability	78	83	87	86	86	90	90	93	100

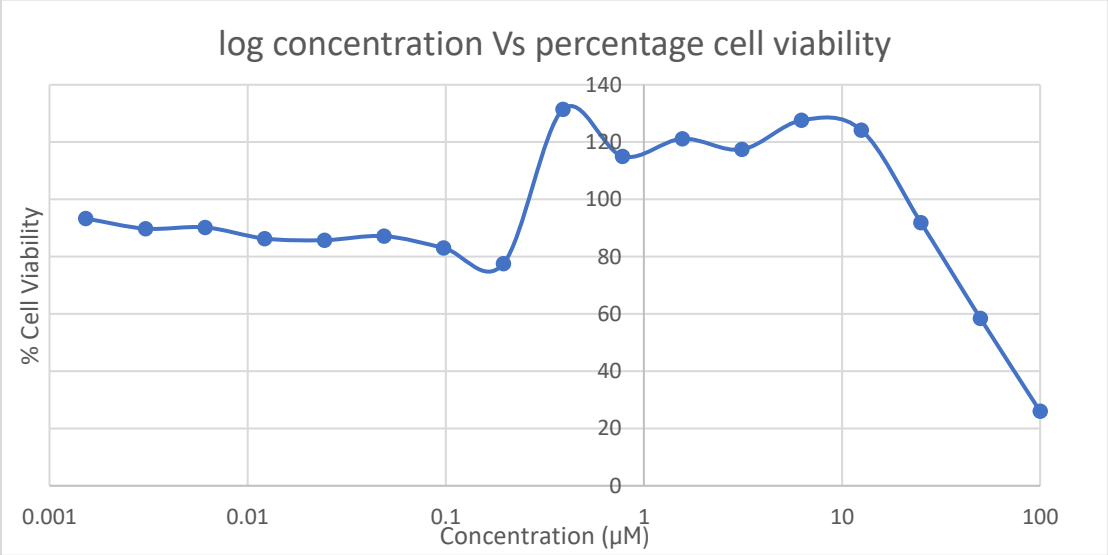

Figure 3.10. Percentage cell viability of 10,000 Caco-2 cells treated with docetaxel for 24 h

From the results obtained above, we noticed that the concentrations of docetaxel needed to obtain 50% cell viability can be narrowed. Therefore, further testing was conducted using Docetaxel concentration ranging from 100 µM to 1 µM. Furthermore, as the doubling time of Caco-2 cells is longer, docetaxel-treated cells were incubated for 72 hours before the MTT assay. The results obtained are given below in Table 3.6 and Figure 3.11.

Table 3.6. Percentage cell viability of 10,000 Caco-2 cells treated with docetaxel for 72 h

Concentration (µM)	100.00	50.00	25.00	12.50	6.25	3.13	1.56	0.78	0.00
% Cell viability	0.70	50.73	60.92	63.13	69.01	63.60	49.92	48.62	100.00

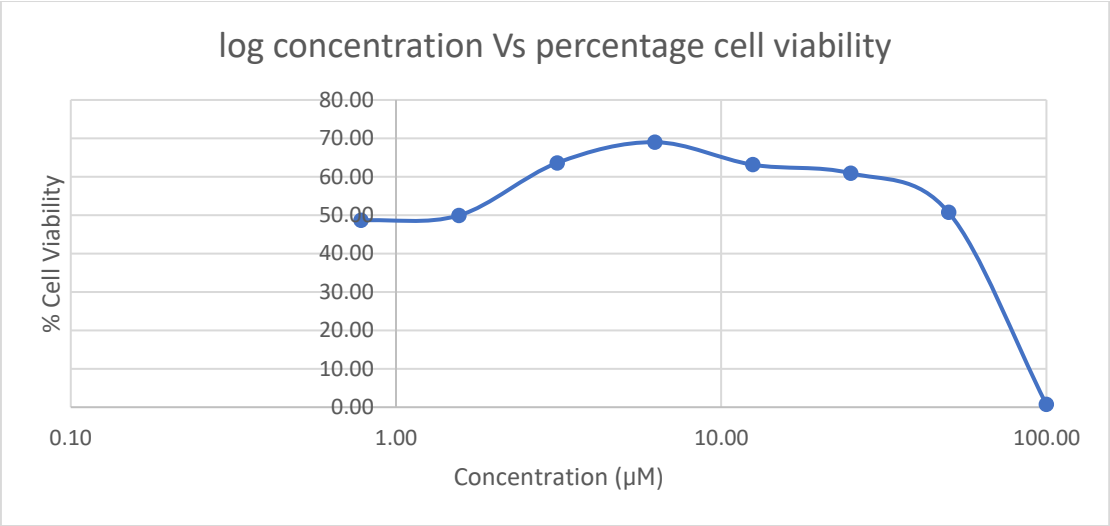

Figure 3.11. Percentage cell viability of 10,000 Caco-2 cells treated with docetaxel for 72 h

As there was a decrease in cell viability when treated with Docetaxel concentration range from 3.13 µM to 0.78 µM compared to higher concentrations (50 µM to 6.25 µM), the experiment was repeated using 5,000 Caco-2 cells per well. The results obtained are displayed below in **Error! Not a valid bookmark self-reference.** and Figure 3.12.

Table 3.7. Percentage cell viability of 5,000 Caco-2 cells treated with docetaxel for 72 h

Concentration (µM)	100.00	50.00	25.00	12.50	6.25	3.13	1.56	0.78	0.00
Mean % Cell viability	0.66	7.53	27.00	30.61	41.37	49.10	51.78	52.55	100.00
SD	0.339	1.963	3.674	5.129	7.946	5.236	2.299	1.947	5.018

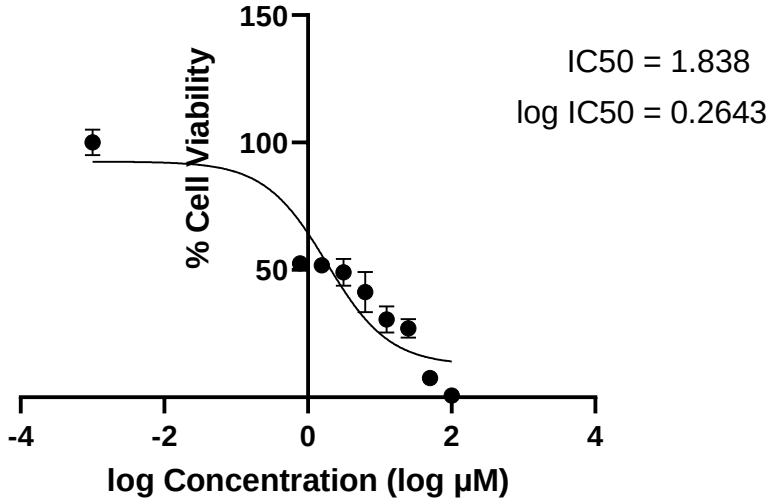

Figure 3.12. Percentage cell viability of 5,000 Caco-2 cells treated with docetaxel for 72 h
Note: IC50 of docetaxel on wild Caco-2 ≈ 2.0 µM (calculated using Prism software).

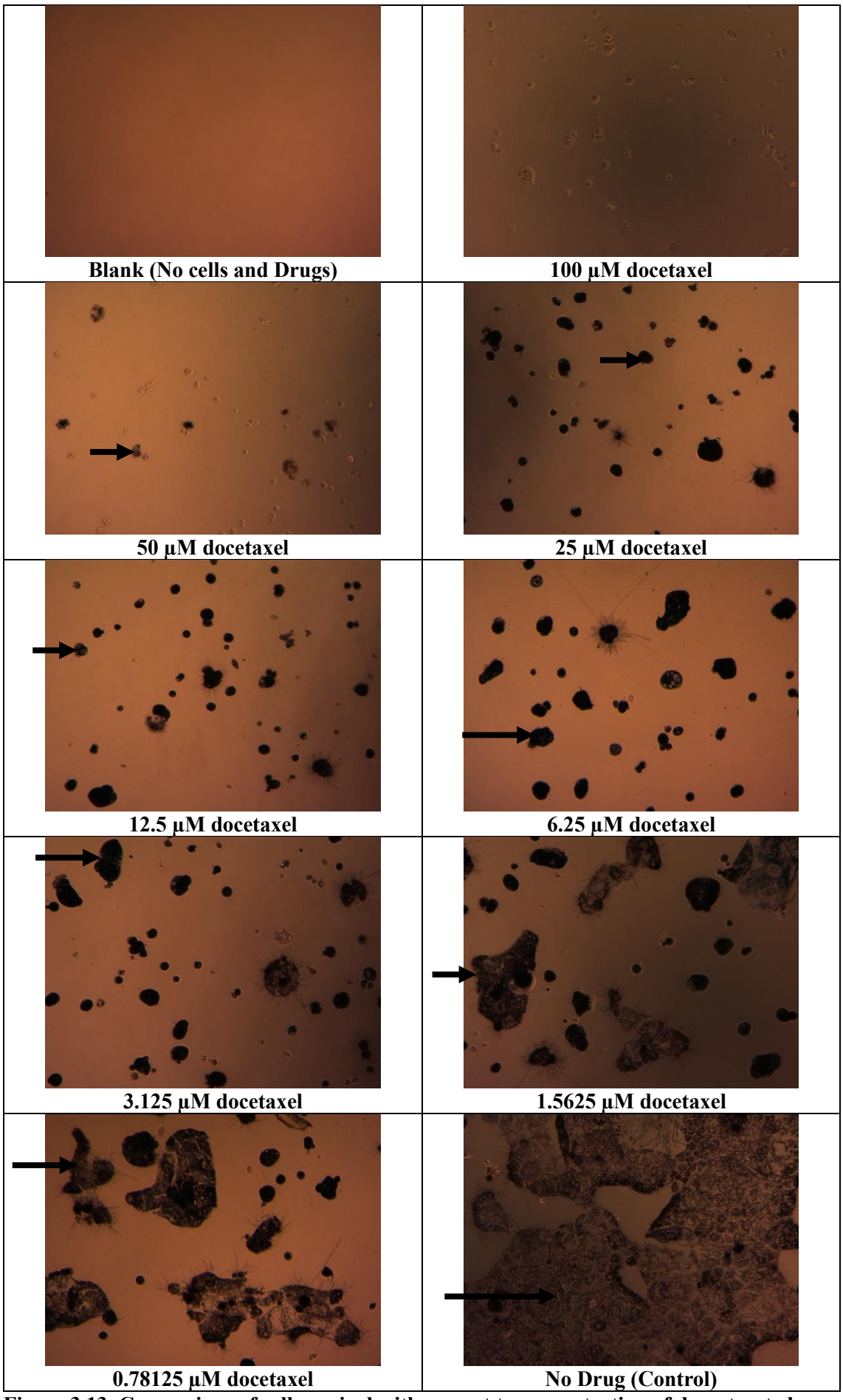

Figure 3.13. Comparison of cell survival with respect to concentration of drug-treated

There was a visible change in the number of cells that survived; when the concentration of docetaxel treated was reduced from 100 µM to 0 µM, the amount of wild Caco-2 cells that survived gradually increased. The cells were observed under the microscope (10X power) after adding MTT. The surviving cells (pointed with arrows) were clearly visible in dark blue (Figure 3.12). The amount of blue colour cells increases with decreasing drug concentration. Therefore, the comparison was easy. If the images were obtained before MTT treatment, the comparison would not be evident as the cells would not be stained. After adding DMSO to the cells reacted with MTT, the formazan produced will be solubilized, and a gradient of purple colour is produced in the 96-Well plates (Figure 3.14) from blank (column 2) and when moving from docetaxel concentration 100 µM to 0 µM (column 3 to column 11).

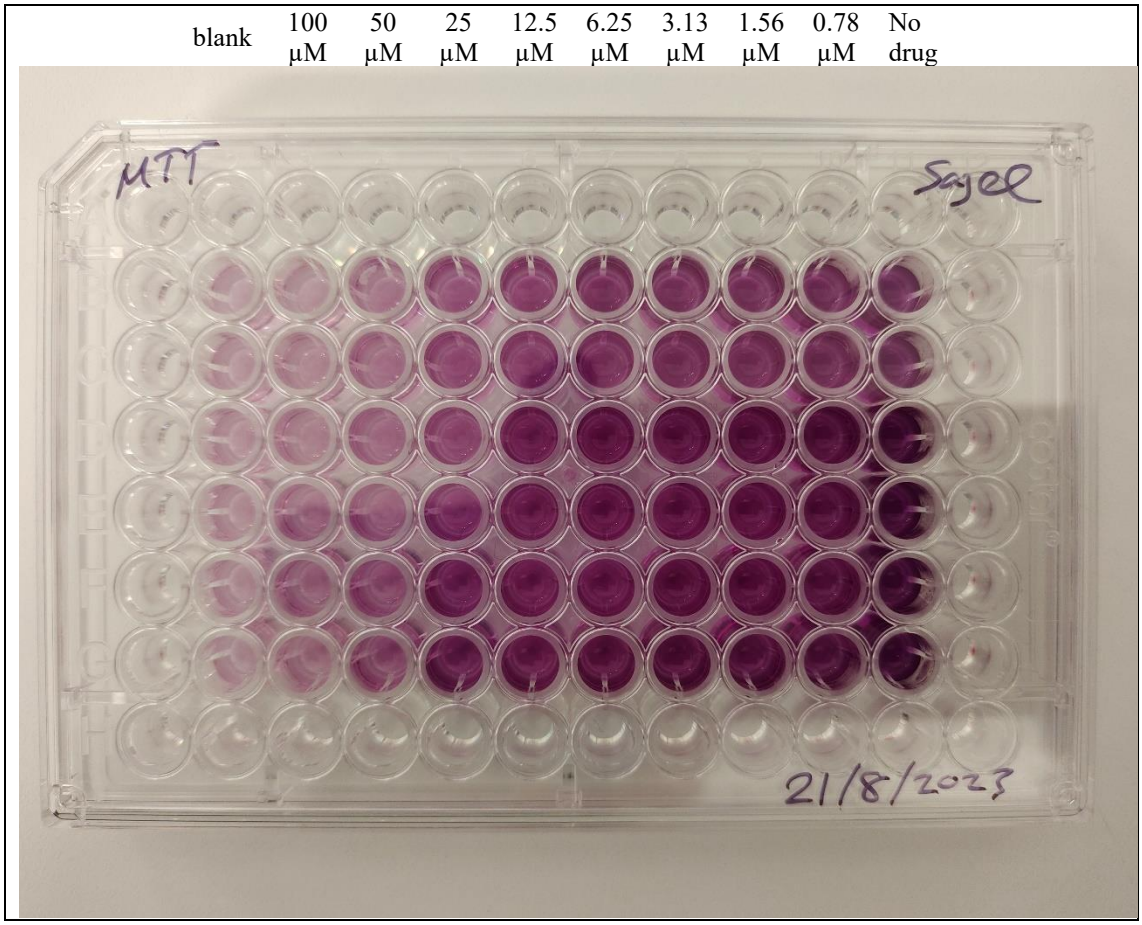

Figure 3.14. IC50 detection of docetaxel for wild Caco-2 cells (96-Well plate following MTT assay)

According to the results obtained following Prism analysis, 50% of wild Caco-2 cells survived when 1.838 µM of docetaxel was treated (Figure 3.12). This value obtained from the software also matched the results of Table 3.7 and Figure 3.12.

3.4.3. Comparison of cell viability of the single clones

All clones isolated were treated with 2 µM docetaxel (IC50 of wild Caco-2 cells), and the cell viability was compared with wild Caco-2 cells. The results obtained shown in Figure 3.15 A - D.

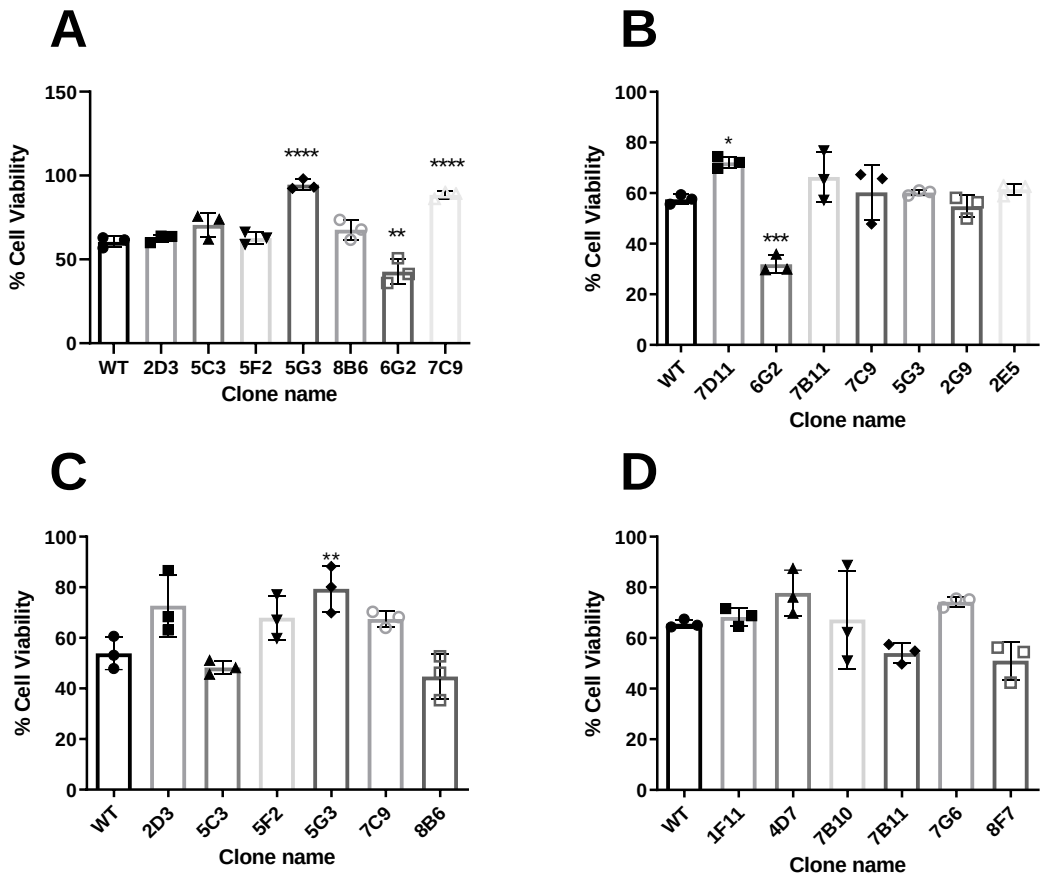

Figure 3.15. Cell viability variations among Caco-2 cell clones treated with docetaxel (2 µM) for 72 h.
Note: * = P < 0.05, ** = P < 0.01, *** = P < 0.001, **** = P < 0.0001
The shapes indicate the values of the triplicated results.

Following the ANOVA test, clones 5G3, 6G2, 7C9, and 7D11 displayed significant variations in cell viability compared to the wild Caco-2 cells. Among them, only 6G2 was shown to have significantly reduced the % cell viability (increasing the death rate of cancer cells) following the treatment. Therefore, only the clone 6G2 has increased the sensitivity for docetaxel. Detailed results from the ANOVA are attached in ANNEX tables A to D.

A concentration gradient of docetaxel varying from 50 µM to 0 µM was used to treat 5000 cells of clone 6G2 for 72 hours the results obtained was compared with the response of wild Caco-2 cells treated with docetaxel (Figure 3.16).

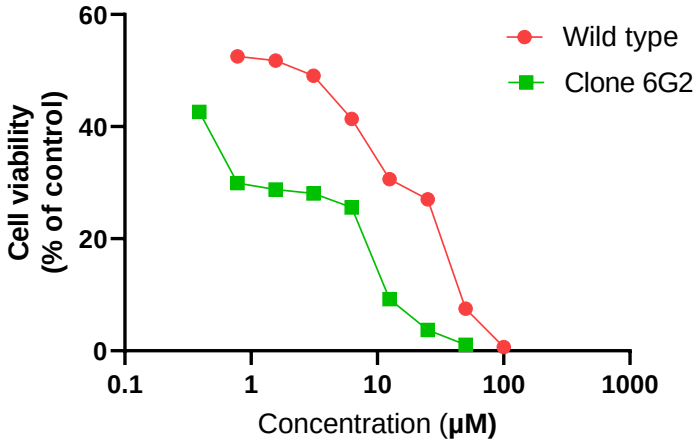

Figure 3.16. Cell viability of WT and clone 6G2 in different docetaxel concentrations

The cell viability of clone 6G2 showed reduced cell viability compared to the wild Caco-2 cells treated with the same concentration of docetaxel. Sensitivity towards docetaxel has increased following CRISPR-Cas 9 transfection. Therefore, the IC50 value was calculated to determine the extent of the increased sensitivity. The IC50 of docetaxel was detected by treating 5000 cells of clone 6G2 per well. The concentration of docetaxel was varied from 50 μM to 0 μM. Following 72 hours of incubation, an MTT assay was performed (Table 3.8). The IC50 value had been reduced by approximately ten-fold compared to the wild type (Figure 3.17).

Table 3.8. Percentage cell viability of 5,000 cells 6G2 clone treated with docetaxel for 72 h

Concentration (μM)	50.00	25.00	12.50	6.25	3.13	1.56	0.78	0.39	0.00
Mean % Cell viability	1.08	3.73	9.23	25.57	28.06	28.80	29.94	42.63	100.00
SD	1.293	1.519	2.422	7.714	10.324	6.814	12.920	5.597	13.724

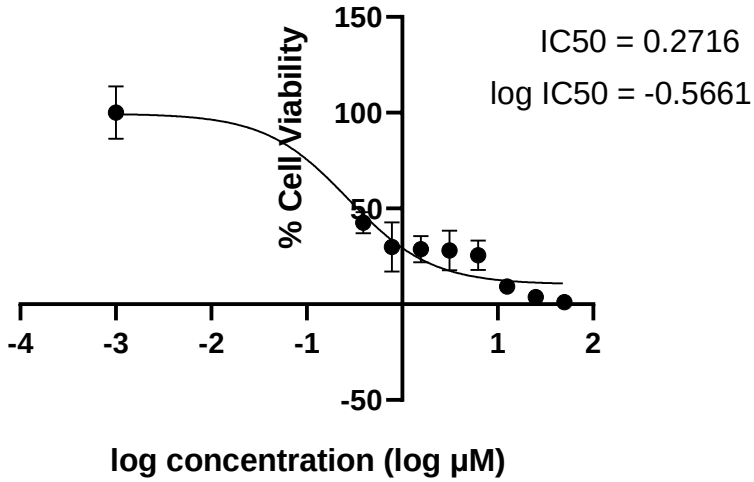

Figure 3.17. Concentration-dependant effect of docetaxel on clone 6G2 (5000 cells per well)

4. Discussion

4.1. Introduction

Colorectal cancer is the third most prominent cancer detected worldwide. According to the data published in GLOBOCAN 2022, Colorectal cancer has the highest incidences reported in New Zealand in 2022. Despite all the new health advances, the incidences are increasing annually. It is prevalent among older adults. Therefore, the increase in life expectancy and lifestyle patterns may contribute immensely to this increase in prevalence reported throughout these years. Furthermore, diagnosis is difficult as the cancer will have spread to a later stage when the symptoms are evident.

There are several treatments for colorectal cancer, out of which chemotherapy plays a crucial role. New Zealand and international clinical practice guidelines, based on robust evidence from randomised controlled trials, now recommend oxaliplatin-based chemotherapy as the preferred regimen for the treatment of metastatic colorectal and other GI cancer types. However, chemotherapy fails to induce durable tumour responses in ~50% of GI cancer patients whose tumours progress early during initial treatment or soon after a short-lived response. Due to the action of multi-drug resistant proteins, the anticancer drugs are prevented from entering the cells. Therefore, the drugs are unable to destroy the cancer cells.

Docetaxel is one of the prominent anticancer drugs used to treat multiple cancers. Pre-clinical studies have shown docetaxel induced significant anti-tumour activities in various colon cancer models (Bissery et al., 1991; Riou et al., 1992). However, it has shown less effect in clinical trials (Clark et al., 1998; Pazdur et al., 1994; Sternberg et al., 1994). Multi-drug resistance is one of the primary reasons for the reduced efficiency in human studies.

The multi-drug resistant protein 7 (MRP7/ABCC10) is the only ABCC transporter that is reported to be responsible for the drug resistance induced in the drug group taxane (Hopper-Borge et al., 2004). Docetaxel and paclitaxel are the main drugs that fall under this group. Furthermore, RT/PCR analysis of ABCC10 has demonstrated that ABCC10 is expressed in colon tissues

(Hopper et al., 2001). Therefore, ABCC10 could have a significant effect on the resistance development toward docetaxel in the treatment of colorectal cancer.

CRISPR-Cas9 is a novel gene editing technique using gRNA and a cas9 protein to incorporate changes into a targeted gene sequence. Previous studies have successfully produced other ABC transporter gene knockouts by using CRISPR-Cas9 (Feng & Huang, 2022), thereby our current project is to explore the feasibility of silencing ABCC10 in human Caco-2 cells by using liposome-mediated delivery of Cas9 protein/gRNA ribonucleoprotein complexes targeting human *ABCC10* locus The effect of silencing ABCC10 on docetaxel sensitivity is also investigated in current project.

4.2. Major Findings of the Study

The Caco-2 cells were transfected with the gRNA selected from in silico analysis (the gRNA with the least number of off-targets). After allowing the clones to grow, fifteen separate clones were identified following limiting dilution.

All the surviving clones were extracted, and the western blotting analysis was performed. The signal corresponding to ABCC10 was observed in the wild Caco-2 cells and all the clones tested. Therefore, the ABCC10 protein is expressed in all the clones even after transfection.

Next, the IC50 value of docetaxel treated for 72h on 5,000 wild Caco-2 cells was identified as 2µM. Therefore, 5,000 cells of all the clones identified were treated with 2µM docetaxel for 72h, and their cell viability was detected. ANOVA was performed to compare the cell viabilities with respect to the wild Caco-2 cells, and only the clones 5G3, 6G2, 7C9, and 7D11 displayed a significant ($P<0.05$) variation.

Only clone 6G2 significantly reduced the cell viability out of the clones tested. Therefore, it was treated with a concentration range of docetaxel for 72h, and its IC50 value was detected. At all concentrations, the cell viability of clone 6G2 was lower than wild Caco-2 cells (Figure 3.16). The IC50 value of clone 6G2 was detected as 0.27, whereas it was 1.84 in the wild Caco-2 cells. Therefore, the sensitivity towards docetaxel has increased approximately tenfold following the CRISPR-Cas9 transfection.

However, even the clone 6G2 produced a signal corresponding to ABCC10 in the western blotting analysis. Therefore, we can assume that following the CRISPR-Cas9 transfection, a heterozygous change is created in the *ABCC10* gene, producing a lower amount of ABCC10 protein than the wild type. Sequencing could have confirmed this assumption, which we could not do due to limited time.

Furthermore, the above findings agree with the results of the cleavage assay. The cleavage efficiency was calculated to be approximately 14%. Therefore, only one produced the expected results from all the clones identified. Though there was no complete knockout, this process produced a clone more sensitive to docetaxel than the wild type.

Therefore, it confirms that CRISPR-Cas9 has successfully increased the antitumor activity of docetaxel by inhibiting the function of the ABCC10 protein. Therefore, the findings of this study will be helpful in further analysis and development of docetaxel in clinical studies.

4.3. Active transportation of Docetaxel via ABCC10

ABCC10 is a recently identified multi-drug-resistant protein family member in the basolateral membrane and belongs to the long MRP subfamily. According to previous studies, it has generated resistance towards many natural products and anticancer drugs. However, it is reported to be the only member of the MRP family that has generated resistance towards the anticancer drug family taxane. It has shown resistance towards docetaxel and paclitaxel (Hopper-Borge et al., 2004).

In the presence of ABCC10 inhibitors, the sensitivity towards docetaxel has increased. Previous studies have proven that in the presence of epidermal growth factor receptor inhibitors (Lapatinib and Erlotinib) (Kuang et al., 2010), Phosphodiesterase type 5 inhibitors (sildenafil and vardenafil) (Chen et al., 2012) and third-generation ABCB1 inhibitor, Tariquidar the sensitivity towards docetaxel has increased in HEK 293 cells (Sun et al., 2013).

However, in another study, ABCC10 knockout mice treated with docetaxel showed increased drug accumulation and hypersensitivity reactions (Hopper-Borge et al., 2011). It is suggested that ABCC10 transporters (MRP7) are necessary for cell functioning. Therefore, complete knockout may lead to a lethal reaction. However, limiting the ABCC10 function to increase the sensitivity

towards anticancer drugs will be a better solution than complete knockout. Therefore, the clone obtained in this study may have more desired properties. Further studies are necessary to evaluate its efficiency and possible toxic reactions generated in animal modules.

4.4. Improvement of chemotherapy with gene editing

Chemotherapy is one of the primary cancer treatments performed. It is done for patients who have undergone surgery and those for whom surgery is not possible. It is done before surgery to reduce the number of affected areas to make the surgery easier. Also, if it is done after surgery, its primary purpose is to remove the cancerous cells left from surgery and to increase the survival rate or delay the death.

Despite the importance of chemotherapy in cancer treatment, it has one primary concern, which is drug resistance, which makes it less effective during treatment. During preclinical studies, docetaxel showed a significant effect in the treatment of colon cancer in murine (Bissery et al., 1991; Riou et al., 1992). However, clinical trials have not shown promising results when treating colorectal cancer patients (Clark et al., 1998; Pazdur et al., 1994; Sternberg et al., 1994). The multi-drug resistance is one reason for the reduced efficiency of anti-cancer drugs.

In addition, Neutropenia was the most common dose-related toxicity associated with docetaxel. Other toxicities, such as hypersensitivity reactions, Mucositis, and Alopecia, develop when the dose increases (Burris et al., 1993; Pazdur et al., 1992).

Both the above drawbacks of chemotherapy can be reduced by using gene editing. The function of the proteins responsible for drug resistance is removed by altering the gene. At the same time, as the sensitivity towards the drug increases, a lower dose can produce the same effect, done using a higher dose before gene editing. Therefore, the dose-related toxicities will be eliminated, and the patient's quality of life will be increased.

In this study, ABCC10 was selected as the gene target as it is the only multi-drug resistant protein that confers resistance towards docetaxel. By altering the MRP7/*ABCC10* gene, the efflux of the drug has been reduced. The accumulation of the drug has increased. Therefore, the sensitivity for the drug has increased, and the same anticancer effect is observed using a lower drug dose.

Therefore, this study confirms that chemotherapy and gene editing effectively reduce tumour cell growth. Therefore, combining gene editing and chemotherapy using in vitro CRISPR-Cas9 is feasible. However, further studies are necessary to implement this approach in animal models and clinical trials.

4.5. Gene knockout efficiency and off-target effect

According to previous studies and according to the findings of this study, it is evident that CRISPR-Cas9 has excellent therapeutic potential in generating gene knockouts. However, despite all its benefits, this technique has a significant drawback known as the off-target effect. These are mutations generated by binding the gRNA to DNA sequences with less-than-perfect complementary sites (Hsu et al., 2013).

According to previous studies, to minimise off-target effects, the sgRNA should be designed to match precisely to the Protospacer Adjacent Motif (PAM) sequence NGG and the "Seed sequence," which is 8 to 12 bases from the 3' end of the gRNA (Mali et al., 2013). It is also reported that the mismatches in the PAM-proximal sites are less tolerated than the PAM-distal mismatches (Zheng et al., 2017).

It is reported that up to five mismatches in the gRNA can be tolerated (Fu et al., 2013). However, it is recommended to perform sequencing on the target cell line before the experiment to check if it matches the sequence generated from in silico analysis software (Campenhout et al., 2019). For example, reports show that the commonly used cell line HeLa displayed a different gene expression pattern compared to the Human cells (Landry et al., 2013).

The gRNA should be designed to have a higher GC content to prevent off-target effects. GC content between 40%-60% is ideal as higher GC content will stabilize the DNA-RNA duplex (Naeem et al., 2020). Furthermore, according to research, at position 20 of the gRNA, Guanine is preferred, and at position 16, Cytosine is preferred to increase on-target editing (Doench et al., 2014).

To minimize off-targets, the gRNA should be designed to target the N-terminal coding exons of the protein-coding gene (Shi et al., 2015). Furthermore, the knockout experiment should be

designed to disrupt the exon shared by all variants of the specific gene (Endo et al., 2015). The genetic polymorphisms in the target region (Endo et al., 2015) and the SNP in the PAM region should be considered as they may affect the Cas 9 binding (Zheng et al., 2017).

Apart from the base pair sequence, the chromatin structure also affects the binding of Cas9 in vertebrates. Nucleosomes are the basic units of chromatin. It is reported that Cas9 is found to bond to regions with low nucleosome content (Horlbeck et al., 2016). Furthermore, studies have demonstrated varied effects on Cas9 binding depending on whether it is an open chromatin (Euchromatin) or a closed chromatin (Heterochromatin). Closed chromatin hinders Cas9 binding at the target site and editing the specific target (Daer et al., 2017).

As mentioned above, the gRNA and the Cas9 protein are essential for proper targeting. Therefore, improved Cas9, too, has been engineered to reduce off-target effects. A study has demonstrated a reduced off-target effect using a Cas9 nickase mutant and paired gRNA, which binds to two locations. Therefore, it increases the number of bases required for recognition and decreases off-targets by 50 to 1500 fold (Ran et al., 2013).

Also, when the single clones are obtained from the limiting dilution method, the dilution process should be conducted as soon as the transfection is completed. This is because the non-edited wild-type cells will outgrow the knockouts if the transfected cells are left to grow for a long time. Finally, the isolated single clone should be sequenced to identify on-targets and changes to the sequence following the transfection (Campenhout et al., 2019).

4.6. Future Directions

In this study, the clone 6G2 had shown a significant increased sensitivity towards docetaxel compared to the wild-type control. However, the wild type and the clone 6G2 have produced the signal corresponding to ABCC10 protein in the western blot analysis. Therefore, clone 6G2 may be a heterozygous of ABCC10 knockout. This could be confirmed by performing a genomic sequence analysis and comparing the sequences of the wild type, 6G2 clone and the proposed knockout. On the other hand, it has been reported that residual protein expression occurred in HAP1 cells for about one third of the genetically verified CRISPR knockouts (Smits et al., 2019).

Two causal mechanisms have been proposed, including 1) translation reinitiation leading to N-terminally truncated target proteins or 2) skipping of the edited exon leading to protein isoforms with internal sequence deletions.

Furthermore, the western blot analysis produced two signals for each sample. The signal that corresponds to the ABCC10 appeared around 158 kD, and a second signal appeared around 37 kD. Therefore, further analysis is required to identify the reasons for the 37 kD signal. Different ABCC10 antibodies can be tested, which bind to different locations of the ABCC10 protein to detect if the band is available in all cases. Also, different cell lines can be compared to check whether the pattern is common to all tissues when using the same antibody and if it is still available with different antibodies. Furthermore, it must be analysed if the 37 kD band is available even in the knockout. Typically, a known western blot target such as the PDL-1 or the total protein analysis is used as a positive control to compare the signals of the knockout. Therefore, further analysis must be performed to detect the ability to use the 37 kD band as an internal control of the western blot in a knockout clone.

In this study, the MTT assay was performed to detect the IC50 of docetaxel following 72 hours of treatment. Five thousand cells per well of both wild-type and knockout clones were tested, and it was identified that clone 6G2 had significantly higher sensitivity towards docetaxel compared to the wild-type. Several inhibitors of ABCC10 have been identified so far. Further analysis could be performed to check the IC50 of docetaxel on wild Caco-2 cells in the presence of the inhibitors. From such a study, we could predict whether the ABCC10 knockout clone is more efficient in increasing the sensitivity compared to the ABCC10 inhibitors. Also, Further studies are necessary to compare the docetaxel dose-related toxicities generated in the event of knockout and the ABCC10 inhibitors.

Oxaliplatin is one of the most common drugs used to treat colorectal cancer. Therefore, the sensitivity of the wild and knockout Caco-2 cells can also be compared to check if the CRISPR-Cas9 transfection had increased the sensitivity of the knockout clones towards oxaliplatin, too or was the effect specific only to docetaxel.

Docetaxel is a prominent drug used to treat breast cancer. Therefore, further studies can be performed to create CRISPR-Cas9 knockout clones using breast cancer cell lines. Following limiting dilution, the isolated clones can be tested using MTT assay, western blotting, and sequencing to check the feasibility of obtaining ABCC10 knockout clones that are more sensitive to docetaxel.

As explained in section 4.5, the off-target effect can be reduced using improved gRNA and modified Cas9. Therefore, CRISPR/Cas 9 transfection can be performed using different gRNAs or modified Cas9 nickase with paired gRNA. The functional analysis needs to be performed on the clones obtained using different methods, and the efficiency of producing the expected knockout can be compared.

4.7. Conclusion

This thesis demonstrates that liposome-mediated delivery of ABCC10 guide-RNA/Cas9 protein ribonucleoprotein complexes to Caco-2 cells achieved an on-target *ABCC10* editing with a gene cleavage efficiency of 13.8%. The subsequent limiting dilution cloning identified a single Caco-2 clone that are significantly more sensitive to an ABCC10 substrate drug docetaxel. Furthermore, it demonstrates that by inhibiting the ABCC10 protein using a gene editing technique, the function of docetaxel is increased. Therefore, this research's findings confirm previous studies' data that ABCC10 acts as a resistor towards docetaxel. As the sensitivity increases, lower concentrations are sufficient to treat tumour cells. Therefore, the dose-related toxicities are reduced, and the patient's quality of life is increased. However, several factors, such as the gRNA, Cas9 protein, the cell line used, and the target gene-modified, play a crucial role in generating the intended knockout. Further studies are necessary to increase the efficiency of producing complete knockouts and develop methods to test in animal models and clinical trials. In short, this study provides evidence for invitro gene alteration of ABCC10 protein and decreases its resistance towards docetaxel, increasing the sensitivity of Caco-2 cells. Therefore, this therapeutic strategy provides a novel approach to increase docetaxel sensitivity in colorectal cancer patients.

References

Abar, L., Vieira, A. R., Aune, D., Sobiecki, J. G., Vingeliene, S., Polemiti, E., Stevens, C., Greenwood, D. C., Chan, D. S. M., & Schlesinger, S. (2018). Height and body fatness and colorectal cancer risk: an update of the WCRF–AICR systematic review of published prospective studies. *European journal of nutrition*, *57*, 1701-1720.

Abshire, D., & Lang, M. K. (2018). The evolution of radiation therapy in treating cancer.

Ajouz, H., Mukherji, D., & Shamseddine, A. (2014). Secondary bile acids: an underrecognized cause of colon cancer. *World journal of surgical oncology*, *12*(1), 1-5.

American Cancer Society. (2020). *Colorectal Cancer Early Detection, Diagnosis, and Staging*. https://www.cancer.org/cancer/types/colon-rectal-cancer/detection-diagnosis-staging.html

Amersi, F., Agustin, M., & Ko, C. Y. (2005). Colorectal cancer: epidemiology, risk factors, and health services. *Clinics in colon and rectal surgery*, *18*(03), 133-140.

Arvelo, F., Sojo, F., & Cotte, C. (2015). Biology of colorectal cancer. *Ecancermedicalscience*, *9*.

Aune, D., Chan, D. S. M., Lau, R., Vieira, R., Greenwood, D. C., Kampman, E., & Norat, T. (2011). Dietary fibre, whole grains, and risk of colorectal cancer: systematic review and dose-response meta-analysis of prospective studies. *Bmj*, *343*.

Baliou, S., Adamaki, M., Kyriakopoulos, A. M., Spandidos, D. A., Panayiotidis, M., Christodoulou, I., & Zoumpourlis, V. (2018). CRISPR therapeutic tools for complex genetic disorders and cancer. *International journal of oncology*, *53*(2), 443-468.

Baskar, R., Lee, K. A., Yeo, R., & Yeoh, K.-W. (2012). Cancer and radiation therapy: current advances and future directions. *International journal of medical sciences*, *9*(3), 193.

Bernstein, C. N., Blanchard, J. F., Kliewer, E., & Wajda, A. (2001). Cancer risk in patients with inflammatory bowel disease: a population ‐ based study. *Cancer*, *91*(4), 854-862.

Bissery, M.-C., Guénard, D., Guéritte-Voegelein, F., & Lavelle, F. (1991). Experimental antitumor activity of taxotere (RP 56976, NSC 628503), a taxol analogue. *Cancer research*, *51*(18), 4845-4852.

Blum, J. L., Savin, M. A., Edelman, G., Pippen, J. E., Robert, N. J., Geister, B. V., Kirby, R. L., Clawson, A., & O'Shaughnessy, J. A. (2007). Phase II study of weekly albumin-bound paclitaxel for patients with metastatic breast cancer heavily pretreated with taxanes. *Clinical breast cancer*, *7*(11), 850-856.

Botteri, E., Iodice, S., Bagnardi, V., Raimondi, S., Lowenfels, A. B., & Maisonneuve, P. (2008). Smoking and colorectal cancer: a meta-analysis. *Jama*, *300*(23), 2765-2778.

Bruntsch, U., Heinrich, B., Kaye, S. B., De Mulder, P. H. M., Vermorken, J. B., Wanders, J., Franklin, H., & Bayssas, M. (1994). Docetaxel (Taxotere) in advanced renal cell cancer. A phase II trial of the EORTC Early Clinical Trials Group. *European Journal of Cancer*, *30*(8), 1064-1067.

Burris, H., Irvin, R., Kuhn, J., Kalter, S., Smith, L., Shaffer, D., Fields, S., Weiss, G., Eckardt, J., & Rodriguez, G. (1993). Phase I clinical trial of taxotere administered as either a 2-hour or 6-hour intravenous infusion. *Journal of clinical oncology*, *11*(5), 950-958.

Campenhout, C. V., Cabochette, P., Veillard, A.-C., Laczik, M., Zelisko-Schmidt, A., Sabatel, C., Dhainaut, M., Vanhollebeke, B., Gueydan, C., & Kruys, V. (2019). Guidelines for optimized gene knockout using CRISPR/Cas9. *Biotechniques*, *66*(6), 295-302.

Canavan, C., Abrams, K. R., & Mayberry, J. (2006). Meta ‐ analysis: colorectal and small bowel cancer risk in patients with Crohn's disease. *Alimentary pharmacology & therapeutics*, *23*(8), 1097-1104.

Catimel, G., Verweij, J., Mattijssen, V., Hanauske, A., Piccart, M., Wanders, J., Franklin, H., Le Bail, N., Clavel, M., & Kaye, S. B. (1994). Docetaxel (Taxotere®): an active drug for the treatment of patients with advanced squamous cell carcinoma of the head and neck. *Annals of oncology*, *5*(6), 533-537.

Chen, J. J., Sun, Y. L., Tiwari, A. K., Xiao, Z. J., Sodani, K., Yang, D. H., Vispute, S. G., Jiang, W. Q., Chen, S. D., & Chen, Z. S. (2012). PDE 5 inhibitors, sildenafil and vardenafil, reverse multidrug resistance by inhibiting the efflux function of multidrug resistance protein 7 (ATP ‐ binding Cassette C 10) transporter. *Cancer science*, *103*(8), 1531-1537.

Chen, M., Mao, A., Xu, M., Weng, Q., Mao, J., & Ji, J. (2019). CRISPR-Cas9 for cancer therapy: Opportunities and challenges. *Cancer letters*, *447*, 48-55.

Chen, Z.-S., Hopper-Borge, E., Belinsky, M. G., Shchaveleva, I., Kotova, E., & Kruh, G. D. (2003). Characterization of the transport properties of human multidrug resistance protein 7 (MRP7, ABCC10). *Molecular pharmacology*, *63*(2), 351-358.

Chen, Z. S., & Tiwari, A. K. (2011). Multidrug resistance proteins (MRPs/ABCCs) in cancer chemotherapy and genetic diseases. *The FEBS journal*, *278*(18), 3226-3245.

Cirocchi, R., Trastulli, S., Boselli, C., Montedori, A., Cavaliere, D., Parisi, A., Noya, G., & Abraha, I. (2012). Radiofrequency ablation in the treatment of liver metastases from colorectal cancer. *Cochrane Database of Systematic Reviews*(6).

Clark, T. B., Kemeny, N. E., Conti, J. A., Huang, Y., Andre, A. M., & Stockman, J. (1998). Phase II trial of docetaxel (Taxotere®) for untreated advanced colorectal carcinoma. *Cancer investigation*, *16*(5), 314-318.

Clarke, S. J., & Rivory, L. P. (1999). Clinical pharmacokinetics of docetaxel. *Clinical pharmacokinetics*, *36*, 99-114.

Cox, D. B. T., Platt, R. J., & Zhang, F. (2015). Therapeutic genome editing: prospects and challenges. *Nature medicine*, *21*(2), 121-131.

Cross, A. J., Boca, S., Freedman, N. D., Caporaso, N. E., Huang, W.-Y., Sinha, R., Sampson, J. N., & Moore, S. C. (2014). Metabolites of tobacco smoking and colorectal cancer risk. *Carcinogenesis*, *35*(7), 1516-1522.

Daer, R. M., Cutts, J. P., Brafman, D. A., & Haynes, K. A. (2017). The impact of chromatin dynamics on Cas9-mediated genome editing in human cells. *ACS synthetic biology*, *6*(3), 428-438.

de Weger, V. A., Beijnen, J. H., & Schellens, J. H. M. (2014). Cellular and clinical pharmacology of the taxanes docetaxel and paclitaxel–a review. *Anti-cancer drugs*, *25*(5), 488-494.

Deng, W., Dai, C.-L., Chen, J.-J., Kathawala, R. J., Sun, Y.-L., Chen, H.-F., Fu, L.-W., & Chen, Z.-S. (2013). Tandutinib (MLN518) reverses multidrug resistance by inhibiting the efflux activity of the multidrug resistance protein 7 (ABCC10). *Oncology reports*, *29*(6), 2479-2485.

Devkota, S. (2018). The road less traveled: strategies to enhance the frequency of homology-directed repair (HDR) for increased efficiency of CRISPR/Cas-mediated transgenesis. *BMB reports*, *51*(9), 437.

Doench, J. G., Hartenian, E., Graham, D. B., Tothova, Z., Hegde, M., Smith, I., Sullender, M., Ebert, B. L., Xavier, R. J., & Root, D. E. (2014). Rational design of highly active sgRNAs for CRISPR-Cas9–mediated gene inactivation. *Nature biotechnology*, *32*(12), 1262-1267.

Dreyfuss, A. I., Clark, J. R., Norris, C. M., Rossi, R. M., Lucarini, J. W., Busse, P. M., Poulin, M. D., Thornhill, L., Costello, R., & Posner, M. R. (1996). Docetaxel: an active drug for squamous cell carcinoma of the head and neck. *Journal of clinical oncology*, *14*(5), 1672-1678.

Dvorak, P., Hlavac, V., Mohelnikova-Duchonova, B., Liska, V., Pesta, M., & Soucek, P. (2017). Downregulation of ABC transporters in non-neoplastic tissues confers better prognosis for pancreatic and colorectal cancer patients. *Journal of Cancer*, *8*(11), 1959.

Einzig, A. I., Schuchter, L. M., Recio, A., Coatsworth, S., Rodriquez, R., & Wiernik, P. H. (1996). Phase II trial of docetaxel (Taxotere) in patients with metastatic melanoma previously untreated with cytotoxic chemotherapy. *Medical Oncology*, *13*, 111-117.

Eisenhauer, E. A., & Trudeau, M. (1995). An overview of phase II studies of docetaxel in patients with metastatic breast cancer. *European Journal of Cancer*, *31*, S11-S13.

Ellis, L., Abrahão, R., McKinley, M., Yang, J., Somsouk, M., Marchand, L. L., Cheng, I., Gomez, S. L., & Shariff-Marco, S. (2018). Colorectal cancer incidence trends by age, stage, and racial/ethnic group in California, 1990–2014. *Cancer Epidemiology, Biomarkers & Prevention*, *27*(9), 1011-1018.

Endo, M., Mikami, M., & Toki, S. (2015). Multigene knockout utilizing off-target mutations of the CRISPR/Cas9 system in rice. *Plant and Cell Physiology*, *56*(1), 41-47.

Extra, J.-M., Rousseau, F., Bruno, R., Clavel, M., Bail, N. L., & Marty, M. (1993). Phase I and pharmacokinetic study of Taxotere (RP 56976; NSC 628503) given as a short intravenous infusion. *Cancer research*, *53*(5), 1037-1042.

Fauzee, N. J., Dong, Z., & Wang, Y. L. (2011). Taxanes: promising anti-cancer drugs. *Asian Pac J Cancer Prev*, *12*(4), 837-851.

Feng, D., & Huang, L. (2022). Knockout of ABC transporters by CRISPR/Cas9 contributes to reliable and accurate transporter substrate identification for drug discovery. *Frontiers in Pharmacology*, *13*, 1015940.

Fossella, F. V., Lee, J. S., Murphy, W. K., Lippman, S. M., Calayag, M., Pang, A., Chasen, M., Shin, D. M., Glisson, B., & Benner, S. (1994). Phase II study of docetaxel for recurrent or metastatic non-small-cell lung cancer. *Journal of clinical oncology*, *12*(6), 1238-1244.

Francis, P., Schneider, J., Hann, L., Balmaceda, C., Barakat, R., Phillips, M., & Hakes, T. (1994). Phase II trial of docetaxel in patients with platinum-refractory advanced ovarian cancer. *Journal of clinical oncology*, *12*(11), 2301-2308.

Francis, P. A., Rigas, J. R., Kris, M. G., Pisters, K. M., Orazem, J. P., Woolley, K. J., & Heelan, R. T. (1994). Phase II trial of docetaxel in patients with stage III and IV non-small-cell lung cancer. *Journal of clinical oncology*, *12*(6), 1232-1237.

Fromm, M. F., & Kim, R. B. (2010). *Drug transporters* (Vol. 201). Springer Science & Business Media.

Fu, Y., Foden, J. A., Khayter, C., Maeder, M. L., Reyon, D., Joung, J. K., & Sander, J. D. (2013). High-frequency off-target mutagenesis induced by CRISPR-Cas nucleases in human cells. *Nature biotechnology*, *31*(9), 822-826.

Fulco, C. P., Munschauer, M., Anyoha, R., Munson, G., Grossman, S. R., Perez, E. M., Kane, M., Cleary, B., Lander, E. S., & Engreitz, J. M. (2016). Systematic mapping of functional enhancer–promoter connections with CRISPR interference. *Science*, *354*(6313), 769-773.

Gallamini, A., Zwarthoed, C., & Borra, A. (2014). Positron emission tomography (PET) in oncology. *Cancers*, *6*(4), 1821-1889.

Garcia-Larsen, V., Morton, V., Norat, T., Moreira, A., Potts, J. F., Reeves, T., & Bakolis, I. (2019). Dietary patterns derived from principal component analysis (PCA) and risk of colorectal cancer: a systematic review and meta-analysis. *European journal of clinical nutrition*, *73*(3), 366-386.

Ghosh, D., Venkataramani, P., Nandi, S., & Bhattacharjee, S. (2019). CRISPR–Cas9 a boon or bane: the bumpy road ahead to cancer therapeutics. *Cancer cell international*, *19*, 1-10.

Golden, R. J., Chen, B., Li, T., Braun, J., Manjunath, H., Chen, X., Wu, J., Schmid, V., Chang, T.-C., & Kopp, F. (2017). An Argonaute phosphorylation cycle promotes microRNA-mediated silencing. *Nature*, *542*(7640), 197-202.

Granados-Romero, J. J., Valderrama-Treviño, A. I., Contreras-Flores, E. H., Barrera-Mera, B., Herrera Enríquez, M., Uriarte-Ruíz, K., Ceballos-Villalba, J. C., Estrada-Mata, A. G., Alvarado Rodríguez, C., & Arauz-Peña, G. (2017). Colorectal cancer: a review. *Int J Res Med Sci*, *5*(11), 4667.

Guo, X., Chitale, P., & Sanjana, N. E. (2017). Target discovery for precision medicine using high-throughput genome engineering. *Precision Medicine, CRISPR, and Genome Engineering: Moving from Association to Biology and Therapeutics*, 123-145.

Hart, T., Chandrashekhar, M., Aregger, M., Steinhart, Z., Brown, K. R., MacLeod, G., Mis, M., Zimmermann, M., Fradet-Turcotte, A., & Sun, S. (2015). High-resolution CRISPR screens reveal fitness genes and genotype-specific cancer liabilities. *Cell*, *163*(6), 1515-1526.

Health New Zealand. (2023, 14 December 2023). *Cancer Web Tool*. https://tewhatuora.shinyapps.io/cancer-web-tool/

Ho, Y.-H., & Ashour, M. A. T. (2010). Techniques for colorectal anastomosis. *World Journal of Gastroenterology: WJG*, *16*(13), 1610.

Hong, A. L., Tseng, Y.-Y., Cowley, G. S., Jonas, O., Cheah, J. H., Kynnap, B. D., Doshi, M. B., Oh, C., Meyer, S. C., & Church, A. J. (2016). Integrated genetic and pharmacologic interrogation of rare cancers. *Nature communications*, *7*(1), 11987.

Hopper-Borge, E., Chen, Z.-S., Shchaveleva, I., Belinsky, M. G., & Kruh, G. D. (2004). Analysis of the Drug Resistance Profile of Multidrug Resistance Protein 7 (ABCC10): Resistance to Docetaxel. *Cancer research*, *64*(14), 4927-4930.

Hopper-Borge, E., Xu, X., Shen, T., Shi, Z., Chen, Z.-S., & Kruh, G. D. (2009). Human multidrug resistance protein 7 (ABCC10) is a resistance factor for nucleoside analogues and epothilone B. *Cancer research*, *69*(1), 178-184.

Hopper-Borge, E. A., Churchill, T., Paulose, C., Nicolas, E., Jacobs, J. D., Ngo, O., Kuang, Y., Grinberg, A., Westphal, H., & Chen, Z.-S. (2011). Contribution of Abcc10 (Mrp7) to in vivo paclitaxel resistance as assessed in Abcc10−/− mice. *Cancer research*, *71*(10), 3649-3657.

Hopper, E., Belinsky, M. G., Zeng, H., Tosolini, A., Testa, J. R., & Kruh, G. D. (2001). Analysis of the structure and expression pattern of MRP7 (ABCC10), a new member of the MRP subfamily. *Cancer letters*, *162*(2), 181-191.

Horlbeck, M. A., Witkowsky, L. B., Guglielmi, B., Replogle, J. M., Gilbert, L. A., Villalta, J. E., Torigoe, S. E., Tjian, R., & Weissman, J. S. (2016). Nucleosomes impede Cas9 access to DNA in vivo and in vitro. *elife*, *5*, e12677.

Hsieh, J.-S., Lin, S.-R., Chang, M.-Y., Chen, F.-M., Lu, C.-Y., Huang, T.-J., Huang, Y.-S., Huang, C.-J., & Wang, J.-Y. (2005). APC, K-ras, and p53 gene mutations in colorectal cancer patients: correlation to clinicopathologic features and postoperative surveillance. *The American Surgeon*, *71*(4), 336-343.

Hsu, P. D., Scott, D. A., Weinstein, J. A., Ran, F. A., Konermann, S., Agarwala, V., Li, Y., Fine, E. J., Wu, X., & Shalem, O. (2013). DNA targeting specificity of RNA-guided Cas9 nucleases. *Nature biotechnology*, *31*(9), 827-832.

Jackson, C., Sharples, K., Firth, M., Hinder, V., Jeffrey, M., Keating, J., Secker, A., Derrett, S., Atmore, C., & Bramley, D. (2015). The PIPER project: An internal examination of colorectal cancer management in New Zealand.

Jones, S. E., Erban, J., Overmoyer, B., Budd, G. T., Hutchins, L., Lower, E., Laufman, L., Sundaram, S., Urba, W. J., & Pritchard, K. I. (2005). Randomized phase III study of docetaxel compared with paclitaxel in metastatic breast cancer. *Journal of clinical oncology*, *23*(24), 5542-5551.

Kao, H.-h., Chang, M.-s., Cheng, J.-f., & Huang, J.-d. (2003). Genomic structure, gene expression, and promoter analysis of human multidrug resistance-associated protein 7. *Journal of biomedical science*, *10*, 98-110.

Karimian, A., Azizian, K., Parsian, H., Rafieian, S., Shafiei‐Irannejad, V., Kheyrollah, M., Yousefi, M., Majidinia, M., & Yousefi, B. (2019). CRISPR/Cas9 technology as a potent molecular tool for gene therapy. *Journal of cellular physiology*, *234*(8), 12267-12277.

Kataoka, K., Shiraishi, Y., Takeda, Y., Sakata, S., Matsumoto, M., Nagano, S., Maeda, T., Nagata, Y., Kitanaka, A., & Mizuno, S. (2016). Aberrant PD-L1 expression through 3′-UTR disruption in multiple cancers. *Nature*, *534*(7607), 402-406.

Kaye, S. B., Piccart, M., Aapro, M., Francis, P., & Kavanagh, J. (1997). Phase II trials of docetaxel (Taxotere®) in advanced ovarian cancer—an updated overview. *European Journal of Cancer*, *33*(13), 2167-2170.

Keum, N., Aune, D., Greenwood, D. C., Ju, W., & Giovannucci, E. L. (2014). Calcium intake and colorectal cancer risk: Dose‐response meta‐analysis of prospective observational studies. *International journal of cancer*, *135*(8), 1940-1948.

Keum, N., & Giovannucci, E. (2019). Global burden of colorectal cancer: emerging trends, risk factors and prevention strategies. *Nature reviews Gastroenterology & hepatology*, *16*(12), 713-732.

Konermann, S., Brigham, M. D., Trevino, A. E., Joung, J., Abudayyeh, O. O., Barcena, C., Hsu, P. D., Habib, N., Gootenberg, J. S., & Nishimasu, H. (2015). Genome-scale transcriptional activation by an engineered CRISPR-Cas9 complex. *Nature*, *517*(7536), 583-588.

Kuang, Y.-H., Shen, T., Chen, X., Sodani, K., Hopper-Borge, E., Tiwari, A. K., Lee, J. W. K. K., Fu, L.-W., & Chen, Z.-S. (2010). Lapatinib and erlotinib are potent reversal agents for MRP7 (ABCC10)-mediated multidrug resistance. *Biochemical pharmacology*, *79*(2), 154-161.

Landry, J. J. M., Pyl, P. T., Rausch, T., Zichner, T., Tekkedil, M. M., Stütz, A. M., Jauch, A., Aiyar, R. S., Pau, G., & Delhomme, N. (2013). The genomic and transcriptomic landscape of a HeLa cell line. *G3: Genes, Genomes, Genetics*, *3*(8), 1213-1224.

Li, B., Chen, L., Luo, H.-L., Yi, F.-M., Wei, Y.-P., & Zhang, W.-X. (2019). Docetaxel, cisplatin, and 5-fluorouracil compared with epirubicin, cisplatin, and 5-fluorouracil regimen for advanced gastric cancer: A systematic review and meta-analysis. *World journal of clinical cases*, *7*(5), 600.

Li, Z.-H., You, D.-Y., Gao, D.-P., Yang, G.-J., Dong, X.-X., Zhang, D.-F., & Ding, Y.-Y. (2017). Role of CT scan in differentiating the type of colorectal cancer. *OncoTargets and therapy*, 2297-2303.

Lian, H., Zhang, T., Sun, J., Liu, X., Ren, G., Kou, L., Zhang, Y., Han, X., Ding, W., & Ai, X. (2013). Enhanced oral delivery of paclitaxel using acetylcysteine functionalized chitosan-vitamin E succinate nanomicelles based on a mucus bioadhesion and penetration mechanism. *Molecular pharmaceutics*, *10*(9), 3447-3458.

Liu, B., Saber, A., & Haisma, H. J. (2019). CRISPR/Cas9: a powerful tool for identification of new targets for cancer treatment. *Drug discovery today*, *24*(4), 955-970.

Lordick, F., Carneiro, F., Cascinu, S., Fleitas, T., Haustermans, K., Piessen, G., Vogel, A., & Smyth, E. C. (2022). Gastric cancer: ESMO Clinical Practice Guideline for diagnosis, treatment and follow-up☆. *Annals of oncology*, *33*(10), 1005-1020.

Ma, P., Yao, Y., Sun, W., Dai, S., & Zhou, C. (2017). Daily sedentary time and its association with risk for colorectal cancer in adults: a dose–response meta-analysis of prospective cohort studies. *Medicine*, *96*(22).

Ma, Y., Yang, W., Song, M., Smith-Warner, S. A., Yang, J., Li, Y., Ma, W., Hu, Y., Ogino, S., & Hu, F. B. (2018). Type 2 diabetes and risk of colorectal cancer in two large US prospective cohorts. *British journal of cancer*, *119*(11), 1436-1442.

Mali, P., Yang, L., Esvelt, K. M., Aach, J., Guell, M., DiCarlo, J. E., Norville, J. E., & Church, G. M. (2013). RNA-guided human genome engineering via Cas9. *Science*, *339*(6121), 823-826.

Maria, A., & Lieske, B. (2020). Colostomy Care.

Mattiuzzi, C., Sanchis-Gomar, F., & Lippi, G. (2019). Concise update on colorectal cancer epidemiology. *Annals of translational medicine*, *7*(21).

Mertens, W. C., Eisenhauer, E. A., Jolivet, J., Ernst, S., Moore, M., & Muldal, A. (1994). Docetaxel in advanced renal carcinoma: A phase II trial of the National Cancer Institute of Canada Clinical Trials Group. *Annals of oncology*, *5*(2), 185-187.

Mizoue, T., Inoue, M., Wakai, K., Nagata, C., Shimazu, T., Tsuji, I., Otani, T., Tanaka, K., Matsuo, K., & Tamakoshi, A. (2008). Alcohol drinking and colorectal cancer in Japanese: a pooled analysis of results from five cohort studies. *American journal of epidemiology*, *167*(12), 1397-1406.

Mollanoori, H., Shahraki, H., Rahmati, Y., & Teimourian, S. (2018). CRISPR/Cas9 and CAR-T cell, collaboration of two revolutionary technologies in cancer immunotherapy, an instruction for successful cancer treatment. *Human immunology*, *79*(12), 876-882.

Montero, A., Fossella, F., Hortobagyi, G., & Valero, V. (2005). Docetaxel for treatment of solid tumours: a systematic review of clinical data. *The lancet oncology*, *6*(4), 229-239.

Morgan, E., Arnold, M., Gini, A., Lorenzoni, V., Cabasag, C. J., Laversanne, M., Vignat, J., Ferlay, J., Murphy, N., & Bray, F. (2023). Global burden of colorectal cancer in 2020 and 2040: Incidence and mortality estimates from GLOBOCAN. *Gut*, *72*(2), 338-344.

Muller, A. D., & Sonnenberg, A. (1995). Prevention of colorectal cancer by flexible endoscopy and polypectomy: a case-control study of 32 702 veterans. *Annals of internal medicine*, *123*(12), 904-910.

Murphy, N., Moreno, V., Hughes, D. J., Vodicka, L., Vodicka, P., Aglago, E. K., Gunter, M. J., & Jenab, M. (2019). Lifestyle and dietary environmental factors in colorectal cancer susceptibility. *Molecular aspects of medicine*, *69*, 2-9.

Muta, M., Yanagawa, T., Sai, Y., Saji, S., Suzuki, E., Aruga, T., Kuroi, K., Matsumoto, G., Toi, M., & Nakashima, E. (2009). Effect of low-dose paclitaxel and docetaxel on endothelial progenitor cells. *Oncology*, *77*(3-4), 182-191.

Naeem, M., Majeed, S., Hoque, M. Z., & Ahmad, I. (2020). Latest developed strategies to minimize the off-target effects in CRISPR-Cas-mediated genome editing. *Cells*, *9*(7), 1608.

National Cancer Institute. (2022, April 6, 2022). *Colon Cancer Treatment (PDQ®)–Patient Version*. https://www.cancer.gov/types/colorectal/patient/colon-treatment-pdq

National Comprehensive Cancer, N. (2009). Guidelines for treatment of cancer by site. *Jenkintown, PA: National Comprehensive Cancer Network*.
Nguyen, T. T., Ung, T. T., Kim, N. H., & Do Jung, Y. (2018). Role of bile acids in colon carcinogenesis. *World journal of clinical cases*, *6*(13), 577.
Nivatvongs, S. (2000). Surgical management of early colorectal cancer. *World journal of surgery*, *24*(9), 1052-1055.
Nygren, P. (2001). What is cancer chemotherapy? *Acta Oncologica*, *40*(2-3), 166-174.
Ojima, I., Lichtenthal, B., Lee, S., Wang, C., & Wang, X. (2016). Taxane anticancer agents: a patent perspective. *Expert opinion on therapeutic patents*, *26*(1), 1-20.
Pang, Y., Kartsonaki, C., Guo, Y., Chen, Y., Yang, L., Bian, Z., Bragg, F., Millwood, I. Y., Shen, L., & Zhou, S. (2018). Diabetes, plasma glucose and incidence of colorectal cancer in Chinese adults: a prospective study of 0.5 million people. *J Epidemiol Community Health*, *72*(10), 919-925.
Pazdur, R., Lassere, Y., Soh, L. T., Ajani, J. A., Bready, B., Soo, E., Sugarman, S., Patt, Y., Abbruzzese, J. L., & Levin, B. (1994). Phase II trial of docetaxel (Taxotere®) in metastatic colorectal carcinoma. *Annals of oncology*, *5*(5), 468-470.
Pazdur, R., Newman, R. A., Newman, B. M., Fuentes, A., Benvenuto, J., Bready, B., Moore Jr, D., Jaiyesimi, I., Vreeland, F., & Bayssas, M. M. G. (1992). Phase I trial of Taxotere: five-day schedule. *JNCI: Journal of the National Cancer Institute*, *84*(23), 1781-1788.
Peeters, P. J. H. L., Bazelier, M. T., Leufkens, H. G. M., de Vries, F., & De Bruin, M. L. (2015). The risk of colorectal cancer in patients with type 2 diabetes: associations with treatment stage and obesity. *Diabetes Care*, *38*(3), 495-502.
Pento, J. T. (2017). Monoclonal antibodies for the treatment of cancer. *Anticancer research*, *37*(11), 5935-5939.
Petrylak, D. P., Tangen, C., Hussain, M., Lara, P. N., Jones, J., Talpin, M. E., Burch, P., Greene, G., Small, E., & Crawford, E. D. (2004). SWOG 99–16: Randomized phase III trial of docetaxel (D)/estramustine (E) versus mitoxantrone (M)/prednisone (p) in men with androgen-independent prostate cancer (AIPCA). *Journal of clinical oncology*, *22*(14_suppl), 3-3.
Piccart, M. J., Gore, M., Huinink, W. T. B., Van Oosterom, A., Verweij, J., Wanders, J., Frankli, H., Bayssas, M., & Kaye, S. (1995). Docetaxel: an active new drug for treatment of advanced epithelial ovarian cancer. *JNCI: Journal of the National Cancer Institute*, *87*(9), 676-681.
Pushpakom, S. P., Liptrott, N. J., Rodríguez-Nóvoa, S., Labarga, P., Soriano, V., Albalater, M., Hopper-Borge, E., Bonora, S., Di Perri, G., & Back, D. J. (2011). Genetic variants of ABCC10, a novel tenofovir transporter, are associated with kidney tubular dysfunction. *Journal of Infectious Diseases*, *204*(1), 145-153.
Ran, F. A., Hsu, P. D., Lin, C.-Y., Gootenberg, J. S., Konermann, S., Trevino, A. E., Scott, D. A., Inoue, A., Matoba, S., & Zhang, Y. (2013). Double nicking by RNA-guided CRISPR Cas9 for enhanced genome editing specificity. *Cell*, *154*(6), 1380-1389.
Ravikumar, T. S., Sotomayor, R., & Goel, R. (1997). Cryosurgery in the treatment of liver metastasis from colorectal cancer. *Journal of Gastrointestinal Surgery*, *1*(5), 426-432.
Ren, J., Zhang, X., Liu, X., Fang, C., Jiang, S., June, C. H., & Zhao, Y. (2017). A versatile system for rapid multiplex genome-edited CAR T cell generation. *Oncotarget*, *8*(10), 17002.
Riou, J.-F., Naudin, A., & Lavelle, F. (1992). Effects of Taxotere on murine and human tumor cell lines. *Biochemical and biophysical research communications*, *187*(1), 164-170.
Robey, R. W., Pluchino, K. M., Hall, M. D., Fojo, A. T., Bates, S. E., & Gottesman, M. M. (2018). Revisiting the role of ABC transporters in multidrug-resistant cancer. *Nature Reviews Cancer*, *18*(7), 452-464.
Rodríguez-Rodríguez, D. R., Ramírez-Solís, R., Garza-Elizondo, M. A., Garza-Rodríguez, M. D. L., & Barrera-Saldaña, H. A. (2019). Genome editing: A perspective on the application of CRISPR/Cas9 to study human diseases. *International journal of molecular medicine*, *43*(4), 1559-1574.
Rossi, M., Jahanzaib Anwar, M., Usman, A., Keshavarzian, A., & Bishehsari, F. (2018). Colorectal cancer and alcohol consumption—populations to molecules. *Cancers*, *10*(2), 38.

Rougier, P., Adenis, A., Ducreux, M., De Forni, M., Bonneterre, J., Dembak, M., Clouet, P., Lebecq, A., Baille, P., & Lefresne-Soulas, F. (2000). A phase II study: docetaxel as first-line chemotherapy for advanced pancreatic adenocarcinoma. *European Journal of Cancer*, *36*(8), 1016-1025.

Royer, I., Monsarrat, B., Sonnier, M., Wright, M., & Cresteil, T. (1996). Metabolism of docetaxel by human cytochromes P450: interactions with paclitaxel and other antineoplastic drugs. *Cancer research*, *56*(1), 58-65.

Saber, A., Liu, B., Ebrahimi, P., & Haisma, H. J. (2020). CRISPR/Cas9 for overcoming drug resistance in solid tumors. *DARU Journal of Pharmaceutical Sciences*, *28*, 295-304.

Sánchez-Alcoholado, L., Ramos-Molina, B., Otero, A., Laborda-Illanes, A., Ordóñez, R., Medina, J. A., Gómez-Millán, J., & Queipo-Ortuño, M. I. (2020). The role of the gut microbiome in colorectal cancer development and therapy response. *Cancers*, *12*(6), 1406.

Saus, E., Iraola-Guzmán, S., Willis, J. R., Brunet-Vega, A., & Gabaldón, T. (2019). Microbiome and colorectal cancer: Roles in carcinogenesis and clinical potential. *Molecular aspects of medicine*, *69*, 93-106.

Sawicki, T., Ruszkowska, M., Danielewicz, A., Niedźwiedzka, E., Arłukowicz, T., & Przybyłowicz, K. E. (2021). A review of colorectal cancer in terms of epidemiology, risk factors, development, symptoms and diagnosis. *Cancers*, *13*(9), 2025.

Schiff, P. B., Fant, J., & Horwitz, S. B. (1979). Promotion of microtubule assembly in vitro by taxol. *Nature*, *277*(5698), 665-667.

Schmid, D., & Leitzmann, M. F. (2014). Television viewing and time spent sedentary in relation to cancer risk: a meta-analysis. *JNCI: Journal of the National Cancer Institute*, *106*(7), dju098.

Schrijvers, D., Wanders, J., Dirix, L., Prove, A., Vonck, I., Van Oosterom, A., & Kaye, S. (1993). Coping with toxicities of docetaxel (TaxotereTM). *Annals of oncology*, *4*(7), 610-611.

Scott, A. M., Allison, J. P., & Wolchok, J. D. (2012). Monoclonal antibodies in cancer therapy. *Cancer immunity*, *12*(1).

Shen, T., Kuang, Y.-H., Ashby Jr, C. R., Lei, Y., Chen, A., Zhou, Y., Chen, X., Tiwari, A. K., Hopper-Borge, E., & Ouyang, J. (2009). Imatinib and nilotinib reverse multidrug resistance in cancer cells by inhibiting the efflux activity of the MRP7 (ABCC10). *PLoS One*, *4*(10), e7520.

Shi, J., Wang, E., Milazzo, J. P., Wang, Z., Kinney, J. B., & Vakoc, C. R. (2015). Discovery of cancer drug targets by CRISPR-Cas9 screening of protein domains. *Nature biotechnology*, *33*(6), 661-667.

Smits, A. H., Ziebell, F., Joberty, G., Zinn, N., Mueller, W. F., Clauder-Münster, S., Eberhard, D., Fälth Savitski, M., Grandi, P., & Jakob, P. (2019). Biological plasticity rescues target activity in CRISPR knock outs. *Nature methods*, *16*(11), 1087-1093.

Smyth, J. F., Smith, I. E., Sessa, C., Schoffski, P., Wanders, J., Franklin, H., & Kaye, S. B. (1994). Activity of docetaxel (Taxotere) in small cell lung cancer. *European Journal of Cancer*, *30*(8), 1058-1060.

Sodani, K., Patel, A., Kathawala, R. J., & Chen, Z.-S. (2012). Multidrug resistance associated proteins in multidrug resistance. *Chinese journal of cancer*, *31*(2), 58.

Song, M., Wu, K., Meyerhardt, J. A., Ogino, S., Wang, M., Fuchs, C. S., Giovannucci, E. L., & Chan, A. T. (2018). Fiber intake and survival after colorectal cancer diagnosis. *JAMA oncology*, *4*(1), 71-79.

Sparreboom, A., Van Tellingen, O., Scherrenburg, E. J., Boesen, J. J., Huizing, M. T., Nooijen, W. J., Versluis, C., & Beijnen, J. H. (1996). Isolation, purification and biological activity of major docetaxel metabolites from human feces. *Drug metabolism and disposition*, *24*(6), 655-658.

St. John, D. J. B., McDermott, F. T., Hopper, J. L., Debney, E. A., Johnson, W. R., & Hughes, E. S. R. (1993). Cancer risk in relatives of patients with common colorectal cancer. *Annals of internal medicine*, *118*(10), 785-790.

Sternberg, C. N., ten Bokkel Huinink, W. W., Smyth, J. F., Bruntsch, V., Dirix, L. Y., Pavlidis, N. A., Franklin, H., Wanders, S., Le Bail, N., & Kaye, S. B. (1994). Docetaxel (TaxotereTM), a novel taxoid, in the treatment of advanced colorectal carcinoma: an EORTC Early Clinical Trials Group Study. *British journal of cancer*, *70*(2), 376-379.

Stryker, S. J., Wolff, B. G., Culp, C. E., Libbe, S. D., Ilstrup, D. M., & MacCarty, R. L. (1987). Natural history of untreated colonic polyps. *Gastroenterology*, *93*(5), 1009-1013.

Sulkes, A., Smyth, J., Sessa, C., Dirix, L. Y., Vermorken, J. B., Kaye, S., Wanders, J., Franklin, H., LeBail, N., & Verweij, J. (1994). Docetaxel (TaxotereTM) in advanced gastric cancer: results of a phase II clinical trial. EORTC Early Clinical Trials Group. *British journal of cancer*, *70*(2), 380-383.

Sun, Y.-L., Chen, J.-J., Kumar, P., Chen, K., Sodani, K., Patel, A., Chen, Y.-L., Chen, S.-D., Jiang, W.-Q., & Chen, Z.-S. (2013). Reversal of MRP7 (ABCC10)-mediated multidrug resistance by tariquidar. *PLoS One*, *8*(2), e55576.

Tannock, I. F., De Wit, R., Berry, W. R., Horti, J., Pluzanska, A., Chi, K. N., Oudard, S., Théodore, C., James, N. D., & Turesson, I. (2004). Docetaxel plus prednisone or mitoxantrone plus prednisone for advanced prostate cancer. *New England Journal of Medicine*, *351*(15), 1502-1512.

ten Bokkel Huinink, W. W., Prove, A. M., Piccart, M., Steward, W., Tursz, T., Wanders, J., Franklin, H., Clavel, M., Verweij, J., & Alakl, M. (1994). A phase II trial with Docetaxel (Taxotere™) in second line treatment with chemotherapy for advanced breast cancer: A study of the EORTC Early Clinical Trials Group. *Annals of oncology*, *5*(6), 527-532.

The Global Cancer Observatory. (2022). *Cancer Today*. International Agency for Research on Cancer. https://gco.iarc.fr/today/home

Tomiak, E., Piccart, M. J., Kerger, J., Lips, S., Awada, A., de Valeriola, D., Ravoet, C., Lossignol, D., Sculier, J.-P., & Auzannet, V. (1994). Phase I study of docetaxel administered as a 1-hour intravenous infusion on a weekly basis. *Journal of clinical oncology*, *12*(7), 1458-1467.

Torkzad, M. R., Påhlman, L., & Glimelius, B. (2010). Magnetic resonance imaging (MRI) in rectal cancer: a comprehensive review. *Insights into imaging*, *1*(4), 245-267.

Urien, S., Barré, J., Morin, C., Paccaly, A., Montay, G., & Tillement, J.-P. (1996). Docetaxel serum protein binding with high affinity to alpha 1-acid glycoprotein. *Investigational new drugs*, *14*, 147-151.

Vaishampayan, U., Parchment, R. E., Jasti, B. R., & Hussain, M. (1999). Taxanes: an overview of the pharmacokinetics and pharmacodynamics. *Urology*, *54*(6), 22-29.

van Hoesel, Q. G. C. M., Verweij, J., Catimel, G., Clavel, M., Kerbrat, P., Van Oosterom, A. T., Kerger, J., Tursz, T., van Glabbeke, M., & Van Pottelsberghe, C. (1994). Phase II study with docetaxel (Taxotere®) in advanced soft tissue sarcomas of the adult. *Annals of oncology*, *5*(6), 539-542.

Wall, M. E., & Wani, M. C. (1995). Camptothecin and taxol: discovery to clinic—thirteenth Bruce F. Cain Memorial Award Lecture. *Cancer research*, *55*(4), 753-760.

Wani, M. C., Taylor, H. L., Wall, M. E., Coggon, P., & McPhail, A. T. (1971). Plant antitumor agents. VI. Isolation and structure of taxol, a novel antileukemic and antitumor agent from Taxus brevifolia. *Journal of the American Chemical Society*, *93*(9), 2325-2327.

Xia, A.-L., He, Q.-F., Wang, J.-C., Zhu, J., Sha, Y.-Q., Sun, B., & Lu, X.-J. (2019). Applications and advances of CRISPR-Cas9 in cancer immunotherapy. *Journal of medical genetics*, *56*(1), 4-9.

Zahavi, D., & Weiner, L. (2020). Monoclonal antibodies in cancer therapy. *Antibodies*, *9*(3), 34.

Zheng, T., Hou, Y., Zhang, P., Zhang, Z., Xu, Y., Zhang, L., Niu, L., Yang, Y., Liang, D., & Yi, F. (2017). Profiling single-guide RNA specificity reveals a mismatch sensitive core sequence. *Scientific reports*, *7*(1), 40638.

Zhou, Y., Hopper-Borge, E., Shen, T., Huang, X.-C., Shi, Z., Kuang, Y.-H., Furukawa, T., Akiyama, S.-i., Peng, X.-X., & Ashby Jr, C. R. (2009). Cepharanthine is a potent reversal agent for MRP7 (ABCC10)-mediated multidrug resistance. *Biochemical pharmacology*, *77*(6), 993-1001.

Zhu, S., Li, W., Liu, J., Chen, C.-H., Liao, Q., Xu, P., Xu, H., Xiao, T., Cao, Z., & Peng, J. (2016). Genome-scale deletion screening of human long non-coding RNAs using a paired-guide RNA CRISPR–Cas9 library. *Nature biotechnology*, *34*(12), 1279-1286.

Annex

Table A: ANOVA results of figure A (% cell viability of clone set A)

Dunnett's multiple comparisons test	Mean Diff.	95.00% CI of diff.	Below threshold?	Summary	Adjusted P Value
WT vs. 2D3	-2.030	-13.65 to 9.587	No	ns	0.9938
WT vs. 5C3	-10.07	-21.69 to 1.546	No	ns	0.1041
WT vs. 5F2	-2.195	-13.81 to 9.421	No	ns	0.9910
WT vs. 5G3	-34.01	-45.63 to -22.40	Yes	****	<0.0001
WT vs. 8B6	-7.165	-18.78 to 4.452	No	ns	0.3522
WT vs. 6G2	17.85	6.231 to 29.46	Yes	**	0.0021
WT vs. 7C9	-27.97	-39.58 to -16.35	Yes	****	<0.0001

Table B: ANOVA results of figure B (% cell viability of clone set B)

Dunnett's multiple comparisons test	Mean Diff.	95.00% CI of diff.	Below threshold?	Summary	Adjusted P Value
WT vs. 7D11	-14.61	-28.21 to -1.014	Yes	*	0.0327
WT vs. 6G2	25.67	12.08 to 39.27	Yes	***	0.0003
WT vs. 7B11	-8.873	-22.47 to 4.723	No	ns	0.3009
WT vs. 7C9	-2.727	-16.32 to 10.87	No	ns	0.9873
WT vs. 5G3	-2.659	-16.25 to 10.94	No	ns	0.9891
WT vs. 2G9	2.722	-10.87 to 16.32	No	ns	0.9874
WT vs. 2E5	-3.905	-17.50 to 9.692	No	ns	0.9255

Table C: ANOVA results of figure C (% cell viability of clone set C)

Dunnett's multiple comparisons test	Mean Diff.	95.00% CI of diff.	Below threshold?	Summary	Adjusted P Value
WT vs. 2D3	-18.83	-37.84 to 0.1873	No	ns	0.0527
WT vs. 5C3	5.553	-13.46 to 24.57	No	ns	0.8953
WT vs. 5F2	-14.06	-33.07 to 4.952	No	ns	0.1905
WT vs. 5G3	-25.51	-44.53 to -6.499	Yes	**	0.0076
WT vs. 7C9	-13.61	-32.62 to 5.403	No	ns	0.2132
WT vs. 8B6	9.132	-9.881 to 28.15	No	ns	0.5608

Table D: ANOVA results of figure D (% cell viability of clone set D)

Dunnett's multiple comparisons test	Mean Diff.	95.00% CI of diff.	Below threshold?	Summary	Adjusted P Value
WT vs. 1F11	-2.681	-23.69 to 18.32	No	ns	0.9977
WT vs. 4D7	-12.17	-33.17 to 8.840	No	ns	0.3882
WT vs. 7B10	-1.650	-22.66 to 19.36	No	ns	0.9997
WT vs. 7B11	11.62	-9.381 to 32.63	No	ns	0.4299
WT vs. 7G6	-8.624	-29.63 to 12.38	No	ns	0.6948
WT vs. 8F7	14.64	-6.364 to 35.65	No	ns	0.2326